The Control of Quantized Conduction Events in Lipid Membranes by Anesthetics

Huiling Wang

Supervisor: Thomas Heimburg

A thesis presented for the degree of Master of Physics

Neils Bohr Institute
University of Copenhagen
Denmark
05.06.2023

Acknowledgments

I would like to express my sincere gratitude to my supervisor, Thomas Heimburg, for his constant support throughout my research. His guidance and assistance were invaluable, from helping me find the necessary materials in the laboratory to providing advice during experiments. He also showed me how to use Igor for data analysis and provided guidance on writing a good thesis. His expertise and different perspectives have broadened my horizons, and I am truly grateful for his kind support.

I would also like to extend my thanks to Karis Zecchi, who generously taught me how to make micropipettes and guided me through performing patch clamp experiments in great detail. Her skillfulness allowed me to witness the occurrence of lipid ion channels, which was a fascinating experience for me. I am thankful for her patience and expertise.

I am grateful to Inger for her kindness and willingness to help me in the laboratory. She provided valuable guidance on using different instruments to prepare various electrolyte solutions, which also contributed to the success of my research.

My heartfelt thanks go to my family, especially my mother-in-law(Ziyin Ni), my sister(Meimei Lin) and my husband(Caiyuan Lin). Their unwavering support and assistance in taking care of my little children have been instrumental in enabling me to pursue my master's degree. I am deeply grateful for their constant care and understanding.

Finally, I would like to express my appreciation to everyone who has been a part of my journey. Your care and thoughtfulness are deeply appreciated.

Abstract

The famous Hodgkin-Huxley model treat lipid bilayer as an insulating barrier that maintains the separation of charges across the membrane when they described action potential in nerve axon. Nowadays, the transport of ions across membrane is thought attributed to protein ion channel. While numerous study has show that lipid bilayer is permeable for ions, even water, when cell membrane close to phase transition regime. The more interesting is the phase transition of lipid bilayer is reported in various cell type close to their biological temperature, include nerve cells. During action potential, the release and reuptake of heat is observed, the area of membrane increased and the thickness of cell membrane decreased. These phenomena strongly suggest that a phase transition of the cell membrane occurs during action potential.

The soliton model proposed by Heimburg et.al takes into account this phase transition in cell membrane and provides a thermodynamic theory to describe the phenomenon of action potential at the macroscopic level. Additionally, the soliton model offers a reasonable explanation for the action of anesthesia using the melting depression law.

Based on the work of Heimburg, this thesis aims to focus on quantized conduction events occurring near phase transitions in the protein-free membrane, which is similar to those described for protein ion channels. Specifically, the focus will be on quantitatively analyzing how anesthetics (such as octanol) affect the conductance of lipid ion channels in protein-free membranes based on the melting depression law.

Contents

Chapter 1

Introduction

1.1 Cell Membrane

Cell membrane(biological membrane), is a critical component of living cells that serves as a selective barrier between the cell's internal environment and the external environment. It plays an essential role in maintaining the cell's shape, regulating the transport of molecules in and out of the cell, and participating in various cellular processes.

1.1.1 Dynamic Cell Membrane

The fluid mosaic model is the prevailing model for describing the structure of the cell membrane. Proposed by S.J. Singer and G.L. Nicolson in 1972, this model suggests that the membrane is composed of a fluid phospholipid bilayer in which proteins are embedded[55].

Nowadays, the structure of cell membranes has been extensively studied. Figure 1.1 shows the cell membrane from a animal's cell. The cell membrane is a highly flexible configuration composed mainly of phospholipids arranged in a bilayer formation. In addition to phospholipids, biological membranes may also contain other types of lipids, such as cholesterol and glycolipids. Proteins are another important component of biological membranes. There are two types of membrane proteins: integral proteins and peripheral proteins. Integral proteins are embedded within the lipid bilayer, and they may span the entire membrane or only a portion of it. One specific type of integral protein is ion channels, which are thought to facilitate the transport of ions across the membrane.

The lipid bilayer consists of two layers of phospholipids, which are amphipathic molecules that have both hydrophobic and hydrophilic regions. In the lipid bilayer, the hydrophobic tails face each other in the interior of the bilayer, while the hydrophilic heads face the aqueous environment on either side of the membrane. This arrangement creates a hydrophobic barrier that separates the internal environment of the cell from the external environment. The head group consists of a phosphate group linked to a small organic molecule, such as choline, serine, or ethanolamine, which contains a polar or charged functional group. The fatty acid tails are long hydrocarbon chains that are nonpolar and hydrophobic.

The fluid mosaic model also takes into account the dynamic nature of biological membranes. The lipid bilayer is not a static structure but rather a dynamic one, with individual phospholipids and proteins able to move laterally within the membrane. This movement is facilitated by the fluid nature of the lipid bilayer. As a result, the composition of biological membranes can change over time, with new lipids and proteins being added and others being removed.

This dynamic nature is essential for the function of membranes, allowing them to respond to changes in their environment and carry out their various functions. The dynamic nature of biological membranes is also reflected in their asymmetry, with different lipids and proteins being distributed unevenly across the membrane.

Mark Bretscher is the first one to report of the asymmetry in pure lipid bilayer[11]. Figure 1.2 show the asymmetric membrane in human red blood cell. In synthetic pure lipid bilayer, One find the membrane is also asymmetric due to uneven distribution of charges or dipoles on the two mono-layers[5][40].

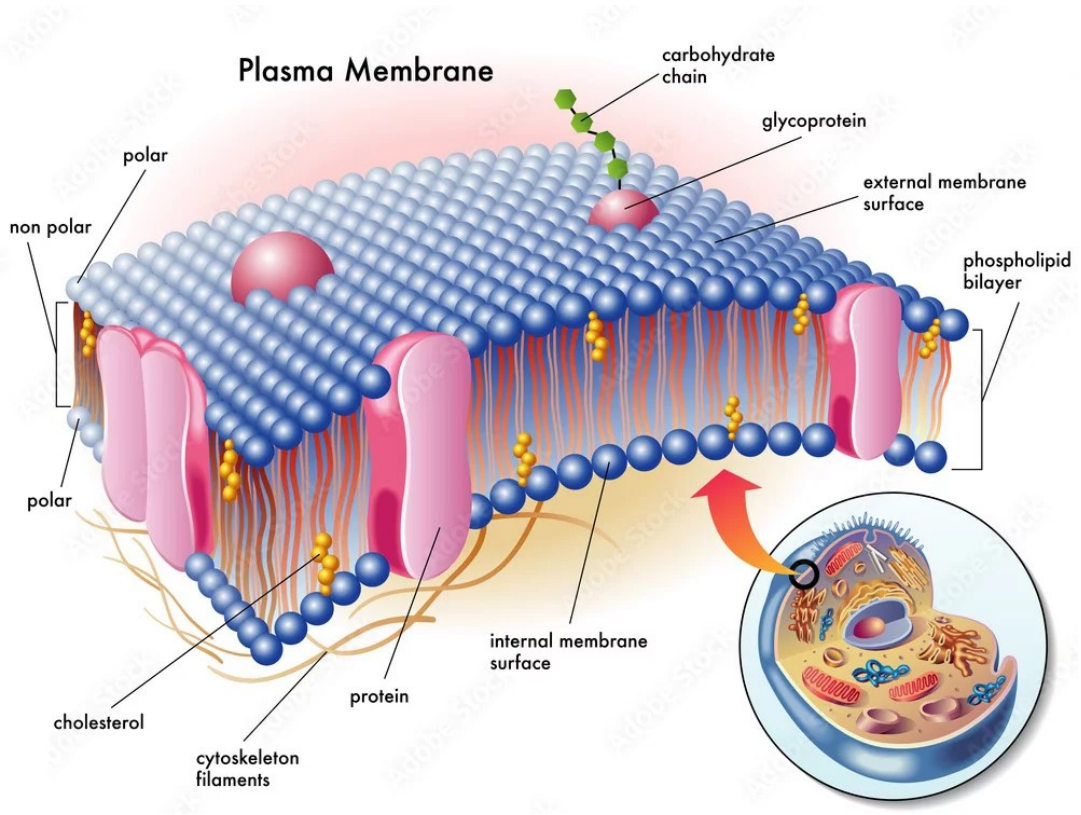

Figure 1.1: The small part of cell membrane from animal cells. The cell membrane is composed of a double layer of phospholipids and encompasses a variety of molecular constituents, such as proteins and cholesterol. Image from newsspace.com.br.

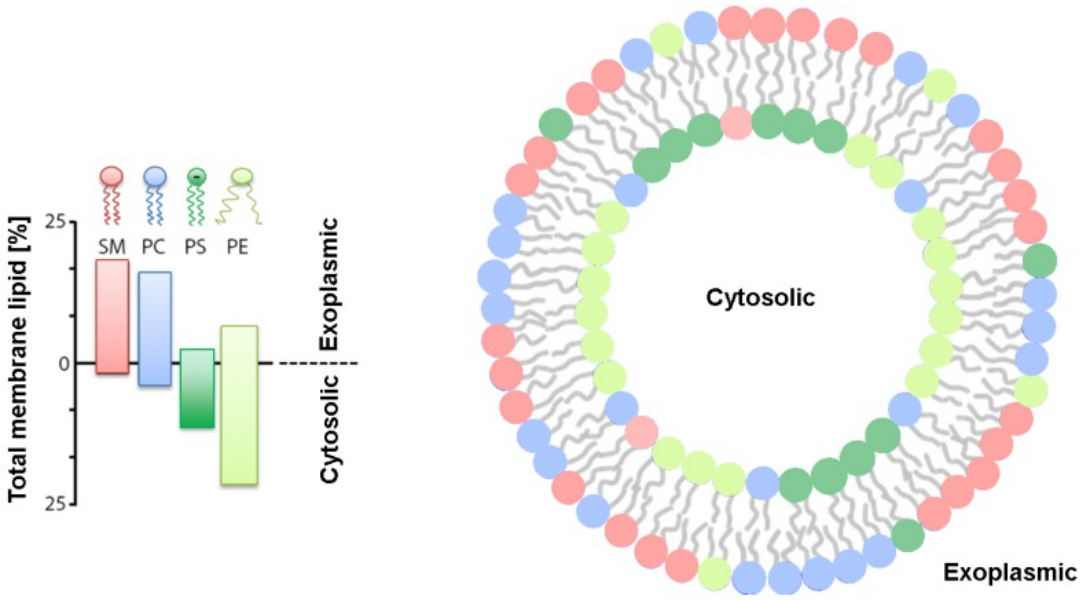

Figure 1.2: The Proposed distribution of phospholipids in human red blood cells put forward by Verkleij et al(1973)[58]. Image from [46]. PE, PS, PC, SM are common abbreviations of phosphatidylethanolamine, phosphatidylserine, phosphatidylcholine, and sphingomyelin.

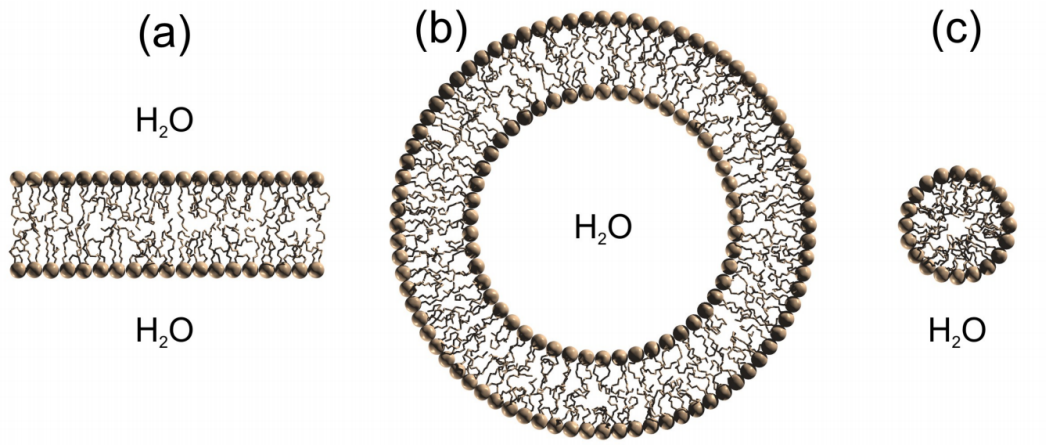

Figure 1.3: Different lipid structures form in water. Image from [6]. (a) Lipid bilayer consists of two layers of amphiphilic molecules arranged in a parallel fashion with their hydrophobic tails facing each other and their hydrophilic heads facing outward. (b) Unilamellar vesicles, also known as liposomes, are spherical structures composed of a single lipid bilayer surrounding an aqueous core. (c) Micelles are formed when amphiphilic molecules are present at concentrations below their critical micelle concentration (CMC).

1.1.2 Lipids

Lipids are a diverse group of biomolecules that play essential roles in various cellular functions. They can be broadly classified into three categories: phospholipids, glycolipids, sterols. Among these lipids, phospholipids are typically the most abundant, accounting for over 50% of all lipids in plasma membranes. In contrast, glycolipids make up only about 2% of the total lipid content, while sterols constitute the remaining percentage[18].

Lipids possess an amphiphilic nature, enabling them to organize into diverse structures when immersed in an aqueous environment. These structures include vesicles, multilamellar/unilamellar liposomes and lipid bilayers. This is illustrated in Figure 1.3, self-assembly lipids in water gives different structure, depending on the lipid concentration, the molecular structure, etc[34].

1.1.3 Melting Phenomenon in Cell Membrane

The melting phenomenon in cell membranes refers to the transition of lipids from a solid-ordered state(S_o, or gel phase) to a liquid-disordered state(L_d, or fluid phase) due to changes in temperature. This transition, also known as the phase transition, occurs at a specific temperature known as the melting temperature(T_m). At temperatures below the T_m, the lipid tails are highly ordered, tightly packed and immobile, while above the T_m, the lipid tails become disordered, more fluid and mobile. The following is a specific example of lipid phase transition.

Figure 1.4 shows phospholipid bilayer undergo a chain-melting transition,where the transition from low to high temperature leads to an elevation in both enthalpy (ΔH) and entropy (ΔS). This temperature shift induces alterations in the chain arrangements, typically causing a reduction in lateral organization. The transition between lipid phases leads to a noticeable alteration in the overall dimensions of the membrane. Specifically, the gel phase exhibits a greater thickness characterized by fully stretched chains, whereas the area is minimized due to the tightly packed head groups. In the case of DPPC(1,2-dipalmitoyl-sn-glycero-3-phosphocholine) bilayer, this transition corresponds to a 25% increase in area and a 16% decrease in thickness from the gel phase to the fluid phase.[26].

For biological membranes these transitions are typically found in the range 10–25 °C. These transitions occur in a wide range of cell types, including bacteria, nerve cells, cancer cells, and even lung surfactant[29][31][34][59]. Interestingly, these transitions below normal body temperature appear to be a common characteristic of most cells[31]. (Thomas and Jacson 2005). Figure 1.5 shows the melting profile of membranes from from the spinal cord of pigs, occurring slightly below their growth temperature. When the temperature exceeds the growth temperature, protein unfolding can be observed, various peaks on the right side related to protein unfolding.[33].(Heimburg and

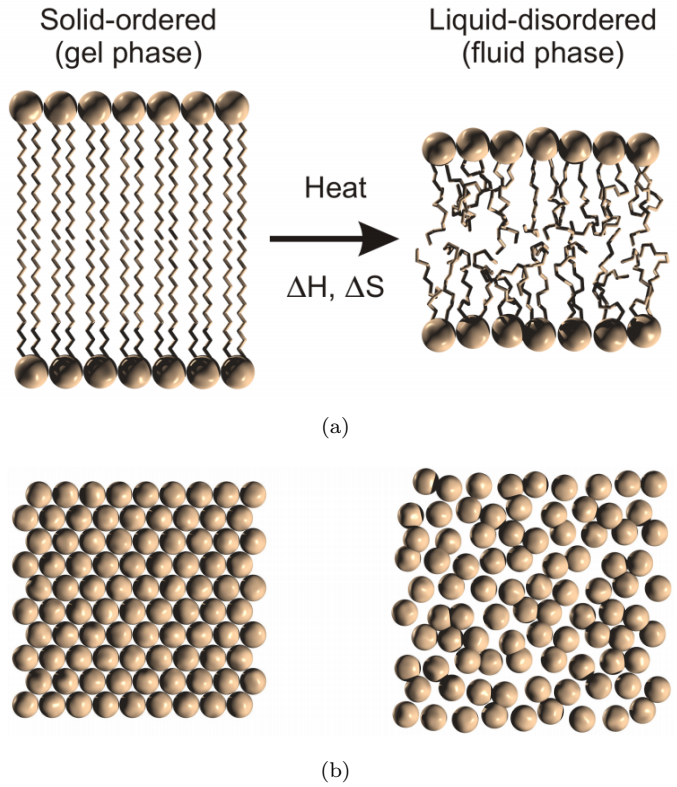

Figure 1.4: Schematic picture of transition of lipids from a solid-ordered to a liquid-disordered phase. During melting process, lipid lost both the order of lipid chain and the order of head group. (a) The loss of order of lipid chains. (b) Lipid head groups lose their crystalline order. Images from [6]

Jackson (2007b))

The melting phenomenon is significant for the function of cell membranes because it affects the fluidity and permeability of the membrane. An increase in temperature above the T_m causes the membrane to become more fluid and permeable, which can affect the stability and function of membrane proteins and the overall integrity of the cell membrane. The melting point can be affected by lipid composition, temperature, hydrostatic and lateral pressure, or ion concentration, pH and the binding or insertion of ligands like proteins or anesthetic drugs[34].

It is worth mentioning that cells have the ability to adapt and regulate the melting phenomenon in order to maintain membrane stability and functionality. For instance, cells can modify the lipid composition of their membranes, thereby altering the melting temperature (T_m), allowing them to adjust to different temperatures[34]. Bacteria, for instance, can increase the proportion of unsaturated fatty acids in their membranes when exposed to lower temperatures, thereby reducing the T_m and preserving membrane fluidity. Figure 1.6 shows the heat capacity profiles of E. coli membranes cultivated at 37 °C and 15 °C exhibit distinct characteristics. The dashed lines indicate the growing temperatures of E.coli. The melting peak of lipids (shown in grey shading area) adjusts according to the growth temperature, while the peaks associated with protein unfolding remain consistent and unaffected.

Membranes lipid melting behavior are also affected by other factors such as pressure. An interesting finding is that bacteria can thrive under elevated pressures exhibited higher quantities of unsaturated fatty acids, indicating that the membrane lipids undergo adaptations to pressures that are relevant to the environment[16]. This indicates that The increase of unsaturated fatty acids is mainly to alter the melting behavior to maintain the stability of cell under changing condition.

The position of transitions of cell membrane also can be affected by anesthetics, pH, neurotransmitters and antibiotics[34][54]. Anesthetics can interaction with membrane by dissolving in and changing the melting behavior of the lipid membrane This effect is well described by melting depression law(see Section 3.2).

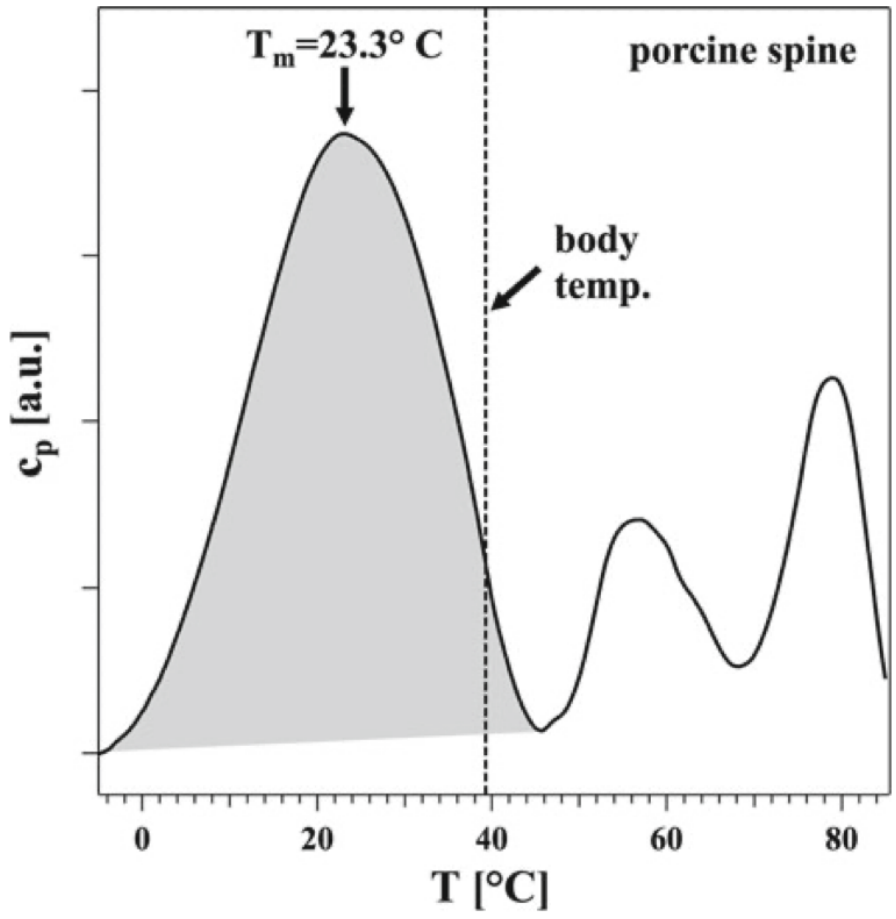

Figure 1.5: Heat capacity profile of membranes from the spinal cord of pigs. The dashed line represents the body temperature of pigs. The phase transition of membrane happened slightly below body temperature(the grey-shaded peak), the peaks above body temperature are related to protein unfolding. Image from [29].

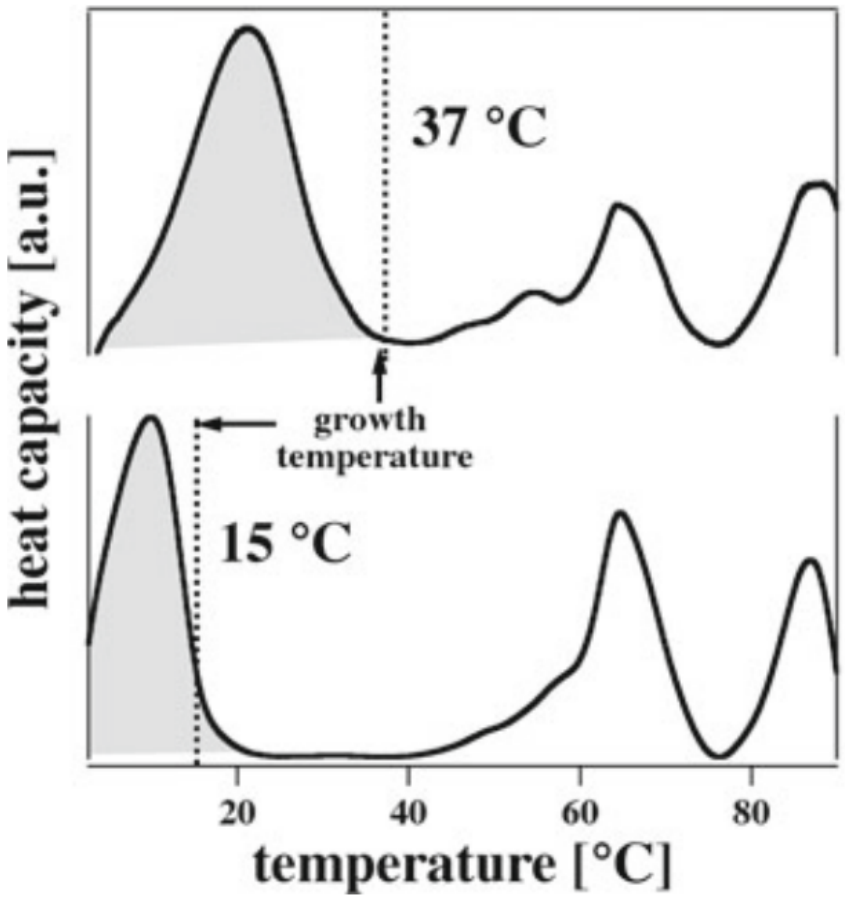

Figure 1.6: Heat capacity profiles of membranes from E.coli growing at two different temperature. The vertical line indicate the cell growing temperature(37 °C and 15 °C). The melting of lipids(the two shaded areas) occurs slightly below the cell's growth temperature in each heat capacity profiles. Above growing temperature, peaks indicate the unfolding of membrane proteins. Image from [34].

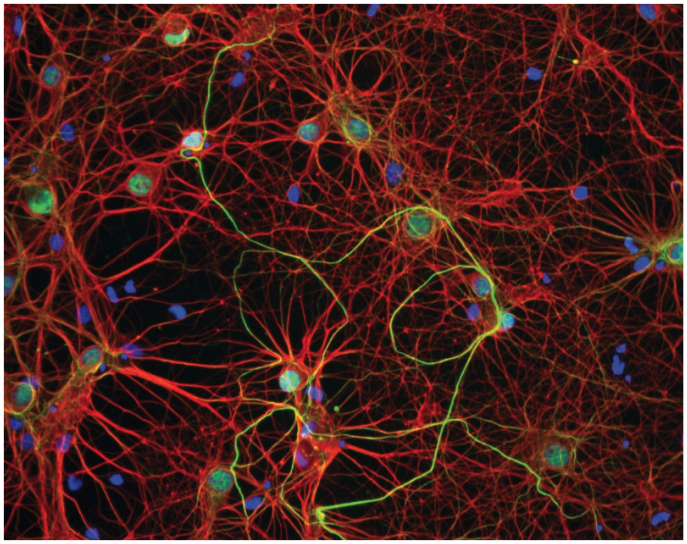

Figure 1.7: A photograph of neurons taken using confocal microscopy. Images from "Introduction to Psychology - 1st Canadian Edition by Jennifer Walinga and Charles Stangor".

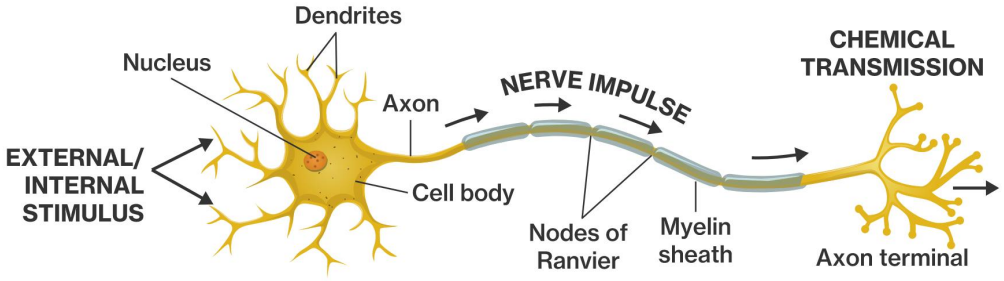

Figure 1.8: A neuron consists of a cell body that contains the nucleus, dendrites, and an axon. When information is received from an external or internal stimulus, it is propagated down the neuron's axon as a nerve impulse and transmitted to another neuron. Image from www.coursehero.com.

1.2 Action Potential in Nerve Cells

1.2.1 Neurons

Neurons(nerve cells) are the remarkable building blocks of the nervous system(Figure 1.7), serving as the essential units for transmitting nerve(electrical) signals and enabling communication within the human body. Neurons can be classified into three types: Sensory neurons, (also known as afferent neurons), motor neurons(efferent neurons), and Interneurons. Beyond these broad categories, neurons exhibit a remarkable diversity in their shapes, sizes, and functions, allowing them to fulfill specialized roles within the nervous system. they also display variations in their physical characteristics[30].

Figure 1.8 shows three primary components of a neuron: the cell body, dendrites, and an axon. The axon serves as the main pathway for transmitting signals away from the neuron's cell body toward other neurons or target. The axon is surrounded by a specialized membrane called the axolemma. To facilitate rapid signal transmission, some axons are enveloped by a myelin sheath — a fatty substance produced by specialized cells.

1.2.2 Action Potential

The primary function of neurons is to transmit and process signals, also known as nerve pulses(action potential) that allow for rapid communication within the nervous system. In text book, these signal is described as electrical signals, known as action potentials, The electrical impulses of nerves can be measured, during a nerve impulse a net change of about 110 milli-volts occurs across the axon's membrane. Nerve impulses are fast:they can travel at a speed of up to 100 meters per second[12]. The basic principle for signal transduction in nerve cells is based on the selective transport of

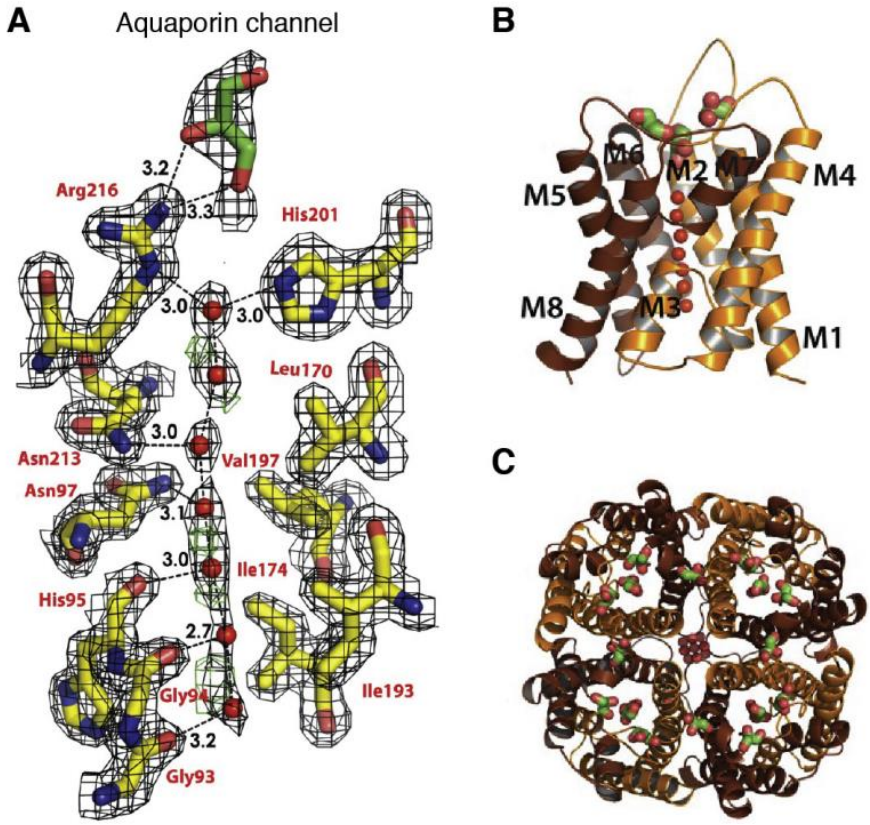

Figure 1.9: The structure of Aquaporin channel(AQP4). A: a line of waters in Aquaporin channel, B: single monomer of AQP4. C: top view of the channel.

the ions(see the Section 1.2.4). It is little know that there is a different way of explaining singles traveling along the neurons,these signals are in soliton form(density wave along with the changes of transmembrane potential) instead of electrical pulses. See Section 1.2.5 for the explanation of signal transduction with the soliton model.

1.2.3 Protein Channels

In textbook, lipid bilayer is thought be impermeable for ions and water. Protein channels are thought to responsible for the transportation of ions and water. The structure of a protein channel basically consists of a pore-forming protein subunit that is composed of multiple transmembrane domains that span the lipid bilayer of the cell membrane[45].

One reported there are over 300 types of ion channels just in the cells of the inner ear[20]. The main ion channels are sodium ion channel and potassium ion channel. Sodium ion channels are integral membrane proteins that are selectively permeable to sodium ions (Na^+), while potassium ion channels are integral membrane proteins that are selectively permeable to potassium ions. It is widely accepted that sodium and potassium channels play a important role during action potential.

The aquaporin channel also reported. Figure 1.9 shows the structure of the aquaporin channel, it act as channels to facilitate the transport of water. While the channel for water transportation is also found in protein free membrane[19].

1.2.4 Hodgkin-Huxley Model

The Hodgkin-Huxley model is a mathematical model that describes the electrical activity of neurons and how action potentials are generated and propagated along their membranes[35]. The model was developed by Alan Hodgkin and Andrew Huxley in 1952 based on the experimental work on the giant axon of the squid by Cole and Curtis in 1939[15]. It describes the behavior of voltage-gated and time dependent ion channels in the neuron's membrane and their role in generating action potentials.

According to Hodgkin-Huxley Model,the action potential is an electric pulses travel along axon membrane. It is initiated and regulated by the complex interplay of ions, particularly sodium (Na^+), potassium (K^+) across the neuron's cell membrane. Before action potential, cell membrane at the resting voltage level(around -70mV[14]), the sodium voltage-gated channels remain closed. However, once the voltage surpasses a specific threshold, these channels rapidly open, allowing a large influx of sodium ions. This influx induces a rapid change in the membrane potential, facilitating the propagation of the action potential.

1.2.5 Soliton Model

In Hodgkin-Huxley Model, They treat membrane as the constant capacitance, and treat the ion channels as resistances. Hodgkin-Huxley (HH) model is dissipative in nature. This is in contrast to the experimental. For example, experimental evidence demonstrates the reversible release and re-uptake of heat during the action potential. Remarkably, the overall heat exchange during the nerve pulse sums up to zero within the precision of the experiments. This finding contradicts a dissipative model based solely on electrical resistors but aligns more closely with the characteristics of an adiabatic wave, such as a sound wave. Furthermore, various experiments have detected mechanical changes occurring alongside the action potential, as evidenced by an increase in nerve thickness and simultaneous shortening[38][23]. These observations indicate the presence of a mechanical pulse accompanying the action potential.

The soliton model is an alternative theoretical framework for explaining the generation and propagation of action potentials in neurons[31]. It was put forth by Heimburg and his colleagues as an alternative to the classical Hodgkin-Huxley Model. According to the soliton model, action potentials are the result of the propagation of soliton-like excitation waves(density wave) in the neuron's membrane. Solitons are self-reinforcing solitary waves that maintain their shape and velocity as they propagate through a medium. In particular, they suggested that the membrane undergoes a phase transition from fluid to gel and back to fluid during the nerve pulse during action potential. Thus, it is an adiabatic process which naturally includes mechanical changes in the membrane.

To be more specify, in the soliton model, the lipid membrane of neurons is considered as a two-dimensional excitable medium. It suggests that action potentials are not primarily driven by the opening and closing of voltage-gated ion channels, as proposed by the Hodgkin-Huxley Model. Instead, the soliton model proposes that changes in the physical properties of the lipid membrane, such as its compressibility and capacitance, play a crucial role in the generation and propagation of action potentials. The model suggests that an external stimulus triggers a local change in the membrane's physical properties, causing a localized compression of the membrane. This compression results in a self-reinforcing excitation wave, or soliton, that propagates along the membrane, similar to a wave traveling through a stretched string[32]. Figure 1.10(bottom) shows the recording of changes of membrane thickness changes due to compression, comparing to the input voltage pulse. These two profiles are surprisingly similar, this indicates the presence of a mechanical pulse during action potential.

The soliton model provides an alternative perspective on the nature of action potentials, emphasizing the physical properties of the membrane rather than the specific dynamics of ion channels. It suggests that modifications in the physical properties of the membrane can significantly influence the propagation of nerve signals within neurons.

1.3 Influence of Anesthetic Drugs on Cell Membrane

1.3.1 Anesthetics

Anesthetics refer to drugs that can cause temporarily lose of consciousness or sensation in parts of the body.According to whether the anesthetics cause the lost of consciousness,anesthetics can be simply divided into two class:general anesthetics and local anesthetics.General anesthetics cause reversibly loss of consciousness while local anesthetics not.

For general anesthetics, approximate categorization of anesthetics has been made, dividing them into three classes: volatile anesthetic gases, alcohols, and intravenous anesthetics. Halothane (2-Bromo-2-chloro-1,1,1-trifluoroethane; BrCH(Cl)CF3) falls into the category of volatile anesthetic gases. Alcohols, including octanol (C_8H_18O), which consists of eight carbon atoms, can also

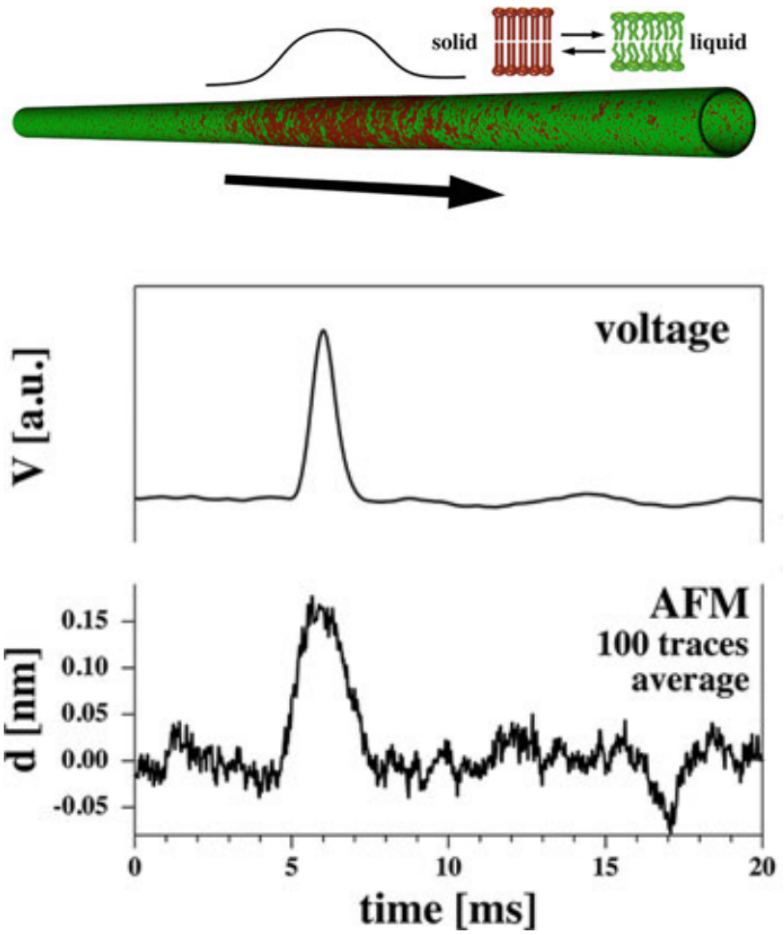

Figure 1.10: The nerve pulse as an electromechanical signal that encompasses phase transitions. Top: A schematic illustration depicts a propagating solitary pulse that involves a transition, represented by the solid phase in red and the liquid phase in green. Bottom: Mechanical pulse (changes in membrane thickness) compare to voltage pulse. Images from [23]

act as anesthetic agents. The last class, intravenous anesthetics such as propofol, etomidate, barbiturates.

1.3.2 Meyer-Overton Correlation

The Meyer-Overton rule emerged from the work of two scientists, Hans Horst Meyer and Charles Ernest Overton. In 1899, Hans Horst Meyer provided the first experimental evidence linking anesthetic potency to lipid solubility. Around the same time, Charles Ernest Overton independently published a similar theory. They independently noticed a striking pattern: the effectiveness of numerous anesthetics appeared to be intimately tied to their ability to dissolve in lipid membranes rather than their affinity[47].

Meyer conducted a study comparing the potency of various anesthetic agents, measured as the reciprocal of the molar concentration required to induce anesthesia in tadpoles, with their olive oil/water partition coefficient. He observed a nearly linear relationship between potency and partition coefficient for different types of anesthetic molecules. Furthermore, he found that the concentration of anesthetic needed to induce anesthesia in 50% of a population of animals (EC50) was independent of the method of administration, whether it was delivered as a gas or in an aqueous phase.

Meyer-Overton correlation held true across a wide range of anesthetics, spanning several orders of magnitude in terms of lipid solubility when olive oil was used as the lipid phase. this rule suggests that the potency and effectiveness of anesthetics are primarily determined by their lipid solubility. It is the ability of anesthetic molecules to dissolve in lipid or fatty tissues that allows them to exert their anesthetic effects, rather than their specific chemical properties.

1.3.3 Hypothesis of the Action of General Anesthetics

Although anesthetics are widely used in surgery, the mechanism of the action of the general anesthesia still unknown. there are variety hypothesis of possible mechanisms of anesthesia[57]. Here we only discuss two possible mechanism.

Protein Hypothesis

Protein hypothesis states that anesthetics work by binding to specific protein ion channels, such as voltage-gated sodium channels or GABA receptors, which are responsible for transmitting signals in the nervous system. By binding to these channels, anesthetics can prevent the normal flow of ions, which disrupts the electrical signaling that is necessary for consciousness and pain perception. One example of how ion channels work to explain the mechanism of anesthetics is the action of general anesthetics on the GABA-A receptor. The GABA-A receptor is a ligand-gated ion channel that is activated by the neurotransmitter gamma-aminobutyric acid (GABA). When GABA binds to the receptor, it causes the channel to open, allowing negatively charged chloride ions (Cl-) to flow into the cell, leading to hyperpolarization of the neuron and inhibition of neurotransmission[50].

General anesthetics, such as propofol, etomidate, and barbiturates, enhance the activity of the GABA-A receptor by increasing the duration and frequency of the channel opening[53]. This leads to a greater influx of chloride ions and an increased inhibitory effect on the neuron, ultimately resulting in the sedative and anesthetic effects of these drugs.

Lipid Hypothesis

While the protein hypothesis provides a compelling explanation for the mechanism of action of anesthetics, it does not fully account for all of the observed effects of these drugs. In particular, the rapid onset and offset of anesthesia observed with some anesthetics is difficult to explain solely in terms of protein binding. This has led some researchers to propose an alternative mechanism of action, also known as the lipid hypothesis. The lipid hypothesis proposes that anesthetics mainly worked by altering the physical properties of cell membranes. The lipid hypothesis suggests that anesthetics dissolve in the lipid bilayer and alter its properties, anesthetics such as halothane and isoflurane are known to alter the fluidity of cell membranes, which can lead to alterations in the activity of ion channels.

Support for the lipid hypothesis comes from a number of studies showing that anesthetics can alter the properties of lipid membranes. For example, Leonenko and Cramb observed changes in the thickness of bilayer in black lipid membranes (BLMs) induced by ethanol, suggesting that the presence of ethanol could trigger lipid phase changes[43]. In one of molecular simulation, the introduction of various volatile anesthetics resulted in significant alterations to the lipid bilayer. These changes included a reduction in lipid order and bilayer thickness, an increase in the overall mobility of lipids laterally, an expansion in the area occupied by each lipid molecule, and a notable decrease in the mechanical rigidity of the membrane[66].

The mechanism of anesthesia is still unknown. based on the soliton model, Heimburg et.al suggests that the action of anesthesia can be explained using the phenomenon called melting depression(see Section 3.2) in the lipid bilayer of cell membranes.

According to melting depression law, anesthesia molecules, such as octanol, interact with the lipid bilayer, leading to a reduction in the phase transition temperature of the membrane. And the soliton model suggests that the lipid bilayer undergoes a phase transition between a gel-like state and a more fluid-like state during the action potential. By modulating the phase transition temperature, anesthetics can alter the fluidity of the lipid bilayer, affecting the conduction properties of cell membrane during neuronal signaling. This proposal provides a thermodynamic explanation for the action of anesthesia, linking the molecular interactions between anesthetics and the lipid bilayer to the observed effects on neuronal activity.

Chapter 2

Lipid Ion Channel

2.1 Channel events in Membrane

Traditionally, the role of ion channels in facilitating ion flow across membranes has been attributed to protein structures. However, recent research has shed light on the intriguing possibility of ion channel activity in protein-free or pure lipid membranes. Many studies have documented remarkable quantized current events observed in pure lipid membranes using techniques such as black lipid membranes or patch pipettes, which closely resemble those observed in biological membranes[8] [1] [2] [39] [3] [61] [64] [21]. Since the channel events happened in protein free membrane is highly resembled the conduction events of protein ion channel . We basically consider the channel-like conduction event observed in pure lipid membranes is attributed to the presence of lipid ion channels. The following explores the fascinating world of lipid ion channels in pure lipid membranes, highlighting key findings and the characteristic of lipid ion channels.

2.1.1 Early Investigations of Channel Events

Patch-Clamp Technique(see Section 4.2.2) developed by Erwin Neher and Bert Sakmann (1976)[49] revolutionized the study of ion channels. This technique allows researchers to directly measure the electrical currents flowing through individual ion channels in cell membranes. (Their work earned them the Nobel Prize in Physiology in 1991). Figure 2.1 shows the current recording from the acetylcholine receptor in fog muscle cell from their paper(1976), they discovered that ion channels can exist in multiple states, opening and closing in response to various stimuli.Through their experiments, Neher and Sakmann elucidated the concept of ion channel gating, which refers to the regulation of channel opening and closing.

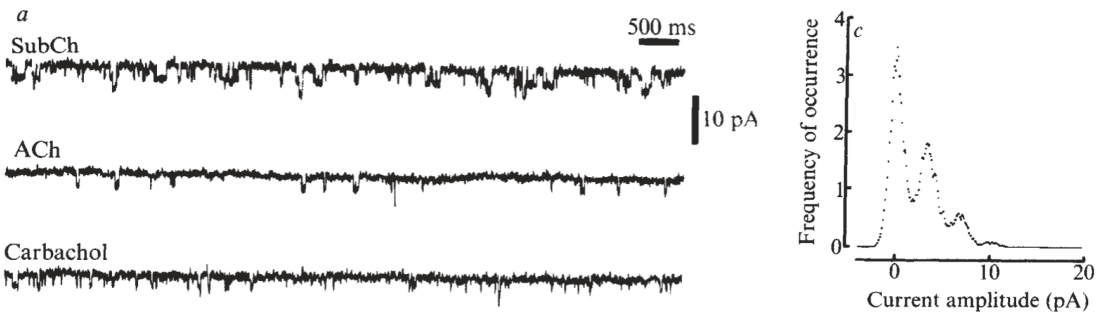

(a) (b)

Figure 2.1: Single-channel current recordings at 8 °C, with membrane potential -120 mV. (a) The channel currents recording with different cholinergic agonists with different concentration. The stochastic feature of current traces can be seen, there are baselines with different frequency of occurrence of deviations from the baseline. (b) Histogram of membrane current,this is the method to analyse stochastic current deviations. Image from[49].

Before this discovery, in 1974 Yafuso et al. published a study documenting spontaneous and multilevel conductance changes in pure lipid membranes[65]. These multistep conductance changes

are believed to be responsible for the formation of channels within the lipid membranes. In 1980, Antonov reported the single ion-channel-likes current recordings in pure lipid membranes of DSPS(Figure 2.2). The step-wise current changing(Figure 2.2 a and b) has been observed in many experiments, which is considered to be the result of lipid channel open and close(reversible formation of these lipid ion channel). Since then, numerous studies have explored the mechanisms and characteristics of pore formation in lipid membranes in the lipid melting regeime.

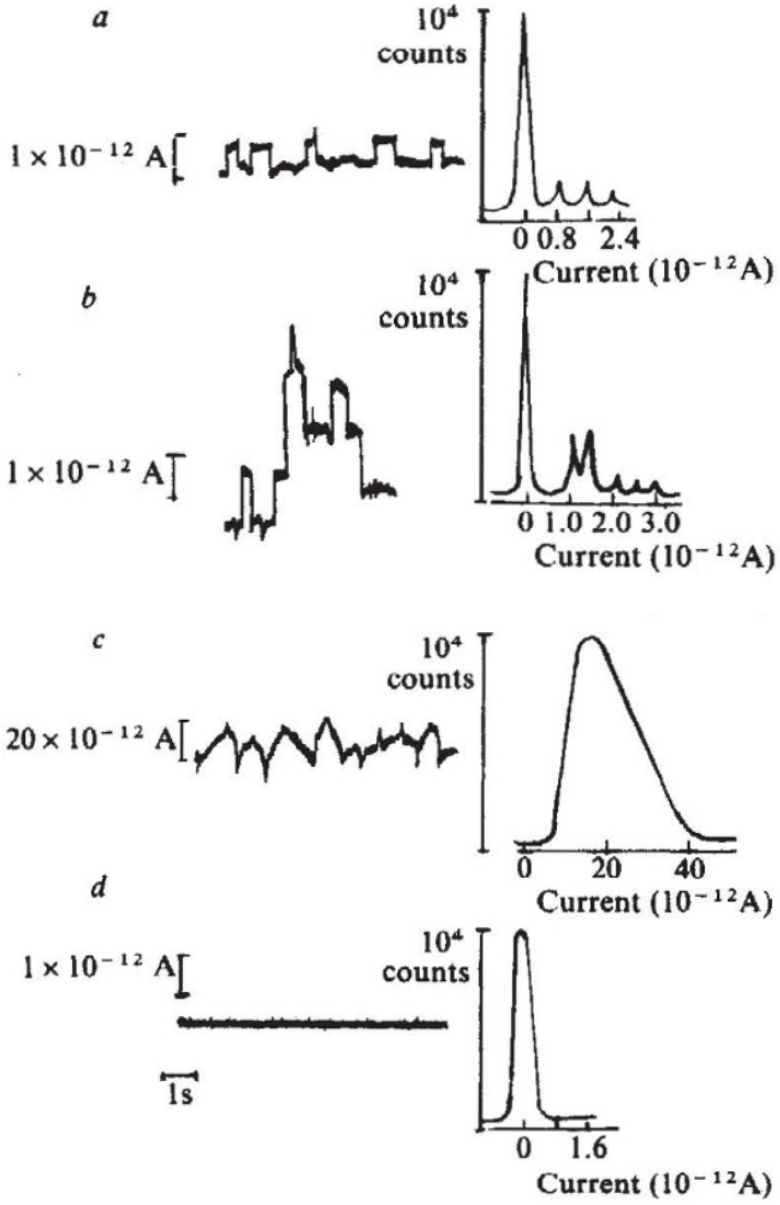

Figure 2.2: First lipid ion channel activity recorded by Antonov. Left: current traces recorded from DSPC membranes at the temperature of 59 °C, which is the melting temperature of the membrane. Right: the current distribution corresponds to each current traces. Image from[1].

2.1.2 Lipid Membrane Permeability Close to Phase Transition

Initially, it was believed that lipid bilayer were only permeable to gases and not to water and ions. However, this notion changes when the lipid membrane approaches its phase transition temperature. Close to the phase transition temperature, lipid membranes become more permeable to various molecules, ions, and even water.

Studies by Pappahadjopoulos et al. (1973)[51], Wu and McConnell (1973)[63], and others have demonstrated that the permeability and conductance of lipid membranes exhibit a pronounced peak at the phase transition temperature. One example from Pappahadjopoulos et al[51]. show

that during the phase transitions of dipalmitoyl phosphatidylglycerol (DPPG) and dipalmitoyl phosphatidylcholine (DPPC), the permeability of sodium ions, as determined using radiolabeled $^{22}Na^{+}$ ions, was observed to increase by a minimum of 100-fold(Figure 2.3 (a)). This is also proved in recent studies, for example, according to Blicher et al.[8], fluorescence correlation spectroscopy measurements revealed that vesicle mixtures containing DPPC and DPPG exhibited a substantial increase in permeability for the positively charged fluorescence marker rhodamine 6G (R6G) during the phase transition. This effect is depicted in Figure 2.3 (b). While the permeation process took several hours in the solid lipid phase, it occurred within a much shorter time frame of approximately 100 seconds or less during the transition regime[8].

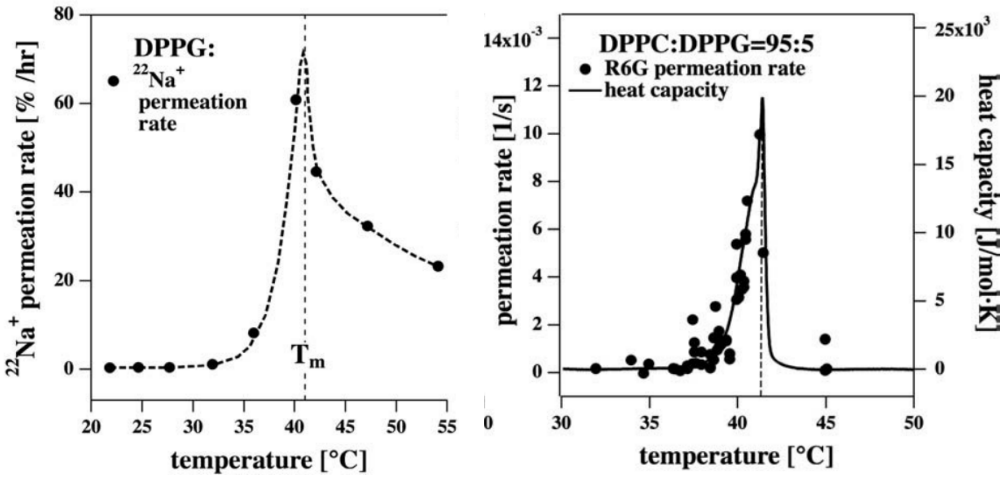

(a) (b)

Figure 2.3: Membrane permeability in pure lipid membrane close to phase transition. The vertical dash lines in both images are corresponding to transition temperature of the membranes. Images from [28]. (a) Permeability rate profile of DPPG vesicles for radioactive sodium, $^{22}Na^{+}$. (b) Permeability rate of DPPC:DPPG=95:5, along with the heat capacity of the membrane.

We can have a sense that the permeability rate is highly related to the melting phase transition. During phase transition, pores can spontaneously formed at low voltage(from 0 mV)[3], this is reasonable because during phase transition there a big fluctuation. Such fluctuations can easily lead to the formation of temporary gaps between the tightly packed lipid molecules and other lipids, resulting in the creation of a transient pore.

2.2 Ion channel Like Behavior of Lipid Pores

Unlike the protein channels, transient pores do not involve specific membrane proteins. The exact mechanism of lipid pore formation is not yet fully understood, but it is thought to involve structural fluctuations or rearrangements of lipid molecules in the membrane. Various factors can influence the formation and stability of these pores, including membrane composition, temperature, pressure, and the presence of other molecules[28].

Glaser et al. proposed pore formation in his paper(1988)[22],which is the most popular mechanism for lipid membrane transportation. In the paper,The formation of hydrophobic pores in the lipid bilayer occurs due to natural fluctuations(Figure 2.4). When these defects reach a size of approximately 0.3 to 0.5 nm, lipid molecules reorient themselves, resulting in the formation of hydrophilic pores. This reorientation process is facilitated by a potential difference existing across the membrane. Hydrophilic pores with an effective radius ranging from 0.6 nm to over 1 nm are generated, leading to the observed increase in membrane conductivity.

Lipid pores exhibit a wide range of conductance values, typically ranging tens or hundreds of picosiemens[42][7]. The conductance is often measured experimentally using techniques such as patch clamping, or single-channel recording. These methods allow researchers to observe and characterize the discrete events of ion conduction through the lipid channels.

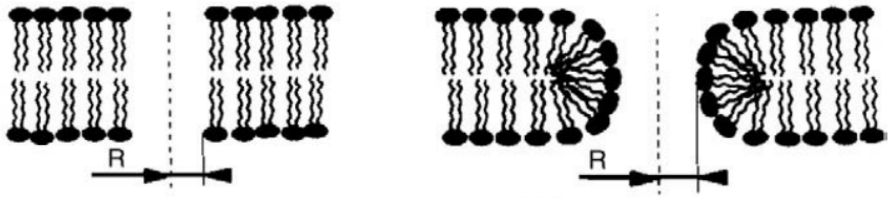

(a) (b)

Figure 2.4: Proposed pore formation in pure lipid membrane. (a) Hydrophobic pore. (b) Hydrophilic pore

2.2.1 Quantized Conductance

Quantized conduction refers to the discrete and stochastic nature of ion movement through these lipid channels. The conductance occurs in discrete steps or events, where the ion flux across the membrane happens in individual packets or bursts. These bursts of ion flow are often attributed to the transient opening and closing of lipid pores.

When the membrane close to phase transition, lipid ion channels spontaneously appear in lipid bilayers, even without additional membrane components. Yafuso et al. (1974)[65], Antonov et al. (1980)[1], and other researchers have associated these fluctuating channels with transient pores formed due to structural changes in the lipid bilayer during the melting transition of phospholipids. One striking finding reported by Antonov et al is that the current change is in quantized manner during the opening and close of lipid pores[1][2][3]. When subjected to a relatively low transmembrane voltage of 100 mV, distinct "channels" exhibiting consistent conductance within the range of picosiemens to nanosiemens were observed to undergo opening and closing. This behavior closely resembles the characteristics observed in ion channel proteins.

2.2.2 Voltage-gated Lipid Ion Channel

Like protein-based voltage-gated channels, the open probability of voltage-gated lipid ion channels also depend on membrane potential. The opening of the channel can be triggered by a change in the voltage across the membrane.[7].

The relationship between voltage and channel opening is typically characterized by a voltage-dependent activation curve. This curve describes the probability or likelihood of channel opening at different voltage levels. It often exhibits a sigmoidal shape, indicating that the channel's response is nonlinear and undergoes cooperative transitions. The open probability $P_{open}(V_m)$ is calculated by the following equation:

$$\begin{aligned} P_{open}(V_m) &= \frac{K(V_m)}{1+K(V_m)} \\ K(V_m) &= exp(-\frac{\Delta G}{kT}) \end{aligned} \tag{2.1}$$

where $K(V_m)$ is the equilibrium constant between open and closed states of a single pore, which can be deduced from the two peak areas in the histogram(Figure 2.5 (a)), From the equilibrium constant one can deduce the free energy difference of the two states(Figure 2.5 (b))[7].

The probability of channel opening is increasing with applied voltage(Figure 2.5(c)), and the relation is nonlinear. Figure 2.5 (d) is the open probability curve of voltage-gated protein channel, we can see they are in same shape.

The properties of lipid ion channels are also influenced by pressure, with the size and frequency of channels increasing as the pressure increases. What's more, the occurrence of lipid ion channels depends on the relevant intensive thermodynamic variables, e.g. temperature, hydrostatic pressure, lateral pressure, voltage, pH, calcium concentration[28].

2.2.3 Comparison of Lipid Ion Channel with Protein Ion Channel

The behavior of lipid ion channel was found to be similar to the protein ion channel decades of year ago[62]. The stepwise conductance change and flickering behavior even the behavior of ion

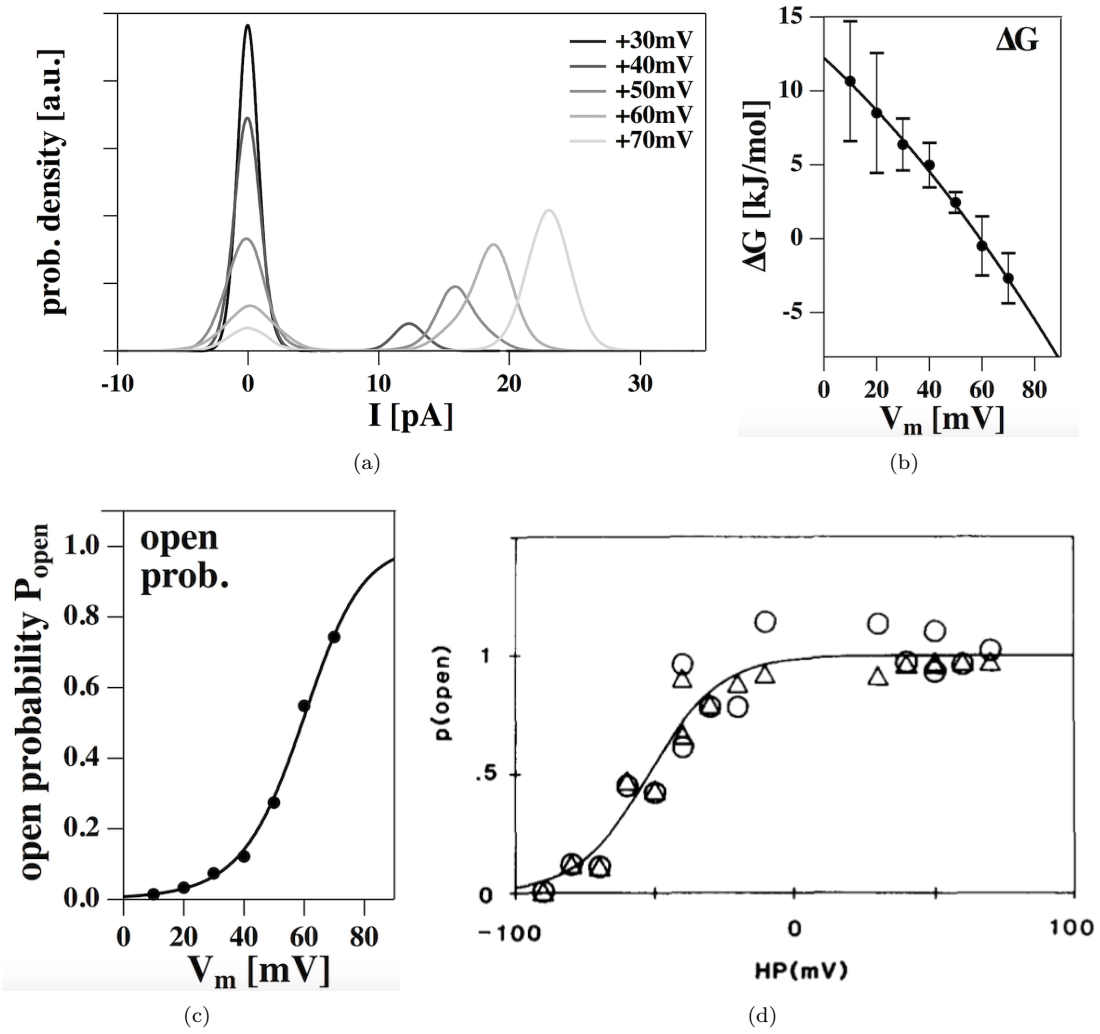

Figure 2.5: Opening probability curves of lipid ion channel and protein ion channel. Images (a)(b)(c) from [7], image (d) from [13]. (a) The probability of open and close of lipid ion channel at different voltages. (b) The calculated free enengy of pores at different voltages. (c) The open probability of lipid ion channel from DMPC:DLPC = 10:1 mol:mol membrane at 30 °C. The open probability shows a transition at the voltage around 60 mV. (d)Open probability of Ca^{2+}-activated K channel with half maximal activation was found to be at the voltage of - 52 mV.

selectivity of the lipid ion channel are repoted[62][3]. More recent paper show the surprising typical current recordings from pure lipid membrane, and it has the same characteristics(unitary current, burst behavior, Flickering, Multistep-conductances, spikes) as protein ion channel[41][61]. The following are the main results from the paper[41]:

Unitary Current

Unitary currents refer to the individual electrical signals produced by a single ion passing through an ion channel. These signals are incredibly small, typically on the order of picoamperes. Figure 2.6 shows the single channel recording of from membrane DMPC:DLPC = 10:1 with current of 3.5 pA, is similar with the recording from protein ion channel.

Burst Behavior

Burst behavior is a pattern of activity in which a group of ion channels open and close together in rapid succession. This behavior can result in a brief surge of ion flow, followed by a period of inactivity. Burst behavior is important because it allows cells to respond quickly to changes in their environment, such as changes in the concentration of a particular ion. Figure 2.7 shows the indistinguishable current activities from lipid ion channel and protein ion channel.

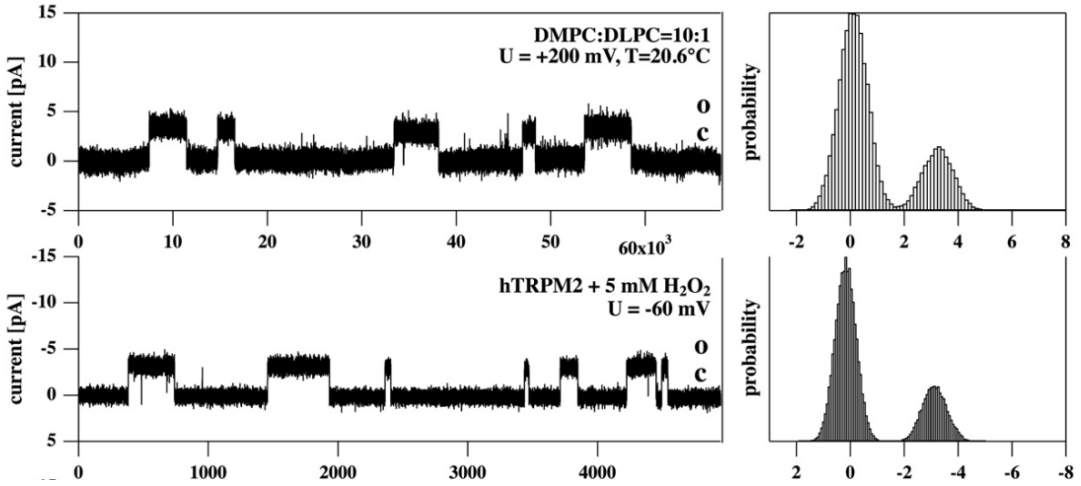

Figure 2.6: Channel events in pure lipid membrane and biological membrane. Top: DMPC:DLPC= 10:1, 150 mM KCl, T= 20.6 °C and U=+200 mV, the current step is about 3.5 pA. Bottom: hTRPM channel activated by H_2O_2 at U= -60 mV, the current step is around 3.5 pA. Images from [41]

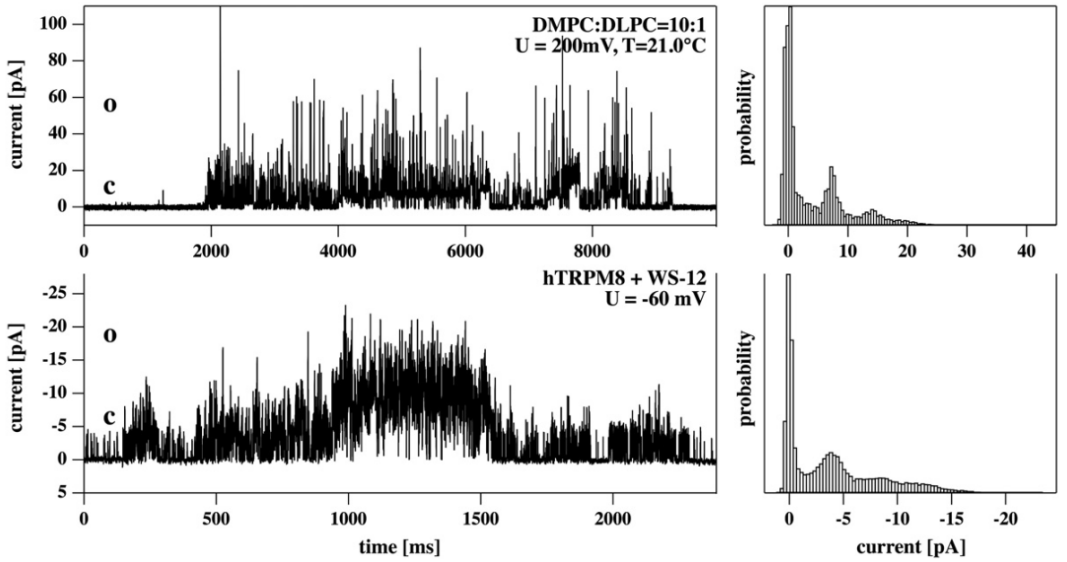

Figure 2.7: Burst behavior in both pure synthetic membranes and cell membranes containing TRP channels, with corresponding current histograms. Top: In the synthetic membrane, the conduction burst lasted approximately 6 seconds. Bottom: In the cell membrane the burst duration was about 2.5 seconds. The conductances of the two preparations were found to be comparable. Images from [41]

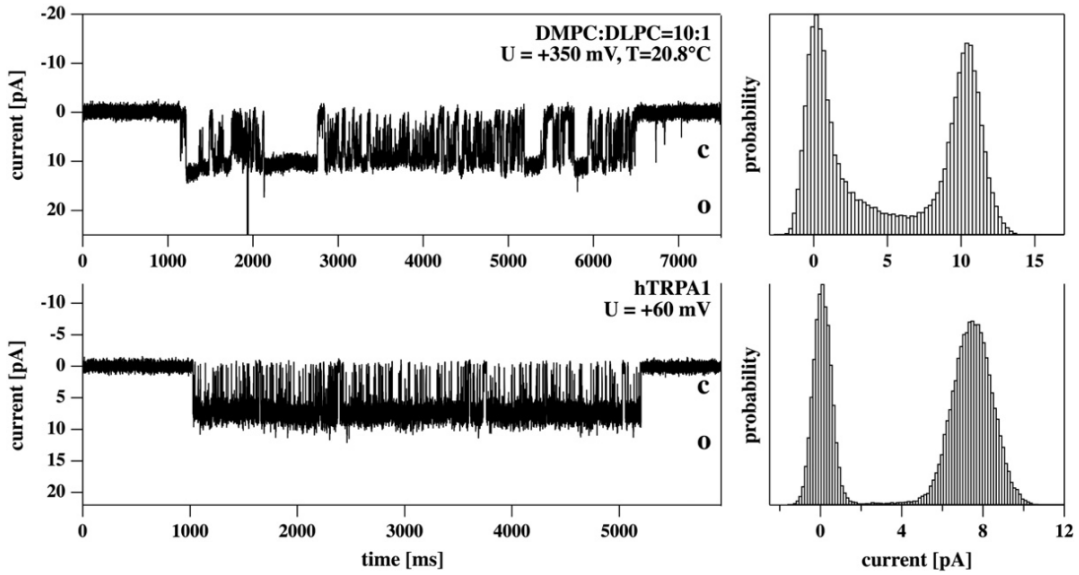

Figure 2.8: Flickering in a synthetic and a cell membrane containing TRP channels. The time scale of these two events are similar. Images from [41]

Flickering

Flickering is a phenomenon in which an ion channel opens and closes rapidly, producing short-lived bursts of ion flow. Flickering behavior is thought to play a role in fine-tuning cellular signaling pathways by allowing small amounts of ions to enter or leave the cell over short periods of time. In Figure 2.8, the flickering are both observed in pure lipid membrane and protein ion channel.

Multistep conductances

Multistep conductances refer to the ability of some ion channels to conduct ions in discrete steps, rather than in a continuous flow. This behavior can result in a staircase-like pattern of ion flow, with each step representing a different conductance level. Multistep-conductances are important because they allow cells to regulate ion flow more precisely, making it easier to maintain proper ion concentrations. Figure 2.9 shows multistep conductance also frequently observed in lipid ion channel in our research.

Spikes

Spikes behavior is a pattern of activity in which ion channels rapidly switch between open and closed states, producing a series of sharp electrical spikes. Spikes behavior is particularly important in neurons, where it is thought to be involved in the generation of action potentials, the electrical signals that allow neurons to communicate with one another. Figure 2.10 shows the similar spikes in the current traces from protein-free membrane and protein ion channel.

These observations indicate that lipid membranes possess channel-like behavior that closely resembles that of protein ion channels. Remarkably, the exact mechanism behind lipid ion channels remains elusive, necessitating further research to comprehensively unravel the underlying processes and mechanisms at play.

2.3 lipid Ion Channel in Molecular Simulations

To gain further insights into the behavior of ion channels in pure lipid membranes, researchers have turned to molecular dynamics simulations. These computational approaches allow for the exploration of the spontaneous formation, stability, and conductive properties of lipidic channels. These simulations provided valuable information on the structural features and dynamics of these channels.

One notable finding from these simulations is the discovery of single-file water pores within lipid bilayers[9]. These transient water wires span the pure lipid membrane, and when a pore forms, the

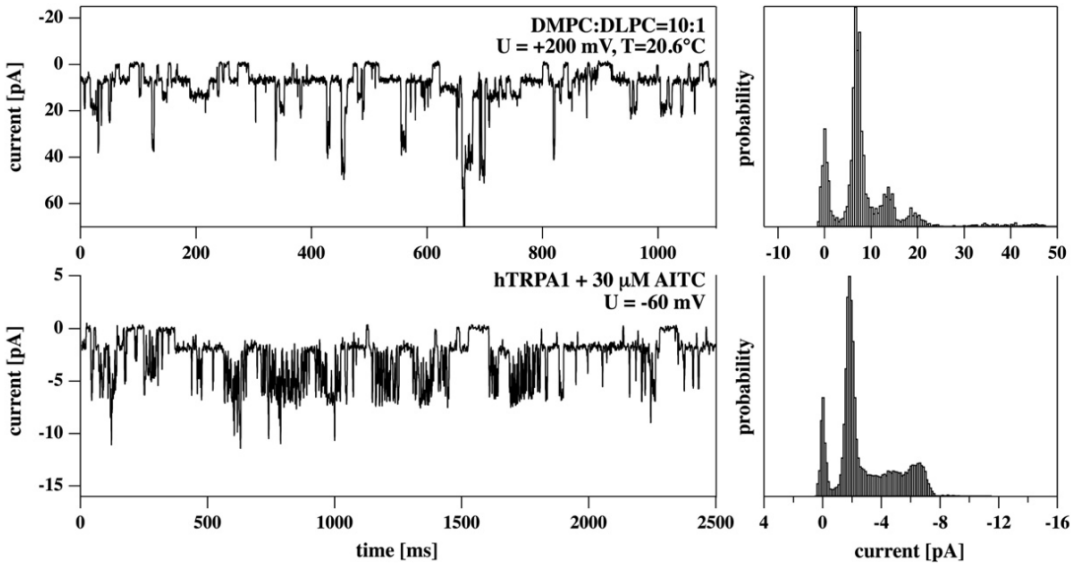

Figure 2.9: Multistep conductance in synthetic membranes and in a TRP channels. Images from [41]

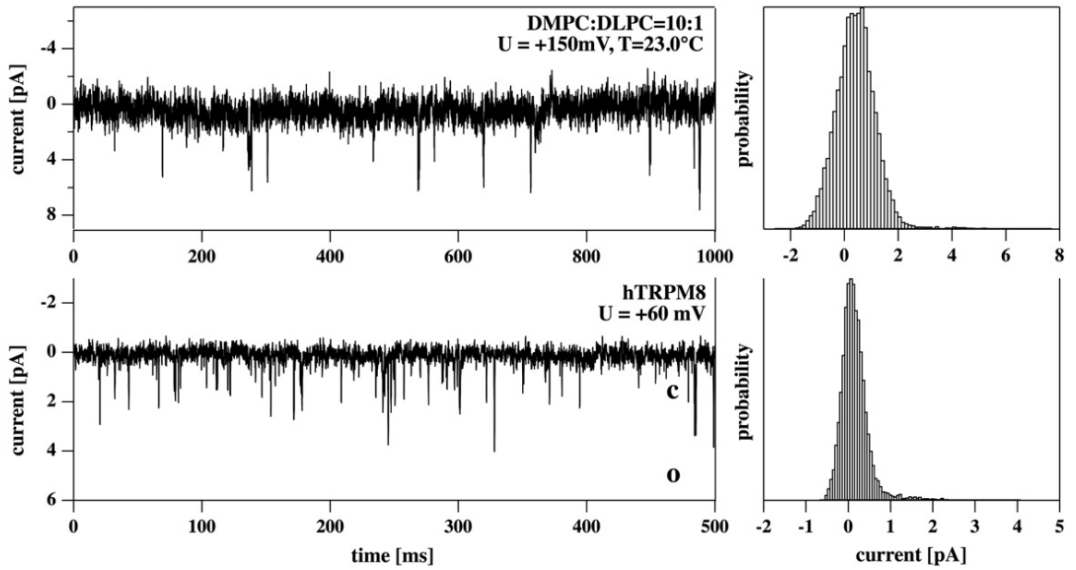

Figure 2.10: Spikes in biological membrane and sythetic membrane. Images from [41]

lipid headgroups reposition themselves towards the pore region. As a result, a hydrophilic pore may emerge, capable of stabilizing water molecules within its structure. This reciprocal stabilization of water molecules contributes to the overall stability of the pore, potentially facilitating the transfer of ions and polar molecules across the membrane. This pore formation process is illustrated in Figure 2.11.

Leontiadou et al. have reported the presence of hourglass-like pores in DPPC membranes (see Figure 2.12)[44]. These pores exhibit stability when their radius is approximately 0.7 nm, which closely aligns with the pore size determined experimentally by Katarzyna, estimated to be 0.75 ± 0.11 nm[60]. This consistency between simulation and experimental results further supports the validity of the observed pore formation.

Another noteworthy simulation study conducted by Hu et al[36]. (Figure 2.13) explored the movement of nona-arginine, a large molecule, freely within lipid pores. The findings revealed that the lipid bilayer can exhibit permeability to such sizable molecules.

These molecular dynamics simulations provide valuable insights into the behavior of ion channels within pure lipid membranes, offering a deeper understanding of their structural characteristics and permeability properties. However, further research is still required to fully elucidate the intricate mechanisms underlying lipidic channel formation and function, and to bridge the gap between simulation and experimental observations.

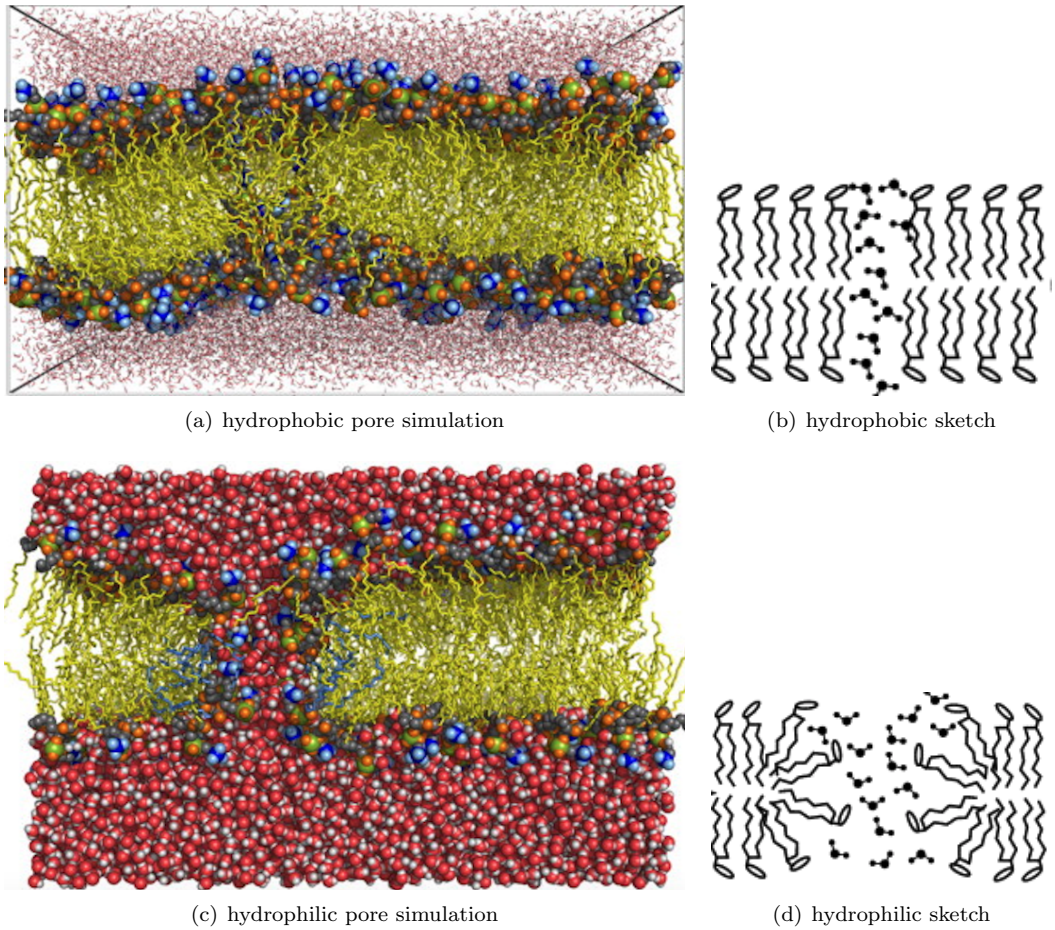

(a) hydrophobic pore simulation

(b) hydrophobic sketch

(c) hydrophilic pore simulation

(d) hydrophilic sketch

Figure 2.11: Membrane pore simulation with POPC. Top: Hydrophobic pore and corresponding lipid arrangement. Bottom: Hydrophilic pore with the schematicl drawing of pore structure. Images from [9]

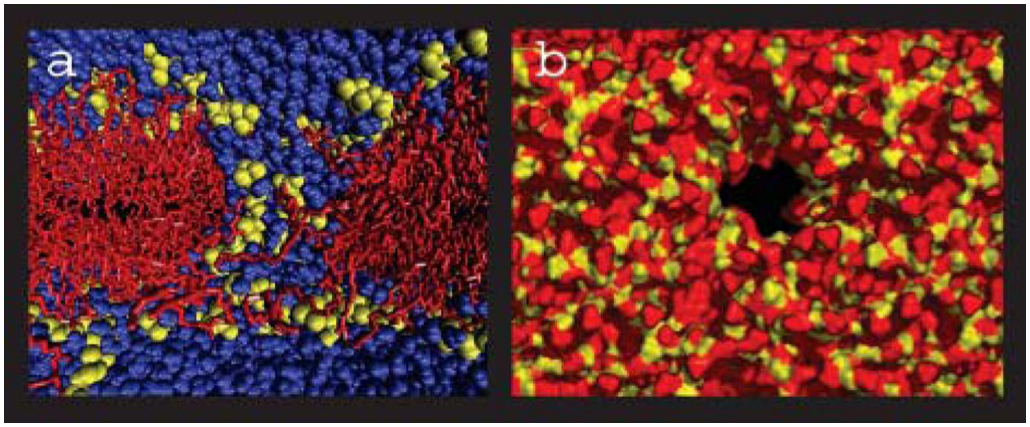

Figure 2.12: Structure of the stabilized hydrophilic pore in DPPC membrane. The lipid headgroups are shown in orange, lipid tails in red, and water molecules in cyan. (a)T he hourglass like pore formation. (b) Top view of the pore. Water molecules are removed from the top view for clarity. Image from [44].

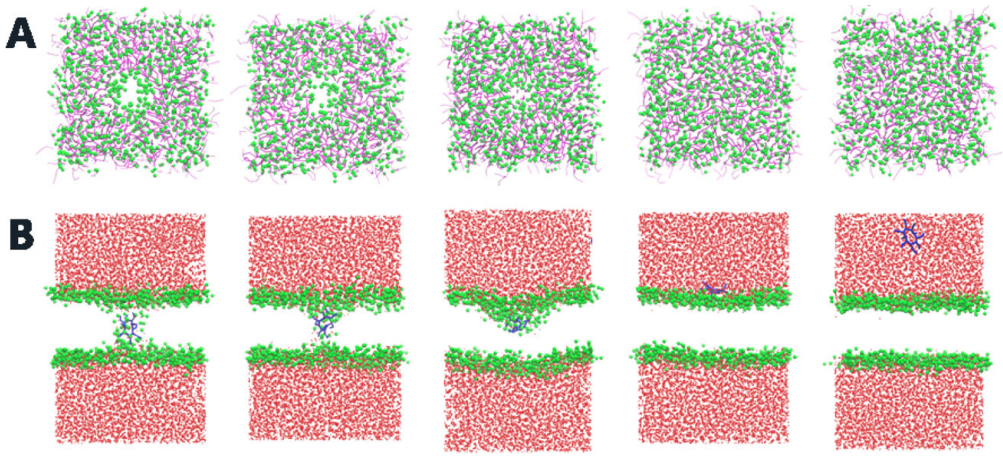

Figure 2.13: Hydrophilic lipid pores in DPPC by umbrella sampling(US) molecular dynamics simulation. (A) The depicted images show a top view of the DPPC system, excluding water, ions, and peptide for clarity. In the images, lipid headgroups are represented by green spheres, while lipid tails are represented by purple lines. (B) The corresponding configurations are displayed in a side view. In this view, lipid tails are not shown, but lipid headgroups are represented by green spheres. The peptide Arg9 is depicted as a blue line, and water and ions are shown as red points. Once the pore is formed, water and ions can move freely into the pore regions. Images from [36].

Chapter 3

Effect of Anesthetics on Lipid Ion Channel

3.1 From Phase Diagrams to Melting Depression Law

3.1.1 Phase Transition and Heat Capacity

The melting temperature(transition temperature), T_m, can be defined as the temperature at which a lipid bilayer undergoes a phase transition from the ordered, gel phase to the disordered, fluid phase.

Assume that the lipid molecule can exist in either a gel phase or a fluid phase during phase transition. Below T_m, most lipids are in the gel phase, where they are tightly packed and have limited mobility. Above T_m, most lipids transition to the fluid phase, where they have increased mobility and are more disordered(Figure 1.4). At T_m, the fraction of gel lipids and the fraction of fluid lipids are equal, and two states are found at the same probability. The free energy difference between the ordered and disordered phases becomes zero at this point. We have:

$$\Delta G = \Delta H - T_m \Delta S = 0 \tag{3.1}$$

$$T_m = \frac{\Delta H}{\Delta S} \tag{3.2}$$

Where ΔH and ΔS are the enthalpy and the entropy difference between the fluid and the gel phase. They can be calculated from the heat capacity profile of the lipid sample.

Figure 3.1 displays the heat capacity of DMPC (1,2-dimyristoyl-sn-glycero-3-phosphocholine), indicating both the pretransition (T_p) and the main transition (T_m). The main transition is the most interested in this research. The main transition is characterized by a distinct peak in the profile, while the pretransition occurs at temperatures lower than T_m. The occurrence of the pretransition is associated with the ripple phase of lipids, which involves the formation of a fluid line defect on one layer of the lipid membrane, resulting in localized bending of the membrane[27]. The main transition temperature of DMPC is known to be around 23-24 degrees Celsius. The transition temperature can vary depending on factors such as changes in lateral pressure, hydrostatic pressure[34], voltage[4], lipid composition (such as the presence of cholesterol), pH[56][10], the ionic environment[56], and the presence of proteins, peptides[37], as well as other substances like anesthetics and neurotransmitters[54].

3.1.2 Lipid Mixtures and Phase Diagrams

Given that biological membranes consist of complex combinations of various lipids, each with its own unique melting temperature and enthalpy, it is expected that their melting behavior would be intricate. The individual lipid species in these mixtures are unlikely to undergo melting independently. Instead, in mixtures, they are influenced by the melting characteristics of neighboring lipids with different chemical properties. Moreover, since these lipids are all dissolved within a matrix, which is the membrane itself, they possess chemical potentials that are closely tied to the concentrations (or molar fractions) of the respective lipids. The chemical potentials of the different

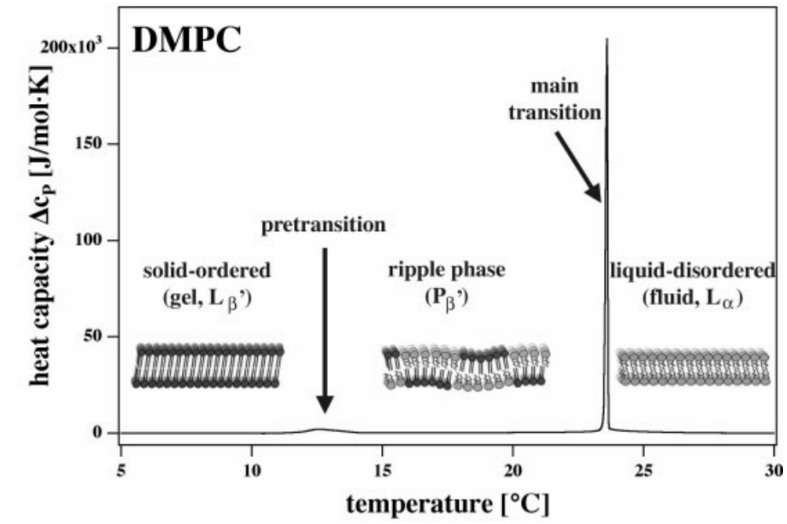

Figure 3.1: Membrane states at different temperature and the corresponding heat capacity.

lipids will vary between the gel and fluid phase. In the following, we will talk about the phase behavior of ideal mixture of two lipid species at the temperature between the their individual transition temperature.

Let's consider a special case, ideal mixture of two lipid species, A and B. Assume that each lipid shall exist in two state: gel state(g) and fluid state(f). And the lipids interact with each other in the same way no matter what lipid species is(the free energy of the interaction between all lipids is the same). Let us say the melting temperature of lipids A is $T_{m,A}$, the melting temperature of lipids B is $T_{m,B}$. In melting regime, The gel and fluid phase of species A and B coexistence. In thermal equilibrium, chemical potential the gel and fluid phase for each lipid species is the same, $\mu^g = \mu^f$. We have

$$\begin{aligned} \mu_A^g &= \mu_A^f \\ \mu_B^g &= \mu_B^f \end{aligned} \tag{3.3}$$

where the index g denotes the gel state, and the index f denotes the fluid state.

Assume the fraction of species A in gel and fluid phase are x_A^g and x_A^f, the fraction of species B in gel and fluid phase are x_B^g and x_B^f. With $x_A^g + x_A^f = 1$, $x_B^g + x_B^f = 1$.

We can write equations according to the definition of chemical potential:

$$\begin{aligned} \mu_A^g &= \mu_{A,0}^g + RT \ln x_A^g \\ \mu_A^f &= \mu_{A,0}^f + RT \ln x_A^f \\ \mu_B^g &= \mu_{B,0}^g + RT \ln x_B^g \\ \mu_B^f &= \mu_{B,0}^f + RT \ln x_B^f \end{aligned} \tag{3.4}$$

It follows:

$$\frac{x_A^f}{x_A^g} = exp(-\frac{\mu_{A,0}^f - \mu_{A,0}^g}{RT}) = exp(-\frac{\Delta H_{A,0}}{R}(\frac{1}{T} - \frac{1}{T_{m,A}})) \equiv e^{-A} \tag{3.5}$$

Where $\Delta\mu_{A,0} = \Delta H_{A,0} - T\Delta S_{A,0}$ and $S_{A,0} = \Delta H_{A,0}/T_m$ has been used in the derivation. And $A = \Delta\mu_{A,0}/RT$.

Similarly, we obtain:

$$\frac{x_B^f}{x_B^g} = exp(-\frac{\mu_{B,0}^f - \mu_{B,0}^g}{RT}) = exp(-\frac{\Delta H_{B,0}}{R}(\frac{1}{T} - \frac{1}{T_{m,B}})) \equiv e^{-B} \tag{3.6}$$

Additionally, one finds:

$$\begin{aligned} x_A^g + x_B^g &= 1 \\ x_A^f + x_B^f &= 1 \end{aligned} \tag{3.7}$$

One obtained the following relations:

$$\begin{aligned} x_A^g &= \frac{e^{-B} - 1}{e^{-B} - e^{-A}} \\ x_B^g &= \frac{e^{-A} - 1}{e^{-A} - e^{-B}} \end{aligned} \tag{3.8}$$

and

$$\begin{aligned} x_A^f &= \frac{e^{-A}(e^{-B} - 1)}{e^{-B} - e^{-A}} \\ x_B^f &= \frac{e^{-B}(e^{-A} - 1)}{e^{-A} - e^{-B}} \end{aligned} \tag{3.9}$$

Where $0 \leq x_A^g, x_B^g, x_A^f, x_B^f \leq 1$.

Furthermore, the amount of lipid mixture in gel phase, x^g, and the amount of lipid mixture in fluid phase, x^f, with $x^g + x^f = 1$ and x_B is the amount of lipid B in the mixture, we can write x_B as:

$$x_B = x^f \cdot x_B^f + x^g \cdot x_B^g = x^f \cdot x_B^f + (1 - x^f) \cdot x_B^g = x^f(x_B^f - x_B^g) + x_B^g \tag{3.10}$$

We finally arrive at lever rule:

$$\begin{aligned} x^f &= \frac{x_B^g - x_B}{x_B^g - x_B^f} \\ x^g &= 1 - x^f \end{aligned} \tag{3.11}$$

The lever rule allows us to calculate the fractions of gel and fluid phase as a function of the fraction of component B and the temperature. In Figure 3.2, The relative amounts of gel phase, x_B^g, and fluid phase, x_B^f for given x_B and temperature obtained from using the lever rule.

3.2 Melting Depression Law

When anesthetics, such as general anesthetics or local anesthetics, interact with lipid membranes, they can alter the physical properties of the membrane. One of the effects observed is the depression of the membrane's melting point, meaning that the phase transition temperature of membrane will shift towards lower temperature when adding anesthetic.

The melting depression law describes the relationship between the decrease in the melting point of a lipid membrane and the concentration of anesthetic present. For a given anesthetic does, we can calculate the shift of melting temperature by equation: $\Delta T_m = (\frac{RT_m{}^2}{\Delta H})x_A$. Where T_m is the melting temperature of lipid(without anesthetics), ΔH is the enthalpy change of lipid membrane(without anesthetics) during phase transition, R is the gas constant($8.314 J/mol \cdot K$), and x_A is the molar fraction of the anesthetics A in lipid membrane.

Figure 3.3 shows the effect of octanol on the phase transition of DPPC vesicles when adding different molar fractions of octanol. The melting depression behavior of membrane can be easily tell from the heat capacity of membranes with different molar fraction of anesthetics. And the calculated heat capacity profiles are consistent with the experiment data. For a given anesthetic dose $x_A = 1 mol\%$ in DPPC membrane will leads to temperature shift of -0.24 °C[33].

3.2.1 The Derivation of Melting Depression Law

Calculating the melting point depression in the case of anesthetics and pure lipid membranes, as proposed by Thomas Heimburg, involves considering the chemical potentials of the lipid membrane in the fluid and gel phase. Here, our derivation is analogous to the calculation of phase diagram of ideal mixture of two lipid species[34]. The following steps outline a general approach to derive the melting depression:

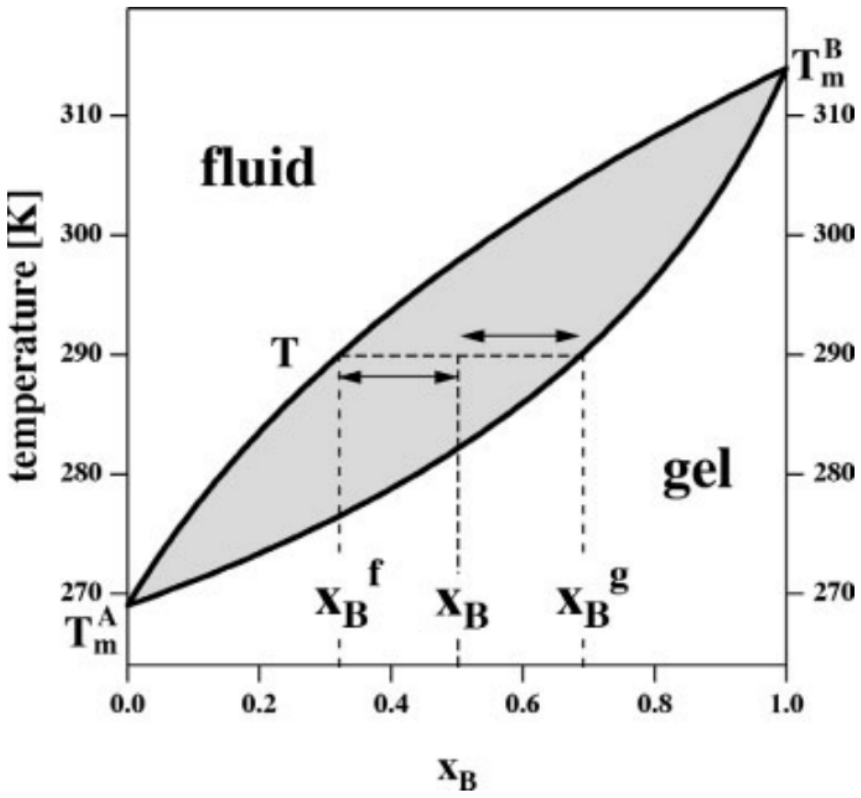

Figure 3.2: Lever rule, for a given x_B and temperature, The relative amounts and the compositions of gel phase, x_B^g, and fluid phase, x_B^f can be read from the curves. Image from [34].

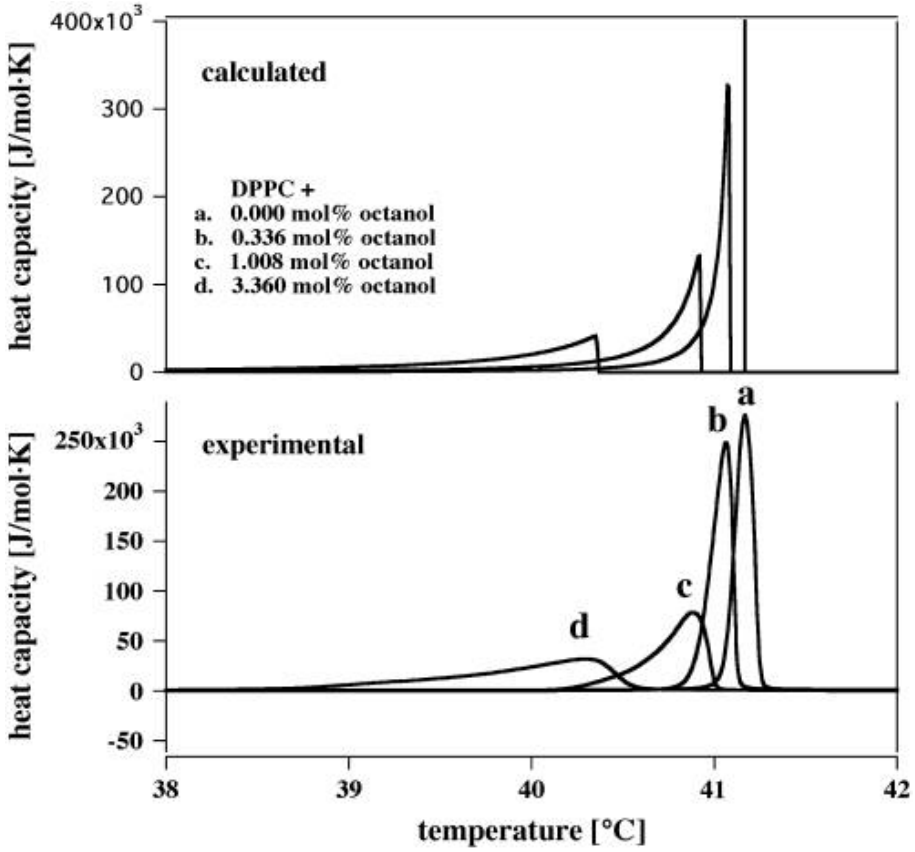

Figure 3.3: Melting point depression law. The heat capacity profile for DPPC membrane with different molar fractions of octanol. Upper: The calculate heat capacity. Bottom: The heat capacity obtain from experiment(DSC).

Let's examine a scenario involving a lipid membrane with a specific melting temperature and an anesthetic molecule A. In this case, molecules A dissolve ideally in the fluid phase of the lipid but not in the gel phase at all.

No anesthetics dissolve in the gel phase of lipid membrane, that means the anesthetics don't interact with the lipid in gel phase. The chemical potential of lipid in gel phase is:

$$\mu_L^g = \mu_{L,0}^g \tag{3.12}$$

All anesthetics dissolve ideally in the fluid phase of lipid membrane,the chemical potential of lipid in fluid phase is:

$$\mu_L^f = \mu_{L,0}^f + RT \ln x_L^f \tag{3.13}$$

Where x_L^f is the molar fraction of the lipid in fluid phase. With $x_L^f + x_A^f = 1$. where x_A^f is the molar fraction the anesthetic drug in fluid phase. What's more,the anesthetics don't have phase transition itself,the molar fraction of anesthetics in fluid phase $x_A^f = x_A$, where x_A is the total molar fraction of anesthetics in lipid membrane

In equilibrium,the chemical potentials of lipid in the two phases are similar,combine equation 3.12 and 3.13, and $\mu_{L,0}^f - \mu_{L,0}^g = \Delta\mu_{L,0} = \Delta H_{L,0} - T\Delta S_{L,0}$; $\Delta S_{L,0} = \Delta H_{L,0}/T_{m,L}$.We have:

$$\ln(x_L^f) = -\frac{\mu_{L,0}^f - \mu_{L,0}^g}{RT} = -\frac{\Delta H_{L,0}}{R}(\frac{1}{T} - \frac{1}{T_{m,L}}) \tag{3.14}$$

With $x_L^f = 1 - x_A^f = 1 - x_A (for T > T_{m,L})$, We obtain

$$\ln(1 - x_A) = -\frac{\Delta H_{L,0}}{R}(\frac{T_{m,L} - T}{T_{m,L}T}) \tag{3.15}$$

If the added amount x_A of the molecule is small and consequently also the shift in melting point, one can write: $\ln(1 - x_A) \approx x_A$ and $T_{m,L}T \approx T_{m,L}^2$,

$$x_A = \frac{\Delta H_{L,0}}{R}(\frac{T_{m,L} - T}{T_{m,L}^2}) \tag{3.16}$$

$$\Delta T_m = T_{m,L} - T = (\frac{RT_{m,L}^2}{\Delta H_{L,0}})x_A \tag{3.17}$$

where $T_{m,L}$ is the melting temperature of lipid, $\Delta H_{L,0}$ is the enthalpy change of lipid membrane during phase tansition, R is the gas constant($8.314 J/mol \cdot K$), and x_A is the molar fraction of the anesthetics A in lipid membrane.

It is worth mentioning that alcohols with a chain length greater than 10 carbons do not exhibit anesthetic properties. It's highly possible that longer-chain alcohols can have their own distinct phase behavior within the cell membrane. Due to their limited solubility in the cell membrane and their tendency to display phase behavior, these longer-chain alcohols do not fulfill the requirements for a molecule to act as an anesthetic[34]. Anesthetics need to effectively dissolve in the cell membrane without exhibiting their own phase behavior according to melting depression law.

3.2.2 the Importance of Melting Depression Law

The melting depression law has been substantiated by other studies[24]. Although this law is derived based on lipid membranes of one species lipid, it provides valuable theoretical guidance for investigating the interaction between anesthetics and lipid bilayer. The addictive effect of anesthetics on cell membranes can also be observed through their impact on the phase transition temperature of lipid membranes. This indicates that the pure lipid bilayer plays a significant role in the interaction with anesthetics in biological membranes.

Moreover, the phase transition of the cell membrane may play a crucial role in signal transport during nerve pulses, as discussed in Section 1.2.5. The melting depression law can explain the effects of anesthetics on action potentials. Additionally, the permeability of lipid membranes is closely related to the heat capacity of the membrane during phase transition (see the next

section). Considering that the phase transition likely has a primary role during action potentials, the contribution of conduction events in the lipid bilayer cannot be neglected.

Understanding how anesthetics exert their effects in protein-free membranes is essential for comprehending their broader impacts on cellular processes and the overall anesthesia response. Through direct interaction with lipid membranes, anesthetics can disrupt the physical and functional properties of these membranes, leading to altered cellular signaling, membrane permeability, and ultimately, the desired anesthetic effects. Further research is ongoing to elucidate the precise mechanisms by which anesthetics interact with protein-free membranes.

3.3 Predictable Anesthetic effect

Based on the principles of the melting depression law, all anesthetics are known to shift the heat capacity profile of a membrane by a consistent and known value. As membrane permeability is closely related to the membrane's heat capacity, it can be anticipated that anesthetics will have a predictable impact on permeability according to heat capacity change. Specifically, when measuring permeability below the melting temperature, the addition of anesthetics is expected to result in an increase in permeability. This is because the melting events are shifted towards the experimental temperatures, promoting phase transitions and the formation of ion channels. Conversely, when conducting the same experiment above the melting temperature, the inclusion of anesthetics is predicted to decrease permeability. This is because the transition events are shifted away from the experimental temperatures, hindering phase transitions and the formation of ion channels. Thus, by considering the change in the membrane's heat capacity, one can anticipate and predict the corresponding changes in permeability induced by anesthetics.

3.3.1 Coupling Compressibilities with Heat Capacity

The membrane undergoes large fluctuations of area, volumn etc. during phase transition. According to fluctuation-dissipation theorem, the heat capacity is given by:

$$C_p = \frac{\langle H^2 \rangle - \langle H \rangle^2}{kT^2} \tag{3.18}$$

This implies that the heat capacity is proportional to the fluctuations in internal energy. This relation can be derive by differentiating the statistical mean of the internal energy. Use equations:

$$\begin{aligned} \langle H \rangle &= \frac{\sum_i H_i exp(-\frac{H_i}{kT})}{Z} \\ Z &= \sum_i exp(-\frac{H_i}{kT}) \end{aligned} \tag{3.19}$$

Where $\langle H \rangle$ is ensemble average of enthalpy, Z is the partition function. The following is the derivation:

$$\begin{aligned} C_p &= \frac{d\langle H \rangle}{dT} \\ &= \frac{d}{dT} \cdot \frac{\sum_i H_i exp(-\frac{H_i}{kT})}{Z} \\ &= \frac{\sum_i H_i^2 exp(-\frac{H_i}{kT})}{kT^2 \cdot Z} - \frac{\sum_i H_i exp(-\frac{H_i}{kT})}{Z} \cdot \frac{\sum_i H_i^2 exp(-\frac{H_i}{kT})}{kT^2 \cdot Z} \\ &= \sum_i \frac{\langle H^2 \rangle - \langle H \rangle^2}{kT^2} \\ &= \frac{\langle H^2 \rangle - \langle H \rangle^2}{kT^2} \end{aligned} \tag{3.20}$$

Similar derivations for volume and area compressibility, we can obtain

The isothermal volume compressibility:

$$\kappa_T^V = \frac{\langle V^2 \rangle - \langle V \rangle^2}{VkT} \tag{3.21}$$

the isothermal area compressibility:

$$\kappa_T^A = \frac{\langle A^2 \rangle - \langle A \rangle^2}{AkT} \tag{3.22}$$

From equation 3.20 and 3.21, we can observe that the isothermal volume compressibility κ_T^V is directly proportional to the fluctuations in volume, and the isothermal area compressibility κ_T^A is directly proportional to the fluctuations in area.

What's more, the temperature dependent volume change $\Delta V(T)$ is proportional to the corresponding change in enthalpy $\Delta H(T)$. And a similar relation is also true for area changes in melting transition of membranes[26][17]:

$$\Delta V(T) = \gamma_V \cdot \Delta H(T) \tag{3.23}$$

$$\Delta A(T) = \gamma_A \cdot \Delta H(T) \tag{3.24}$$

Where $\gamma_V = 7.8 \times 10^{-10} m^3/J$, $\gamma_A = 0.89 m^2/J$. Combine equation 3.20 to equation 3.23, we get:

$$\Delta \kappa_T^V = \frac{{\gamma_V}^2 T}{V} \Delta C_p \tag{3.25}$$

$$\Delta \kappa_T^A = \frac{{\gamma_A}^2 T}{A} \Delta C_p \tag{3.26}$$

This means the isothermal volume and area compressibility are proportional to the heat capacity changes in membrane phase transition. At transition temperature, the heat capacity, the volume and area changes will reach maximum.

3.3.2 Relate Membrane Permeability to phase transition

The opening of lipid ion channel is thought to be responsible for the greatly increased permeability in protein-free membranes at the temperature closed to T_m. While the membrane permeability is related to heat capacity of the lipid membrane during phase transition[8]. To some extent, we would say the conduction of lipid ion channel is closely relate to the heat capacity of the membrane. The following will clarify their relation.

It is believed that the area fluctuations is the main factors to form membranes pores(Lateral compressibility of lipid mono- and bilayers.). We also have derived area change reach maximum during phase transition in Section 3.3.1. Similar to Hooke's law, Nagle and Scott[48] calculated the free energy or the work needed to create a pore of area ΔA with lateral compressibility κ_T^A of the membrane is:

$$\Delta F = \frac{1}{2} \frac{1}{\kappa_T^A A} (\Delta A)^2 \tag{3.27}$$

where A is the total area of the membrane, ΔA is the area of a pore, and κ_T^A is the isothermal area compressibility.

The likelihood to find a pore of size ΔA is

$$P(\Delta A) = P_0 exp(-\frac{\Delta F}{kT}) \tag{3.28}$$

This implies that the likelihood for a pore is depend on $(\Delta A)^2/\kappa_T^A$. it was hypothesized that the permeability of the membrane P is correlated with the size of the defects, allowing for a series expansion of the permeability based on the pore area ΔA.

$$P = P_0 + C_1 \Delta A + C_2 (\Delta A)^2 + ... \tag{3.29}$$

and

$$(\Delta A)^2 \propto \kappa_T^A \tag{3.30}$$

where P_0 is the permeability of membrane without fluctuations. In transition the linear term is neglected[48]. The equation is write into:

$$P = P_0 + C_2(\Delta A)^2 = P_0 + C_2{}'\kappa_T^A \tag{3.31}$$

Combined with equation 3.25 and 3.29, we finally arrived at

$$P = P_0 + \alpha \Delta C_p \tag{3.32}$$

where P_0 and α are constants to be determined from experiment.

This expression provides a straightforward relationship that is directly linked to the heat capacity. Specifically, it indicates that the alteration in permeability is proportionate to the excess heat capacity.

Given the close relationship between membrane permeability and heat capacity, as well as the predictable impact of anesthetics on heat capacity according to the melting depression law, it is possible to predict changes in membrane permeability through analysis of the heat capacity profile. Specifically, when anesthetics are added, the permeability of the membrane is expected to decrease when the membrane temperature exceeds the melting temperature ($T \geq T_m$). The objective of this thesis is to quantitatively measure and analyze the changes in permeability caused by anesthetics in order to provide a comprehensive understanding of this phenomenon.

Chapter 4

Materials and Methods

4.1 Materials and Methods

4.1.1 Materials

- Lipids: 1,2-dimyristoyl-sn-glycero-3-phosphocholine(DMPC),

  1,2-dilauroyl-sn-glycero-3-phosphocholine(DLPC)

  1,2-Dipalmitoyl-sn-Glycero-3-Phosphocholine (DPPC)

  were purchased from Avanti Polar Lipids. and stored at the temperature of -18 °C and used without further purification.

  The calorimeter experiment Group A use a combination of DMPC and DLPC in a ratio of 10:1 (mol:mol) as lipid mixture.Group B is DPPC muti-lamellar vesicles.

  The clamp patch experiments also utilized DMPC:DLPC 10:1 (mol:mol). The same sample as Karis and Andreas. This specific mixture was selected due to its characteristic cooperative phase transition that occurs slightly below room temperature. It was also important to choose a mixture with a transition that is wide enough to allow for accurate measurements within the primary phase transition, without being too narrow and posing significant challenges.
- Electrolyte solution:150mM KCl(FLuka,Switzerland),150mM NaCl(VWR,US) buffered with 50mM TRIS(Sigma Aldrich,Germany) to a final PH of 7.6. In addition, electrolyte solutions were passed through a sterile 0.2 µm filter (Minisart Sartorius Stedim Biotech, Germany) to eliminate any dust particles or impurities.
- Organic solvents: hexane and ethanol chloroform
- Anesthetics:1-Octanol, Octanol-D18 were used in the calorimeter scan Group B by accident.
- The water utilized in the experiments underwent purification via a Direct-Q R Water Purification System (Merck Millipore, Germany) and possessed a resistivity greater than 18.1 MΩ·cm.

4.1.2 sample preparation

Stock solutions

- Stock solution 1 was prepared by dissolving the DMPC lipids powder in chloroform to a final concentration of 10mM and stock in the refrigerator.
- Stock solution 2 was prepared by dissolving the DLPC lipids powder in chloroform to a final concentration of 10mM and stock in the refrigerator
- Electrolyte solution:150mM KCl,150mM NaCl buffered with 50mM TRIS, use NaOH OR Hcl adjust the PH to 7.6.
- Stock solution 3 was prepared by mixing octanol in chloroform to a concentration of 10mM.

Sample for Calorimetry Experiment

Group A

- step 1: Add 10mM DMPC in chloroform(stock solution 1) into 5 glass bottles by transferpettor,the solution in each bottle is 1mL.
- step 2: Add 10mM DLPC in chloroform(stock solution 2)into each bottles.each bottle include 0.1mL stock solution 2.
- step 3: Add 55μL, 110μL, 165μL, 220μL octanol in chloroform(stock solution 3) into second,third,forth,fifth bottles.
- step 4: Drying them under a gental stream of air,then putting them under vacuum more than 3 hours.
- step 5: The dried sample mixtures were resuspended in electrolyte solution to a final concentration of 10mM

Group B

- step 1: Dissolving DPPC lipids powder in chloroform to a final concentration of 10mM
- step 2: Mixing octanol in chloroform to a concentration of 10mM.
- step 3: Add DPPC in chloroform into 5 bottles.each bottle 1mL.
- step 4: Add 20μL, 40μL, 60μL,100μL octanol in chloroform to into second,third,forth,fifth bottles.
- step 5: Drying them under a gental stream of air,then putting them under vacuum more than 3 hours.
- step 6: The dried sample mixtures were resuspended in water to a final concentration of 10mM

Pippete patch clamp experiment

- step 1: Add 10mM DMPC in chloroform(stock solution 1) into 5 glass bottles by transferpettor,the solution in each bottle is 0.1mL.
- step 2: Add 10mM DLPC in chloroform(stock solution 2)into each bottles.each bottle include 0.01mL stock solution 2.
- step 3: Add 5.5μL, 11μL, 16.5μL, 22μL octanol in chloroform(stock solution 3) into second,third,forth,fifth bottles.
- step 4: Drying them under a gental stream of air,then putting them under vacuum more than 3 hours.
- The dried sample mixtures were resuspended in the a mixture 4:1 (vol:vol) of hexane and ethanol to a final concentration 2mM. note:since hexane and ethanol is highly volatile,the samples are stored in vials(the volume of the container is smaller than 2mL),and store the samples in a fridge.The concentration of samples should not change too much.Only suspend the sample mixtures in hexane:ethanol=4:1 before experiment,and used it for a maximum of one week.This is one of the keys to form similar lipid bilayer in patch clamp experiment.

4.2 Methods

4.2.1 Differential Scanning Calorimetry(DSC)

Differential scanning Calorimetry is a thermal analysis technique used to measure the heat capacity of a substrate. It works by comparing the heat absorbed or released by a sample to that of a reference material as a function of temperature.

One of the main types of DSC is Power Compensating DSC, which is used in this research(The calorimeter used in this research is VP-DSC,produced by MicroCal). The setup of calorimeter is shown in Figure 4.1, there are two cells in a adiabatic box. The sample is placed in the left cell and the reference material in the right. Both cells will be heated by two separate heaters. A temperature programe is designed to maintain both sample and reference at the same temperature and guarantee

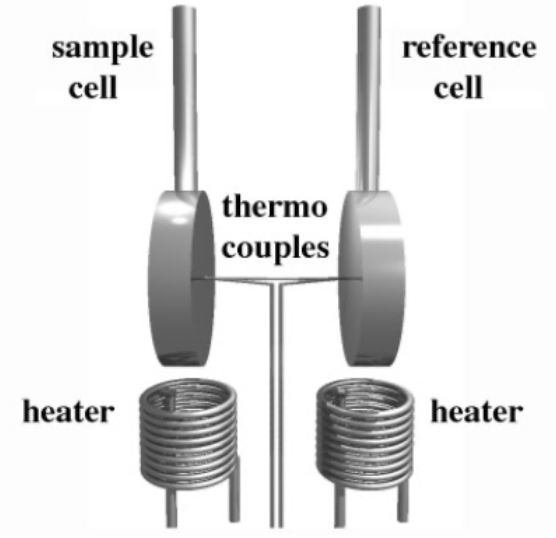

Figure 4.1: Schematic drawing of a calorimeter. The instrument used consisting of a sample and reference cell that are both subjected to a constant rate of heating. The energy required to sustain this heating rate for both cells is measured, and the heat capacity is determined by dividing this energy by the scanning rate. Image from [34]

linear temperature change of them. In a certain up scan of the calorimeter, for example the sample is 5mM DPPC in water,the reference material is water, the excess heat absorbed by sample can be calculate from the difference power supply ΔP of the two cells, by integrating ΔP over time:

$$\Delta Q = \int_{t}^{t+\Delta t} \Delta P(t)\, dt = \Delta P \cdot \Delta t \tag{4.1}$$

The excess heat capacity can be derived:

$$\Delta c_p = (\frac{dQ}{dT})_P = (\frac{\Delta Q}{dT})_P = \frac{\Delta P}{\Delta T/\Delta t} \tag{4.2}$$

From the heat capacity profile, the melting enthalpy and entropy can be obtained by simple integration according to:

$$\Delta H_0 = \int_{T_g}^{T_f} \Delta c_p dT \tag{4.3}$$

In our research, the obtained melting enthalpy is used in the calculation of melting depression law.

4.2.2 Patch Clamp with Droplet Technique

The patch clamp experiment is a widely used electrophysiological technique that allows for the measurement of the electrical activity of individual ion channels or neurons. Sakmann and Neher were awarded the Nobel Prize in 1991 for their development of the patch clamp technique. This technique enables the observation and study of the localized and coordinated opening and closing of ion channels. Figure 4.2 shows the a example result of single ion channel current recording using patch clamp technique, the corresponding current of channel open and close is clear.

The lipid bilayer membranes can be formed on the tip of a patch-clamp glass pipette that is filled with electrolyte solution using the droplet method[25]. To do this, lipids are dissolved in a volatile organic solvent (hexane : ethanol = 4:1(v:v)) and brought into contact with the outer surface of the glass pipette. As the solution flows down the pipette, a membrane spontaneously forms at the tip of the pipette as shown in Figure 4.3(a). The solvent is then allowed to evaporate for at least 30 seconds before the experiment. This method offers several advantages such as practically solvent-free membranes, greater mechanical and electrical stability. Figure 4.3 (b) shows the schematics drawing of lipid bilayer formed on the surface of electrolyte solution.

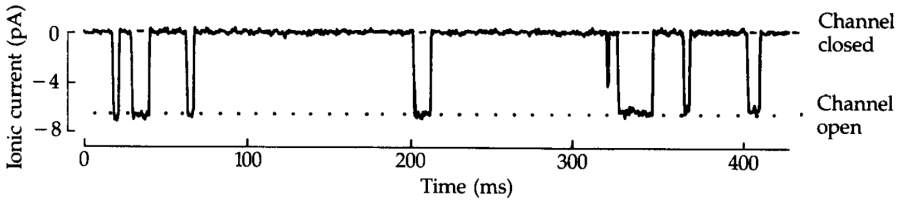

Figure 4.2: Typical patch clamp current trace of a single channel protein, the relative low current corresponds to close state of the channel, the relative high value corresponds to the open state of the channel. Image from [30].

To create the pipettes, borosilicate glass capillaries (1B150F-3, World Precision Instruments, USA) with an outer diameter of 1.0mm and an inner diameter of 0.8mm were pulled using a vertical PC-10 puller. The pulling procedure was a two-step process. The first pull was set to 80% of the instrument's maximum output and produced an 8mm pull. For the second pull, the heating coil was lowered 4mm and the heater setting was reduced to 45%. The pipettes produced were similar to AndreaS[6], which was designed to have a broad and thick-walled structure throughout to minimize both access resistance and pipette capacitance.

Once the glass tip is pulled, it is not initially open, and heat is required to remove the tip. In Figure 4.4 (a), the heated glass on the right side generates the necessary heat. To achieve the desired opening, the pipette tip is brought into contact with the heated bead for approximately 2 seconds. Subsequently, the pipette is fire polished to create a smoother opening, resulting in an opening of approximately $10\mu m$(Figure 4.4(b)). The entire process is performed using a Narishige MF-900 Microforge.

Care was taken to avoid trapping air bubbles in the tip while filling the pipettes with electrolyte solution. In order to avoid any overflow into the pipette holder, the pipettes were filled to a maximum of two-thirds of their total length. It is important to note that overfilling can lead to additional background noise. The electrodes used were made of high-purity, chlorinated silver wires. These wires were frequently re-chlorinated to prevent baseline drift and additional noise[52].

The primary setup, as displayed in Figure 4.5, consisted of a glass beaker containing an electrolyte solution, which was situated in heater jacket, the glass beaker could be heated or cooled using water circulation (Haake DC30-K10, Biolab). Temperature measurements were taken using a thermo-couple (NiCr-Ni, type K) and an in-house-built amplifier that produced an analog output. This output could be linked to the 12-bit analog/digital converter (DigiData 1200B, Axon Instruments Inc.), which digitised signals from the Axopatch 200B patch clamp amplifier (Axon Instruments Inc., Union City/CA, USA). The pipette with electrodes were were fixed in the pipette holder and placed on a capacitor feedback integrating headstage amplifier (Headstage CV 203BU, Axon Instruments Inc.). The headstage was attached to a micro-manipulator (model SM1, Luigs and Neumann, Germany), which allowed for precise manipulation of the pipette's position in relation to the bath surface. Finally, the headstage and micro-manipulators were wrapped in a fine-meshed metal cloth that acted as a Faraday cage. It is crucial to establish a connection between the headstage and the electrolyte solution using the reference electrode to maintain a stable baseline throughout the recording process.

The experimental data was acquired using Clampex 9.2 software (Axon Instruments) and recorded in Whole Cell mode with a headstage gain of $\beta = 1$ in voltage clamp configuration. The data acquisition was performed at a sampling frequency of either 10kHz or 20kHz and the signal was filtered using a 4-pole lowpass Bessel filter with a cut-off frequency of 2kHz and an attenuation of 80dB/decade above the cut-off frequency. The output gain,α, was carefully adjusted to avoid signal clipping and ensure linear amplification. In most cases, an output gain of $\times 50$ was used. Increasing the output gain did not significantly improve the signal-to-noise ratio. All data analysis was carried out using IGOR Pro 6.21 (WaveMetrics, USA) and custom-written(Andreas Blicher) routines.

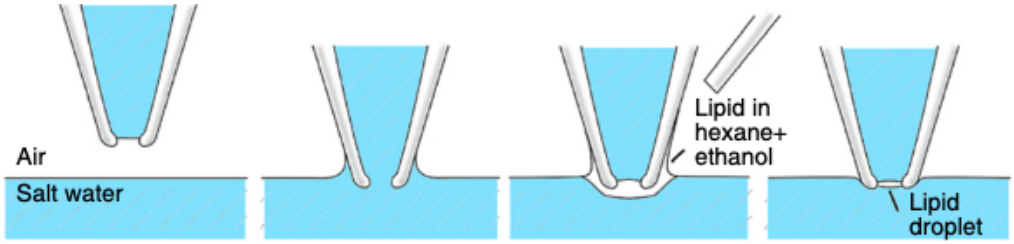

(a) droplet technique

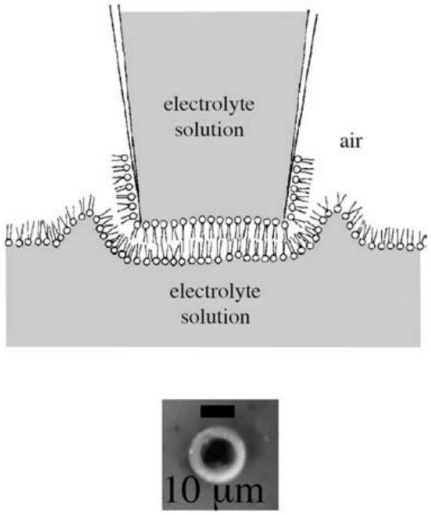

(b) lipid bilayer

Figure 4.3: Patch clamp experiment. (a) Schematics drawings of the droplet technique. Image from [5]. (b) Schematics drawing of lipid bilayer formed on the surface of electrolyte solution, the bottom show the diameter of the pipette tip in our experiments. Images taken from [28].

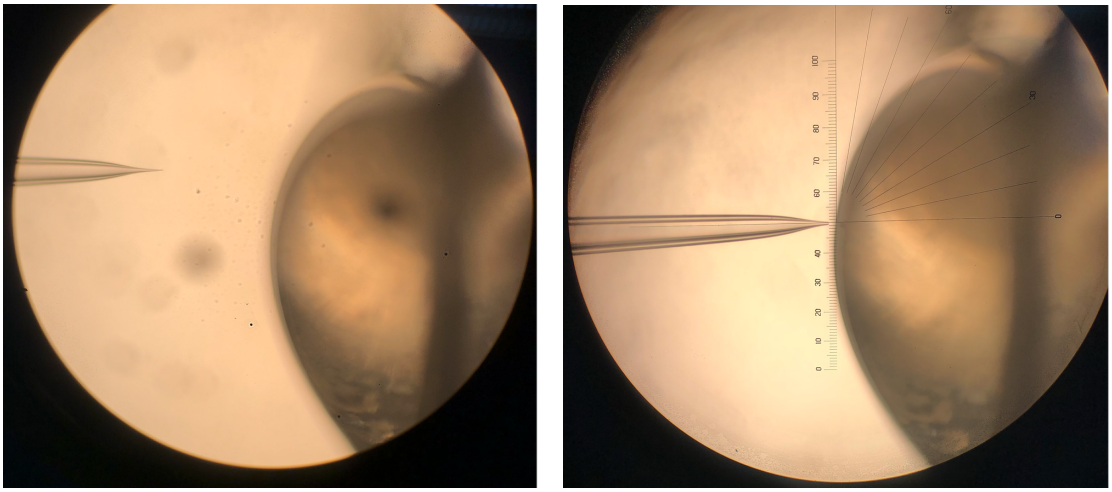

(a) before (b) after

Figure 4.4: Micro pipette creation.(a) Left side: the micro pipette with sealed tip produced by pulling glass capillaries into two parts. Right side: the glass bead used to open the tip of micro pipette when it is heating. (b) Left side: the pipette with open tip with diameter of 10 μm, Right side: the same glass bead used to polish the pipette tip, making the rim of pipette opening more smooth.

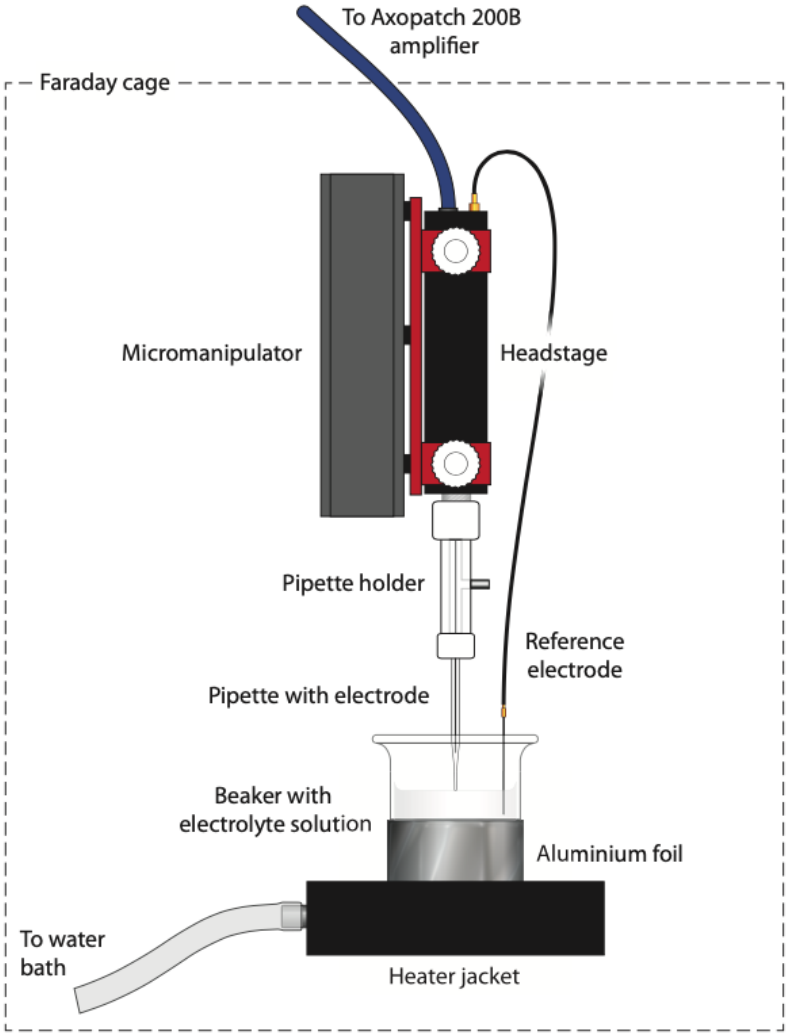

Figure 4.5: The set up of patch clamp experiment, picture from [6].

Chapter 5

Results

5.1 The Result of DSC Experiment

Based on the melting point depression law, when anesthetics are introduced to the membrane, there is a consistent decrease in the membrane's melting temperature, What's more, for given does of anesthetic, the degree of temperature shift can be calculate with the melting temperature and enthalpy change during the phase transition. It is assumed that the anesthetics themselves do not undergo any melting behavior. Moreover, it is desirable for the anesthetics to ideally mix with the fluid phase of the membrane while remaining separate from the gel phase. The experiments of DSC is mainly to determine the melting point depression law in pure lipid membrane. According to equation 3.16, the transition temperature shift is directly proportional to the molar fraction of anesthetic in the membrane when adding anesthetics into membrane:

$$\Delta T_m \propto x_A \tag{5.1}$$

Here we assume T_m is always shift to lower temperature. x_A is the molar fraction of anesthetics in lipid. This also implies that the effect of anesthetics is addictive.

5.1.1 Melting Depression Law in One Species Lipid Membrane

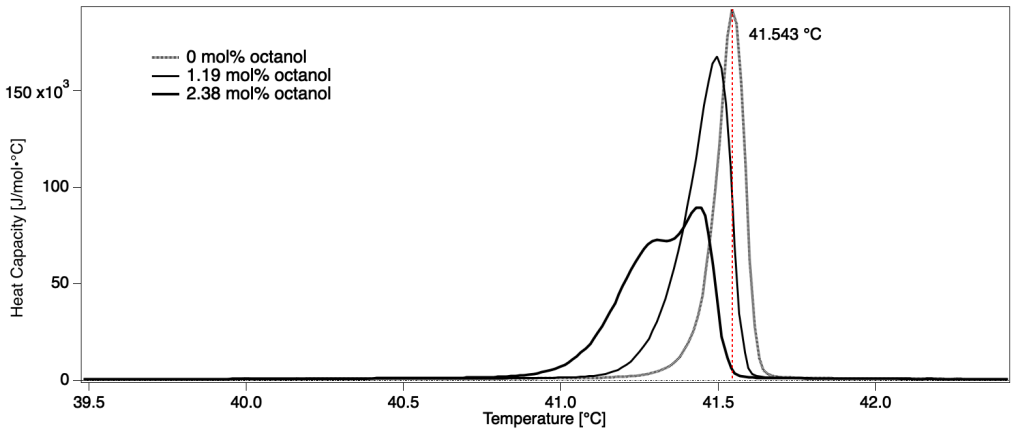

Figure 5.1: Heat capacity of DPPC with different dose of octanol. The red vertical dash line indicates the transition temperature of DPPC vesicles(without octanol) is 41.543 °C. Notice: The anesthetics dose are calculated as molar fraction of octanol dissolved in the membrane.

Figure 5.1 displays three heat capacity profiles of DPPC at different doses of octanol. The calculation of the molar fraction of anesthetics in membrane is the same as Katrzyna Wodzinska(page 65-66)[60]. By visually examining the profiles, it is clear that the addition of anesthetics to lipid membranes results in a shift of the transition temperature towards lower values, accompanied by the broader phase transition area, The changes in the shape of the profiles can be attributed to an increased concentration of octanol within the lipid in its fluid phase[33].

molar ratio of octanol(dissolved in membrane)	transition temperature	ΔT
0 mol%	41.543 °C	
1.19 mol%	41.497 °C	-0.046 °C
2.38 mol%	41.446 °C	-0.097 °C

Table 5.1: The result of DPPC calorimetry scans.

The reported enthalpy change values for the gel-to-liquid crystalline phase transition of DPPC are typically range from 30-40 kJ/mol. These values can vary depending on factors such as the specific experimental conditions, the rate of heating or cooling, and the purity of the DPPC sample. Here we take the value $\Delta H = 35kJ/mol$ from Thomas(this value is also obtained in DSC experiment in this research), if we do the calculation use equation 3.16. And here T_m of DPPC is 41.543 °C, which is consistent with the literature, corresponding to 314.693 K. We obtained ΔT_1 = - 0.28 °C, ΔT_2 = - 0.56 °C if the fraction of octanol in the membrane were 1.19 mol% and 2.38 mol%.

Table 5.1 presents the transition temperatures for different doses of octanol in DPPC obtained in this research. The transition temperature of DPPC without octanol is 41.543°C. When 1.19 mol% of octanol is added to the membrane, the T_m is 41.497°C. This temperature shift ΔT_1 = -0.046°C. Furthermore, when 2.38 mol% of octanol is added, the temperature shift is ΔT_2 = -0.097°C. This observation suggests a clear relationship between the anesthetic dose and the magnitude of the temperature shift. the temperature shift is proportional to the molar fraction of anesthetics in the membrane within experiment error..

Through a comparison between the experimentally obtained temperature shifts and the calculated values, it was observed that the temperature shifts were six times smaller than the theoretical calculations. This difference in magnitude could potentially be attributed to the use of octanol-D18 as an anesthetic, it is highly plausible that its presence has influenced the observed results.

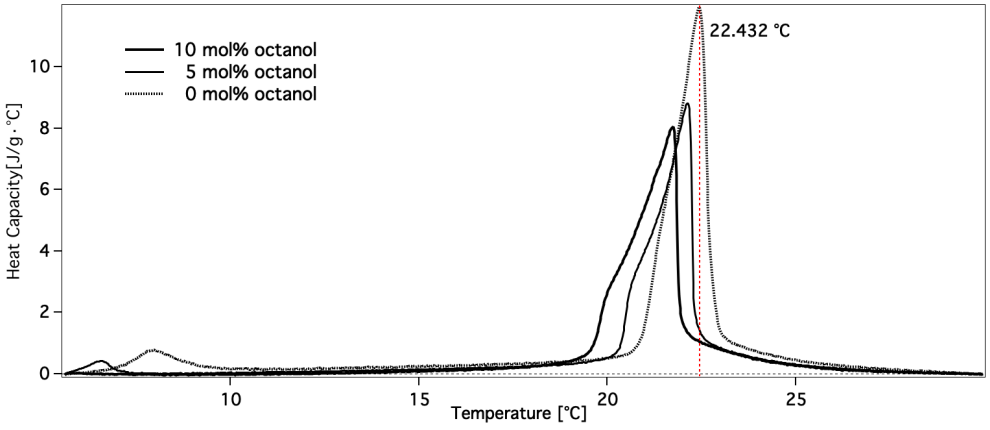

Figure 5.2: Heat capacity of DMPC:DLPC = 10:1(mol:mol) with different dose of octanol. The anesthetic does is calculated as the molar ratio of added octanol and lipid membrane. The red vertical dash line indicates the transition temperature of lipid mixture (without octanol) is 22.432 °C.

5.1.2 Melting Depression in Two species Lipid Membrane

The melting depression law provides an explanation for the influence of anesthetics on lipid membranes in a one species. We cannot employ equation 3.16 to accurately calculate the shifts in transition temperatures, although we have observed the additive effect of anesthetics in pure lipid mixtures. In the following, we will conduct a preliminary analysis of the relationship between the shifts in transition temperatures and the dosage of added anesthetics.

In Figure 5.2, heat capacity scans are depicted for a 10 mM DMPC:DLPC (molar ratio of 10:1) lipid mixture in an electrolyte solution, with varying molar percentages of octanol as anesthetics (0 mol%, 5 mol%, and 10 mol%). The amount of anesthetics added to the membrane is calculated based on the molar percentage between the anesthetic and the membrane in the samples.

Table 5.2 displays the relationship between the transition temperature and the molar percentage

molar ratio of octanol	transition temperature	ΔT
0 mol%	22.432 °C	
5 mol%	22.132 °C	-0.3 °C
10 mol%	21.744 °C	-0.688 °C

Table 5.2: The result of lipid mixture of DMPC:DLPC = 10:1 in DSC experiments.

of octanol in the DMPC:DLPC=10:1 lipid mixture. When 5 mol% octanol is added to the membrane, the transition temperature decreases to 22.132°C. This temperature shift is ΔT_1= -0.3°C. Furthermore, when 10 mol% octanol is added, the temperature shift is ΔT_2 = -0.688°C. Within experimental error, it is evident that the temperature shift is proportional to the anesthetics dose in the sample. Assume the octanol mix ideally in the sample, the transition temperature shift should be proportional to the molar fraction octanol in the membrane.

Given the limitations of our experimental attempts, we can only conclude that the presence of anesthetics, such as octanol, leads to a reduction in the melting temperature (T_m). Furthermore, we have observed a linear relationship between the depression of T_m and the fraction of anesthetics present, which aligns with the principles outlined in the melting depression law.

5.2 Lipid Channel Events

5.2.1 Quantize Conduction Nature of Lipid Ion Channel

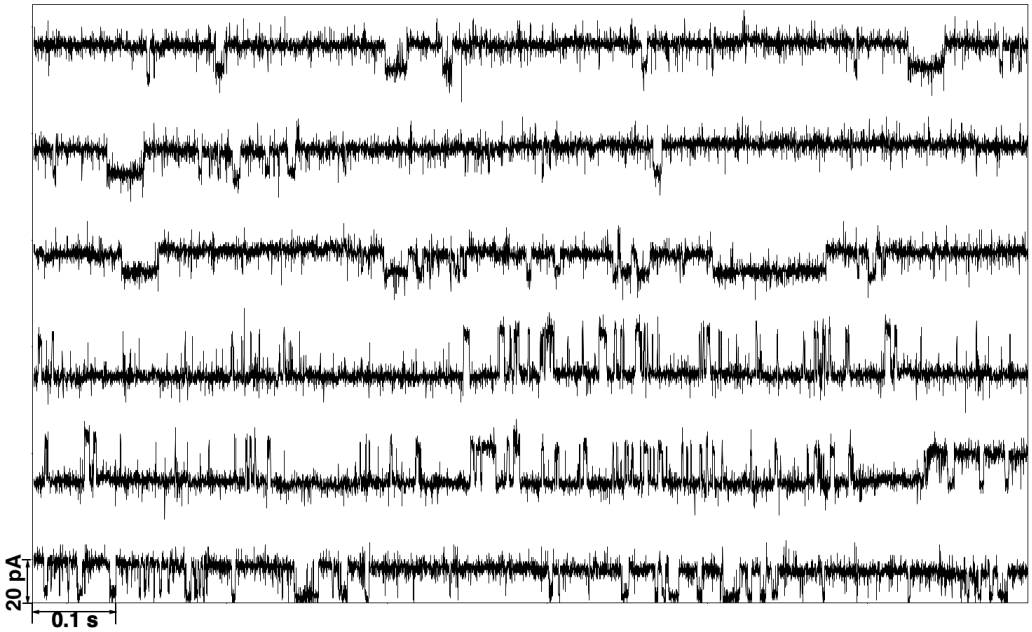

Figure 5.3: Quantized conduction events in DMPC:DLPC = 10:1(mol:mol).V = 70 mV. T = 21 °C. The whole event lasted for around 12 seconds.

In a protein-free lipid membrane, ion conduction occurs through transient nanopores or defects in the lipid bilayer. These nanopores allow the passage of ions across the membrane Many researchers observed the quantized conduction manner of lipid ion channel. It is still surprising that quantize conduction event observed in protein free membrane very similar to that protein ion channel. And the conductance of lipid ion channel is comparable to the conductance of protein ion channel. What's more, lipid nanopores exhibit a wide range of conductance values, typically ranging from picosiemens to hundreds of picosiemens[42].The conductance of lipid ion channel will be quantitatively analyzed in next section.

Figure 5.3 and 5.4 shows the conduction events appear as quantized current events, current traces recorded close to phase transition of lipid membrane. For each traces, It is evident that there are well-defined current step, which mean lipid ion channel allow the passage of ions across the membrane in discrete steps. The observed quantized conduction events in the lipid ion channel suggest that it possesses properties similar to protein ion channels. These quantized events indicate

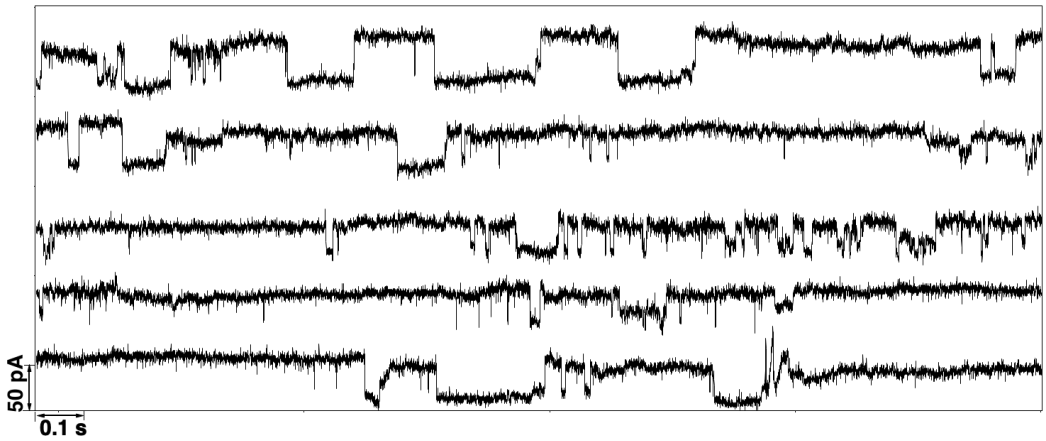

Figure 5.4: Quantized conduction events in DMPC:DLPC = 10:1(mol:mol) with 5 mol% octanol. V = 100 mV. T = 22.4 °C. The whole event lasted for around 14 seconds.

that the passage of ions through the lipid ion channel occurs in discrete steps or events, akin to the quantized conduction observed in protein ion channels.

This finding challenges the conventional notion that ion channels are exclusively protein-based. It suggests that lipid molecules in the membrane can also form structures or arrangements that allow for discrete ion conduction events.

5.2.2 The Conduction of Single Lipid ion channel

The channel events of single lipid pore can be observed in Figure 5.5, which displays the quantized current traces recorded from the channel at different voltages. It is noticeable that the current amplitude increases as the applied voltage increases, with a significant increase in amplitude observed at 88.5 mV.

There are reports suggesting that the size of a single lipid pore may remain constant even as the voltage increases, implying that the conductance of the ion channel remains unchanged [6][60]. In Figure 5.5, when the voltage is set to 65 mV, the conductance of the lipid ion channel measures 261 pS. When the voltage is raised to 77.5 mV, the conductance is 248 pS. These values, accounting for experimental error, it seems that the conductance of the lipid ion channel does not change significantly despite the voltage variation.

At a voltage of 88.5 mV, the conductance of the lipid ion channel increases to 605 pS, indicating a pore size enlargement of approximately 132%. Additionally, significant noise is observed in the current trace. If the arrangement of lipids within the pore remains unchanged, the most plausible explanation for this considerable conductance increase is the occasional presence of dust particles that disrupt the phase transition of the lipid membrane, altering the size of the ion channel. This effect resembles the impact of anesthetics on lipid membranes at temperatures below T_m. However, there is another possibility to consider: between voltages of 51.5 mV and 77.5 mV, the pore exhibits hydrophobic characteristics, but upon reaching 88.5 mV, the lipids reorient themselves, forming a hydrophilic pore, and the conductance of lipid pores could increased[22]. This reorientation may also contribute to the observed noise.

Notably, at a voltage of 51.5 mV, the conductance of the pore is only 175 pS. At our case we would say the pore size keep changing, but the pore size didn't change much at voltages of 65 mV and 77.5 mV. The substantial increase in conductance at the higher voltage could be attributed to external factors, such as the occasional presence of dust particles that disrupted the phase transition of the lipid membrane. This disruption likely altered the size of the lipid ion channel, leading to the observed changes in conductance. Alternatively, the reorientation of lipids from a hydrophobic to a hydrophilic pore could also contribute to the observed noise and significant conductance change.

5.2.3 Multi-step Conduction Event in Lipid Membrane

Figure 5.6 illustrates the recorded current from a membrane under different voltage conditions. At low voltage, a single lipid pore with a conductance of 468 pS is observed. As the voltage increases to 100 mV and 110 mV, several distinct current steps are observed in each trace, with baselines provided as visual aids.

In the current trace at 100 mV, the first current step has an amplitude of 61.99 pA, while the second current step has an amplitude of 74.7 pA. This suggests the presence of two comparable lipid pores with conductances of approximately 620 pS and 747 pS. These pores may open individually or simultaneously.

At 110 mV, it is highly probable that three pores of different sizes are present. The amplitude of the first current step is approximately 50 pA, as evident from the current trace in Figure 5.6 (a). Although it is challenging to discern this step in the corresponding histogram, two small peaks can be observed around 50 pA. The amplitudes of the second and third current steps are 71.4 pA and 94.50 pA, respectively. Based on these observations, it can be concluded that there are three pores (labeled as pore a, b, and c) with conductances of 455 pS, 649 pS, and 859 pS, respectively. The subsequent steps (steps 2 to 6) represent different combinations of open pores: step 2 corresponds to the opening of pore b, step 3 corresponds to the opening of pore c, step 5 is likely the open of pore b and pore c, and step 6 to all three pores being open.

These findings suggest that the individual pore size is not influenced by the applied voltage. Larger pores can be formed at lower voltages, while smaller pores can be found at higher voltages. However, at higher voltages, there is a higher likelihood of the membrane creating new pores, as the opening probability of the lipid ion channel is voltage-dependent(Andreas, 2013). It is also possible for the pore sizes to vary or for pores with similar sizes to coexist. These observations consistent with the previous finding that the single-channel conductance is independent on the applied voltage(Andreas, 2013). Furthermore, it is important to note that these conclusions should based on the assumption that the observed pores are hydrophilic in nature.

5.3 the Effect of Anesthetic in Lipid Ion Channel

Numerous experiments have demonstrated that anesthetics have the ability to lower the melting point of lipid membranes. This implies that anesthetics can influence the phase transition of the membrane, subsequently impacting the formation of lipid ion channels. The melting depression law, as discussed in the previous section, predicts that the addition of a certain amount of anesthetics will systematically decrease the phase transition temperature of a membrane. Figure 5.7 visually illustrates this phenomenon, showing that the inclusion of 5 mol% octanol pushes the phase transition region of the membrane to a lower temperature, resulting in a reduced heat capacity at 22.4 °C.

The objective of the patch clamp experiments is to investigate the impact of anesthetics on conduction events in protein-free membranes. This involves measuring the current flowing through lipid pores in membranes containing varying molar fractions of anesthetics. The ultimate goal is to quantitatively analyze how anesthetics alter the conductance of lipid pores. The experiments are divided into two groups: Group 1, conducted at a temperature of 22.4 °C, and Group 2, conducted at a temperature of 21 °C. By examining the current responses and conductance properties of lipid pores under different experimental conditions, we can gain insights into the effects of anesthetics on lipid ion channel.

5.3.1 Quantized Analysis of the Effect of Anesthetics

Figure 5.7 shows three heat capacity profiles that correspond to membranes with 0 mol%, 5 mol%, and 10 mol% octanol. The experiments was performed at the temperature of 22.4°C, which is in close proximity to the phase transition temperature (22.432°C) of the DMPC:DLPC=10:1 membrane. At this temperature, the heat capacity value of the membrane without octanol is larger than that of the membrane with 5 mol% octanol, and the heat capacity of the membrane with 10 mol% is the smallest. This predicts that the membrane without octanol is more permeable than the membrane with octanol at a temperature of 22.4°C.

The samples used consist of 2mM DMPC:DLPC in a 10:1 (mol:mol) ratio in Hexane: Ethanol in a 4:1 (v:v) mixture. Each sample contains varying amounts of octanol, including 0 mol%, 5

membrane index	molar fraction of octanol	conductance(at the beginning)
Membrane 1	0	$3.84 \times 10^{-4} nA/mV$
Membrane 2	5	$1.99 \times 10^{-4} nA/mV$
Membrane 3	10	$2.17 \times 10^{-4} nA/mV$
Membrane 4	5	$9.09 \times 10^{-4} nA/mV$
Membrane 8	0	$9.62 \times 10^{-4} nA/mV$

Table 5.3: Samples in Group 1 formed on the same pipette, the conductance of the pipette is $3.25 nA/mV$. Five the membranes with different molar fractions of octanol and the conductance of the membranes are measured before current recordings.

mol%, and 10 mol%. It's important to note that all the membranes in each group were formed on the same pipette tip, and the conductance of the pipette was always checked before forming a new membrane. The conductance of the pipette in Group 1 was 3.25 nA/mV, Additionally, the conductance of membranes was always measured after they were formed on the tip of the pipette, and the conductance of the membranes was in the order of $10^{-4} nA/mV$. Eight membranes were formed on the same pipette tip. However, some of the membranes broke during recording, and for the following analysis, data from membranes 1, 2, 3, 4, and 8 were used. The table 5.3 provides basic information about these membranes.

The comparison of channel-like events will only be performed on the membranes containing 0 mol% and 5 mol% octanol at voltages of 60mV, 65mV, and 100mV, as no ion channels were observed in the membrane containing 10 mol% octanol at these voltages.

Figures 5.8 to 5.10 exhibit quantized current traces recorded at different voltages from membranes containing 0 mol% and 5 mol% octanol. These current traces display fluctuations within a specific range, and two distinct baselines can be observed representing the closed and open states of the lipid ion channel. The fluctuations arise from a stochastic process, necessitating an analysis of the current distribution. The corresponding current distributions are depicted in Figures 5.8 to 5.10, revealing two peaks. The current values at these peaks correspond to the mean current when the lipid pore is closed and open, respectively.

In the open state, the lipid pore allows ions to pass through the membrane freely, resulting in a relatively high ion current. Conversely, in the closed state, the lipid membrane restricts ion flow, leading to a relatively low ion current. The separation between the two peaks in each current distribution varies due to differences in the conductance of individual lipid pores. By calculating the difference in current between these peaks, we can determine the conductance of the lipid pores under the given voltage.

The current distributions were fitted using Gaussian distribution function, as depicted in Figures 5.8 to 5.10. It was observed that the majority of the current distributions displayed a good fit to the Gaussian distribution. As the permeability of ions through lipid membranes is associated with the opening of lipid pores, we conducted a comparison of pore conductance between two groups of membranes: one without octanol (0 mol% octanol) and the other with 5 mol% octanol, under the same voltage conditions. This investigation aimed to examine the impact of anesthetics on conduction events in lipid membranes.

At a voltage of 60mV (Figure 5.8), the conductance of lipid ion channels without octanol was measured to be 389 pS, while the conductance of lipid ion channels with 5 mol% octanol was 277 pS, resulting in a 28.8% decrease in conductance for the 5 mol% octanol membrane. Similarly, at a voltage of 65mV (Figure 5.9), the conductance of lipid ion channels without octanol was 468 pS, compared to 334 pS for the 5 mol% octanol membrane, representing a 28.5% decrease in conductance. Finally, at a voltage of 100mV (Figure 5.10), the conductance of lipid ion channels without octanol was 599 pS, whereas it was measured to be 417 pS for the 5 mol% octanol membrane, corresponding to a 30.5% decrease in conductance.

These findings demonstrate a significant reduction in the conductance of lipid pores in the presence of 5 mol% octanol within the membrane. Specifically, our analysis indicates a consistent decrease in pore conductance of approximately 28% under all three tested voltage conditions (60mV, 65mV, and 100mV).

In Group 2, three membranes were formed on the same pipette tip, containing 0 mol%, 5 mol%, and 10 mol% octanol. Table 5.4 provides essential details about these membranes. Figure 5.11 displays the heat capacity of these membranes at a temperature of 21°C. It is observed that the

membrane index	molar fraction of octanol	conductance(at the beginning)
Membrane 1'	0	$2.99 \times 10^{-4} nA/mV$
Membrane 2'	5	$6.76 \times 10^{-4} nA/mV$
Membrane 3'	10	$6.31 \times 10^{-4} nA/mV$

Table 5.4: Samples in Group 2 formed on the same pipette, the conductace of the pipette is $2.38 nA/mV$. Three membranes with different molar fractions of octanol and the conductance of the membranes are measured before current recordings

Voltage	molar fraction of octanol	current step	conductance	conductance change
60 mV	0	23.35 pA	389 pS	
60 mV	5	16.62 pA	277 pS	-28.8%
65 mV	0	30.42 pA	468 pS	
65 mV	5	21.74 pA	334 pS	-28.5%
100 mV	0	59.99 pA	599 pS	
100 mV	5	41.72 pA	417 pS	-30.5%
70mV	10	40.55 pA	579 pS	
70 mV	0	17.81 pA	254 pS	-56%

Table 5.5: The current step of lipid ion channel calculate from the Gaussian fitting and the corresponding conductance.

membrane with 10 mol% octanol exhibits the highest heat capacity, while the membrane with 5 mol% octanol has a lower heat capacity. On the other hand, the membrane with 0 mol% octanol has the lowest heat capacity.

Figure 5.12 presents current traces at a voltage of 70 mV from membranes with 0 mol% octanol and 10 mol% octanol. At a temperature of 21°C, it is observed that the membrane with 10 mol% octanol has higher permeability compared to the membrane with 0 mol% octanol. The conductance of the membrane with 10 mol% octanol is measured at 579 pS, whereas the conductance of the membrane with 0 mol% octanol is measured at 254 pS. Thus, the conductance of the membrane without octanol is significantly smaller, with a decrease of approximately 56% compared to the conductance of the membrane with 10 mol% octanol. These findings suggest that when the membrane is at a temperature above the transition temperature, the conductance is expected to decrease by approximately 56% upon adding 10 mol% octanol.

In conclusion, as presented in Table 5.5, reveals a remarkable consistency in the changes observed in the conductance of the lipid ion channel after the addition of a certain amount of anesthetic agents. The introduction of 5 mol% octanol into the membrane leads to an approximate 29% alteration in the conductance of the lipid ion channel. Furthermore, it suggest that 10 mol% concentration of octanol in the membrane may results in a significant 56% change in the conductance of the lipid ion channel.

5.3.2 The Effect of Anesthetics with Drop-let Technique

The membrane exhibits a high sensitivity to octanol, allowing us to conduct an experiment where anesthetics are directly added to the lipid membrane using a drop-let technique. This approach enables us to dynamically observe the impact of anesthetics on the permeability of the lipid membrane. In accordance with the freezing point depression phenomenon, the presence of anesthetics will shift the heat capacity profile of the membrane towards lower temperatures. Consequently, if the membrane is at a temperature below its melting point (T_m), the addition of anesthetics will further lower the phase transition temperature of the membrane, facilitating a phase transition at a lower temperature.

Figure 5.13 presents the heat capacity profile of a 10 mM DMPC:DLPC (10 mol:1 mol) lipid mixture in an electrolyte solution. The transition temperature observed in this sample is measured to be 22.432 °C, which closely aligns with the value reported by Karis, where the transition temperature was reported as 22.2 °C[5]. The slight discrepancy in the transition temperature could be attributed to the slightly different DMPC to DLPC ratio employed during sample preparation.

To examine the membrane's behavior at different temperatures, we measured the membrane current at two distinct temperatures: 19.9 °C, which is below the transition temperature, and 28.9 °C, which is above the transition temperature.

In Figure 5.14(a), at a temperature of 19.9°C, no current channel events were observed even when the voltage reached the maximum of the applied voltage (1000 mV). At a voltage of 999 mV, triangular signals were observed, but they were not indicative of channel activity. The nature of these triangular signals remains unknown. The current traces for the voltages of 995 mV and 836 mV are not shown. However, at a voltage of 995 mV, a drop of 0.1 mM octanol in ethanol was added to the membrane, resulting in a significant observable change. The current traces were recorded once the membrane reached a stable state.

Figure 5.14(b) displays the current trace recorded after the addition of the octanol solution, while the baseline of the current remained stable. The presence of ion channels indicates an increase in the membrane's permeability. The most plausible explanation is that the anesthetics lower the transition temperature of the membrane, bringing it closer to a phase transition state, thereby facilitating the formation of lipid ion channels.

On the other hand, anesthetics can block the channel events. Figure 5.15(a) presents two current traces recorded at a temperature of 28.9°C, where lipid channels can be observed. However, upon adding a drop of anesthetics, the ion channels quickly disappear (as seen in Figure 5.15(b)), and despite increasing the voltage, no channel events can be observed. This phenomenon can be explained by the shift of the membrane's heat capacity profile towards lower temperatures, resulting in the absence of a phase transition at 28.9°C, with all lipids in the membrane existing in a liquid state.

To further confirm the effect of anesthetics in pushing the membrane away from the phase transition, Figure 5.15(c) shows the reappearance of channels upon cooling the temperature down.

In conclusion, the observed effects of anesthetics on lipid membranes in this experiment align with the predictions of the melting depression law discussed in Section 3.3. This consistency also demonstrates the membrane's permeability is closely related to the membrane's heat capacity.

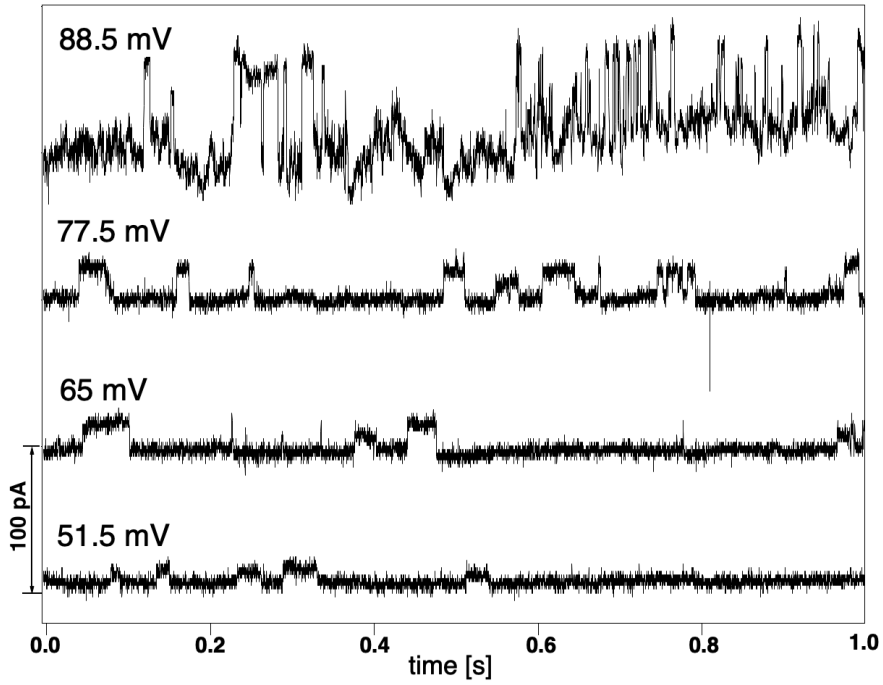

(a)

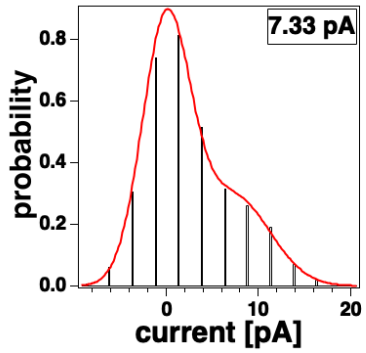

(b) 51.5 mV

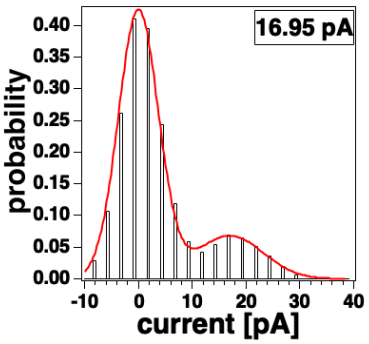

(c) 65 mV

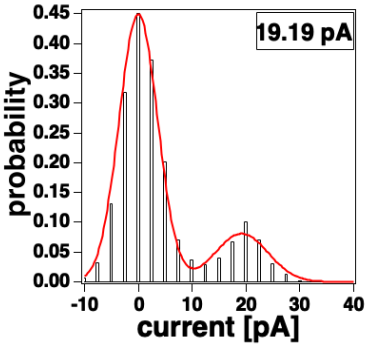

(d) 77.5 mV

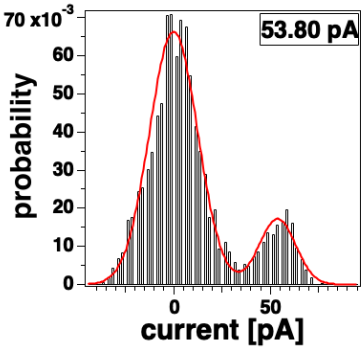

(e) 88.5 mV

Figure 5.5: Single pore current recorded at different voltages and corresponding current histograms. (a) Current traces of DMPC:DLPC = 10:1(mol:mol) from the voltage of 51.5 mV to 88.5 mV. T = 20.1 °C. (b) The current histogram corresponds to the current trace recorded at the voltage of 51.5 mV. The conductance of lipid ion channel is 142 pS. (c) Current histogram corresponds to the current trace 65 mV, the conductance of lipid pore is 261 pS. (d) Current histogram corresponds to the current trace recorded at the voltage of 77.5 mV. The conductance of lipid ion channel is 248 pS. (e) Current histogram corresponds to the current trace recorded at the voltage of 88.5 mV. The conductance of lipid ion channel is 608 pS.

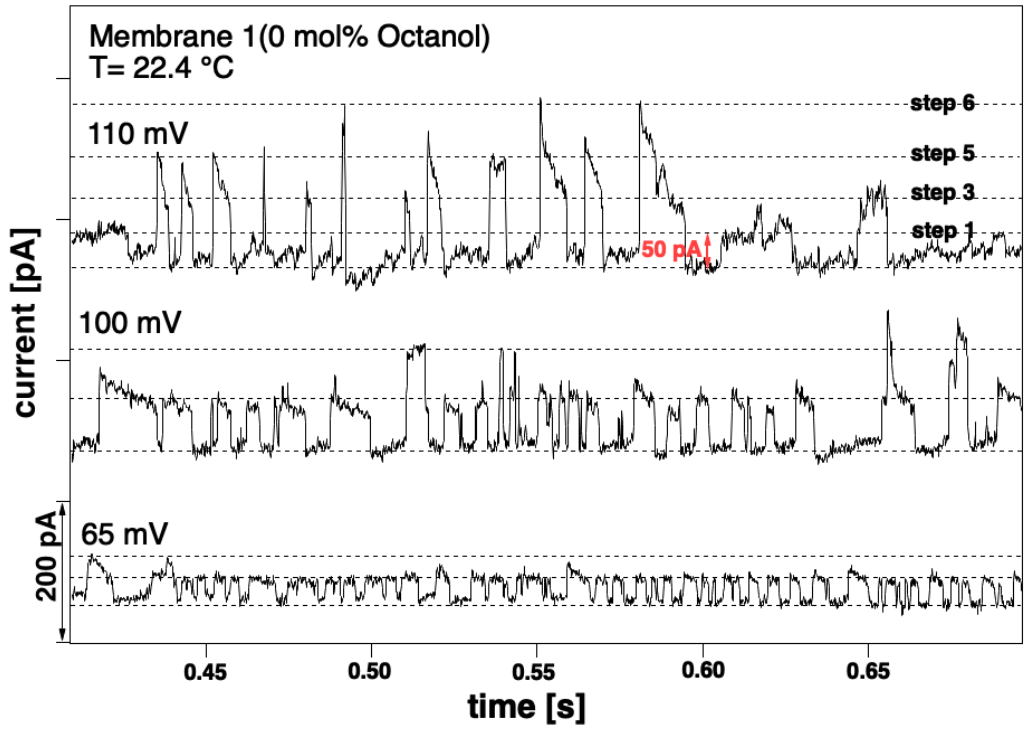

(a)

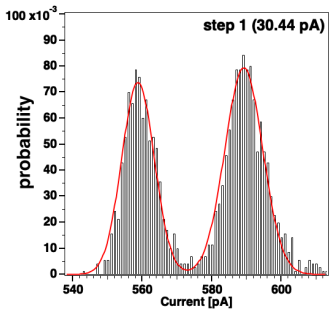

(b) 65 mV

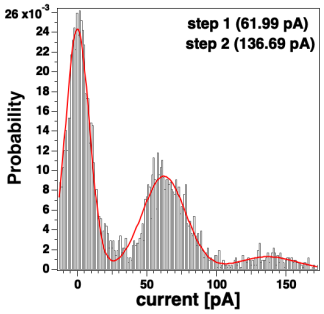

(c) 100 mV

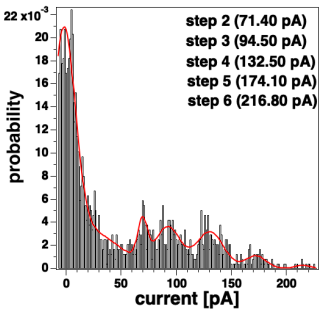

(d) 110 mV

Figure 5.6: Current traces and current histograms, the amplitude of each current step are shown in the right upper corner of histograms. (a)Current traces of DMPC:DLPC = 10:1(mol:mol) from the voltage of 65 mV to 110 mV. T = 22.4 °C. (b) Current histogram corresponds to the current trace recorded at the voltage of 65 mV. The conductance of lipid ion channel is 468 pS. (c)Current histogram corresponds to the current trace 100 mV, the conductance of one lipid pore is 619 pS, the conductance of the other pore is 747 pS. (d) The current histogram corresponds to the current trace recorded at the voltage of 110 mV. The current amplitude of step 2 is 71.40 pA, amplitude of step 3 is 94.50 pA, amplitude of step 3 is 130.5 pA, amplitude of step 4 is 132.50 pA, amplitude of step 5 is 174.10 pA, amplitude of step 6 is 216.80 pA.

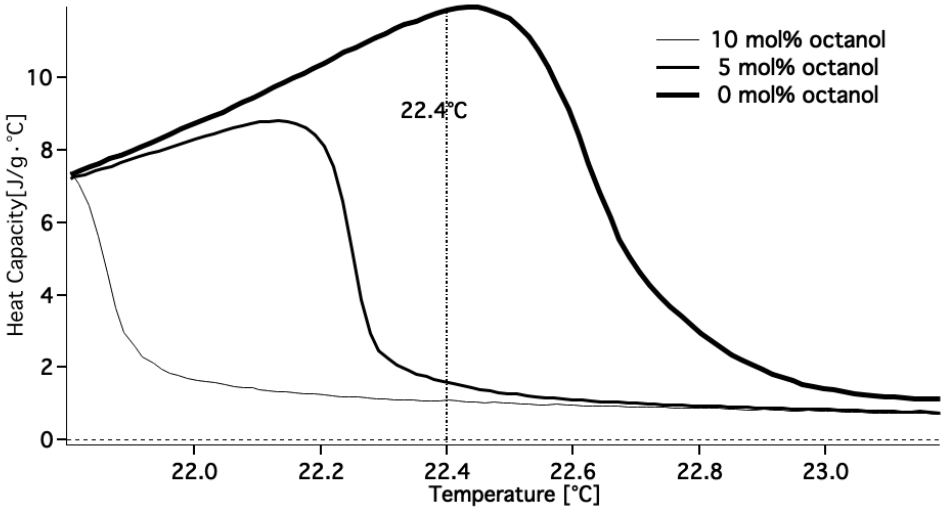

Figure 5.7: Heat capacity profiles of 10mM DMPC:DLPC=10:1(mol:mol) in electrolyte solution with 0 mol%,5 mol% and 10 mol% octanol.The vertical line indicate the experiment temperatrue 22.4°C which is close to the transition temperature of DMPC:DLPC=10:1(mol:mol).Note that the dose of octanol is calculated by the molar ratio between octanol and membrane.

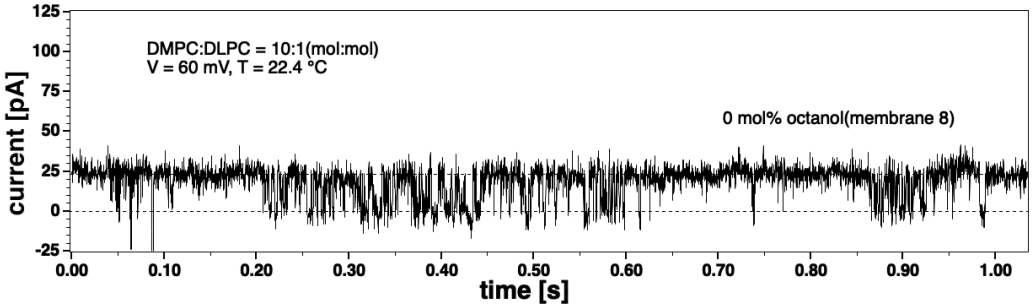

(a)

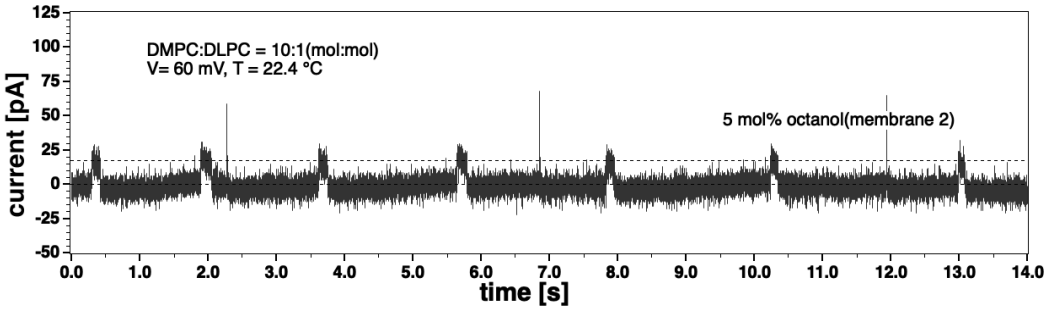

(b)

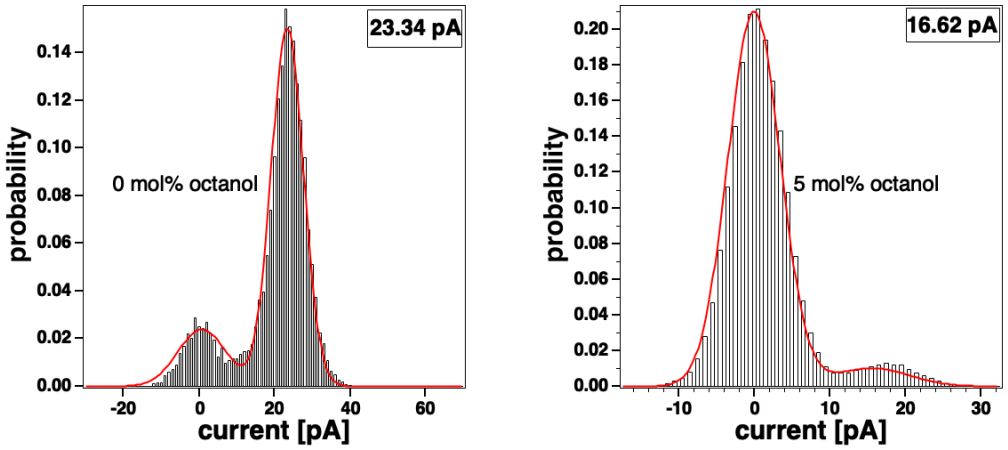

(c) (d)

Figure 5.8: Current traces and current distribution of membranes DMPC:DLPC=10:1 with 0 mol% and 5 mol% octanol. Currents recorded at the same voltage and temperature, T = 22.4 °C, V = 60 mV. Notice the timescale of current recordings are different. (a)The current trace from lipid membrane without octanol. (b)The current trace from lipid membrane with 5 mol% octanol. (c)Current current distribution corresponds to current traces from the membrane with 0 mol% octanol. The red curve is the result of double Gaussian fitting with the current distribution. Left peak corresponds to the mean current when lipid ion channel closed, 0 pA. Right peak corresponds to the mean current when lipid ion channel open, the current step is show in the upper right corner box, which is 23.34 pA. (d)Current distribution correspond to the current traces from the membrane with 5 mol% octanol. The current step is 16.62 pA.

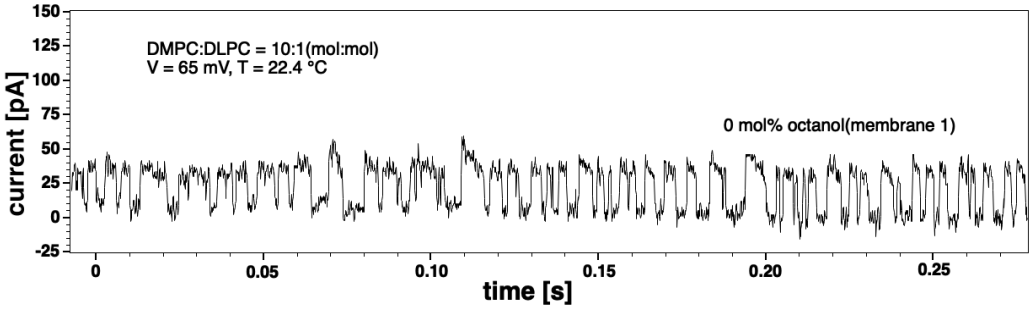

(a)

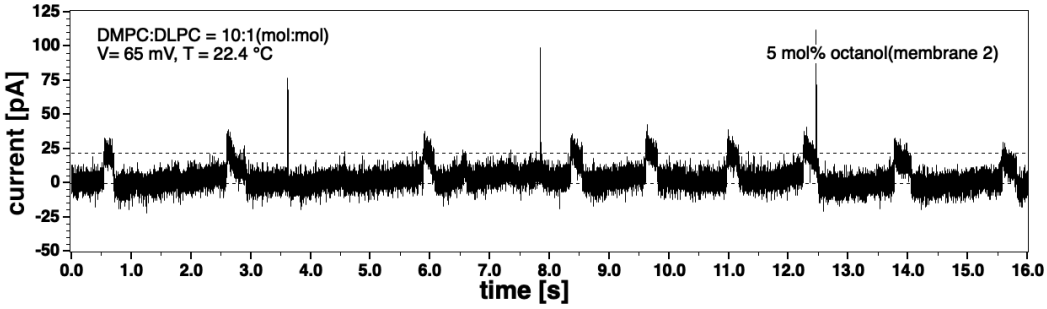

(b)

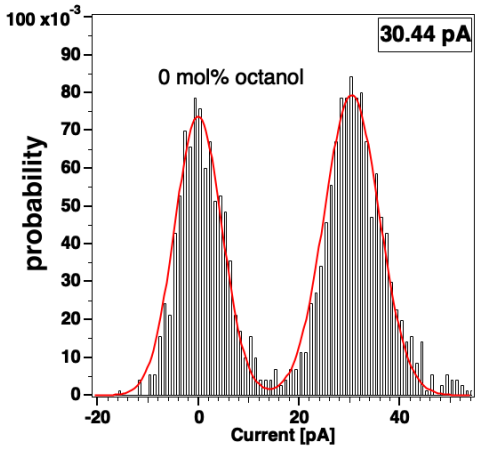

(c)

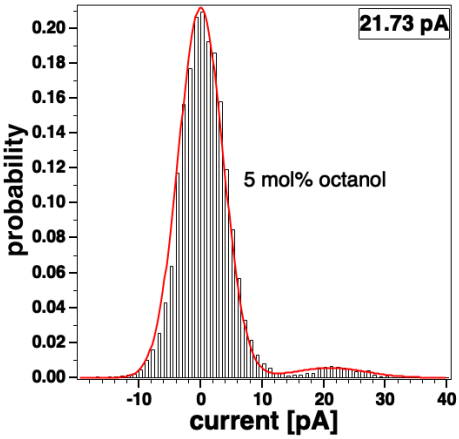

(d)

Figure 5.9: Current traces and current distribution of membranes DMPC:DLPC=10:1 with 0 mol% and 5 mol% octanol. Currents recorded at the same voltage and temperature, T = 22.4 °C, V = 65 mV. Notice the timescale of current recordings are different. (a)The current trace from lipid membrane without octanol. (b)The current trace from lipid membrane with 5 mol% octanol. At the time of around 6.5 s, there is small current step is caused by occasionally touched the cable from headstage to amplifier during the recording. This is not included in the current distribution. (c)Current distribution corresponds to current traces from the membrane with 0 mol% octanol. The red curve is the result of double Gaussian fitting with the current distribution. Left peak corresponds to the mean current when lipid ion channel closed, 0 pA. Right peak corresponds to the mean current when lipid ion channel open, the current step is show in the upper right corner box, which is 30.44 pA. (d)Current distribution correspond to the current traces from the membrane with 5 mol% octanol. The current step is 21.73 pA.

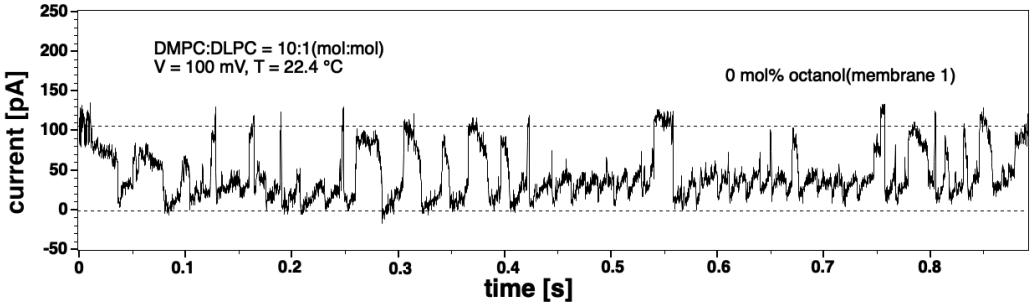

(a)

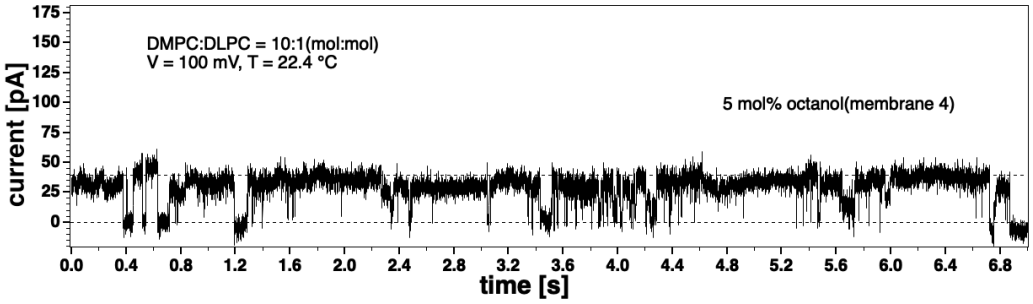

(b)

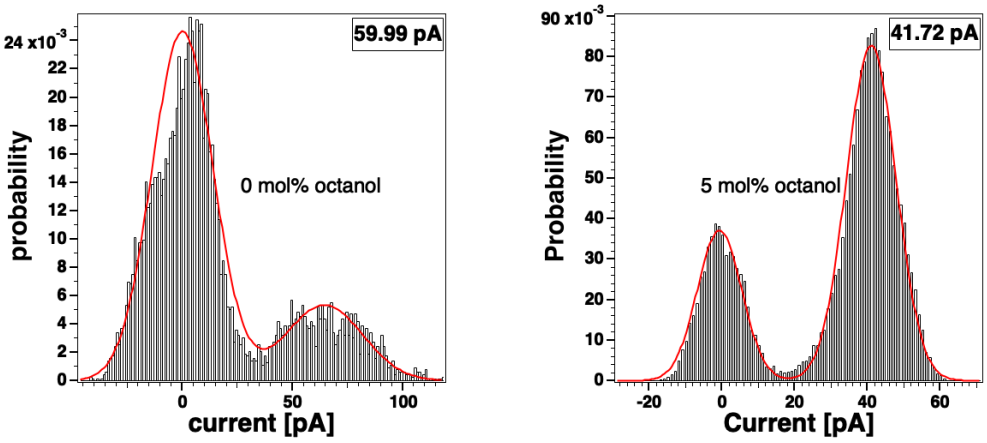

(c) (d)

Figure 5.10: Current traces and current distribution of membranes DMPC:DLPC=10:1 with 0 mol% and 5 mol% octanol. Currents recorded at the same voltage and temperature, T = 22.4 °C, V = 100 mV. Notice the timescale of current recordings are different. (a)The current trace from lipid membrane without octanol. There is some noise in the recordings. This will affect the current distribution at around 0 pA. (b)The current trace from lipid membrane with 5 mol% octanol. (c)Current current distribution corresponds to current traces from the membrane with 0 mol% octanol. The red curve is the result of double Gaussian fitting with the current distribution. Left peak corresponds to the mean current when lipid ion channel closed, 0 pA. Right peak corresponds to the mean current when lipid ion channel open, the current step is show in the upper right corner box, which is 59.99 pA. (d)Current distribution correspond to the current traces from the membrane with 5 mol% octanol. The current step is 41.72 pA.

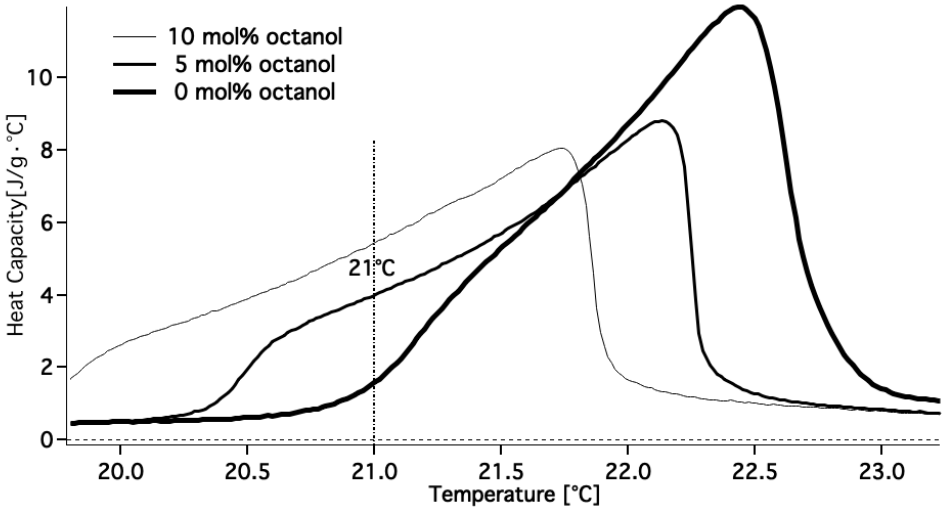

Figure 5.11: Heat capacity profiles of DMPC:DLPC=10:1(mol:mol) in electrolyte solution with 0 mol%,5 mol% and 10 mol% octanol.The vertical line indicate the experiment temperatrue 21°C which is close to the transition temperature of DMPC:DLPC=10:1(mol:mol).Note that the dose of octanol is calculated by the molar ratio between octanol and membrane.

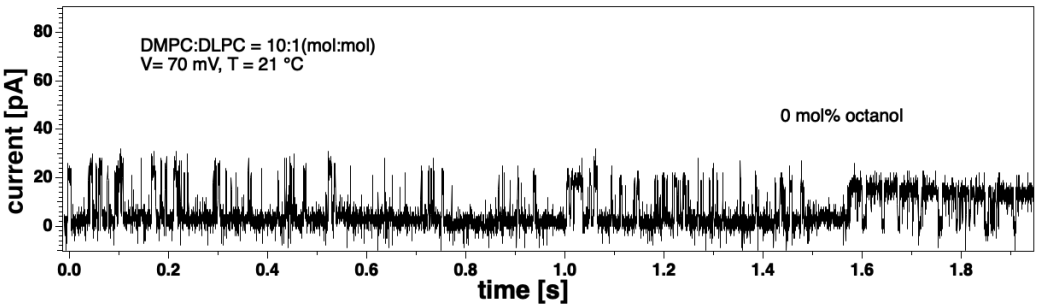

(a)

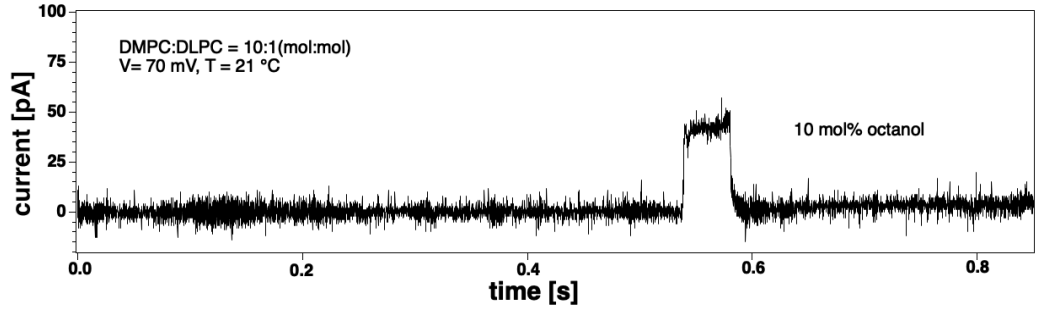

(b)

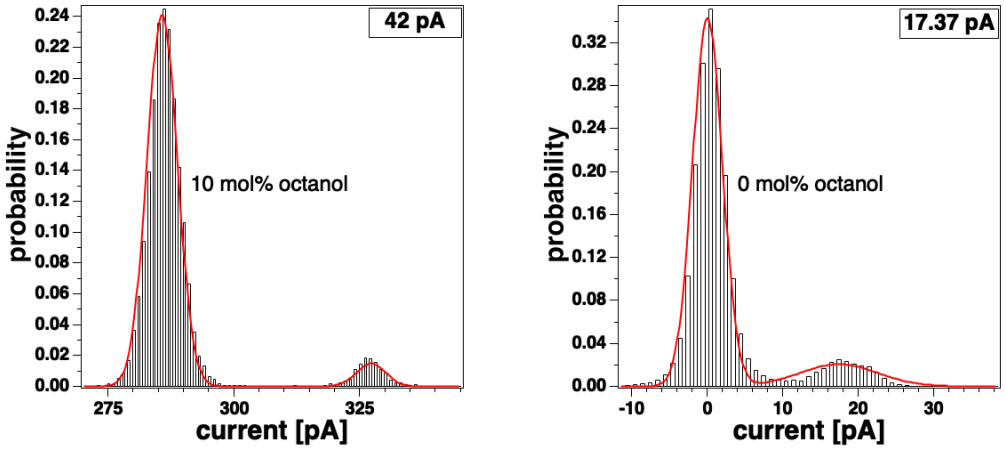

(c) (d)

Figure 5.12: Current traces and current distribution of membranes DMPC:DLPC=10:1 with 0 mol% and 10 mol% octanol. Currents recorded at the same voltage and temperature, T = 21 °C, V = 70 mV. Notice the timescale of current recordings are different. (a)The current trace from lipid membrane without octanol. (b)The current trace from lipid membrane with 10 mol% octanol. (c)Current current distribution corresponds to current traces from the membrane with 10 mol% octanol. The red curve is the result of double-Gaussian fitting with the current distribution. Left peak corresponds to the mean current when lipid ion channel closed, 0 pA. Right peak corresponds to the mean current when lipid ion channel open, the current step is show in the upper right corner box, which is 42.00 pA. (d)Current distribution correspond to the current traces from the membrane with 0 mol% octanol. The current step is 17.37 pA.

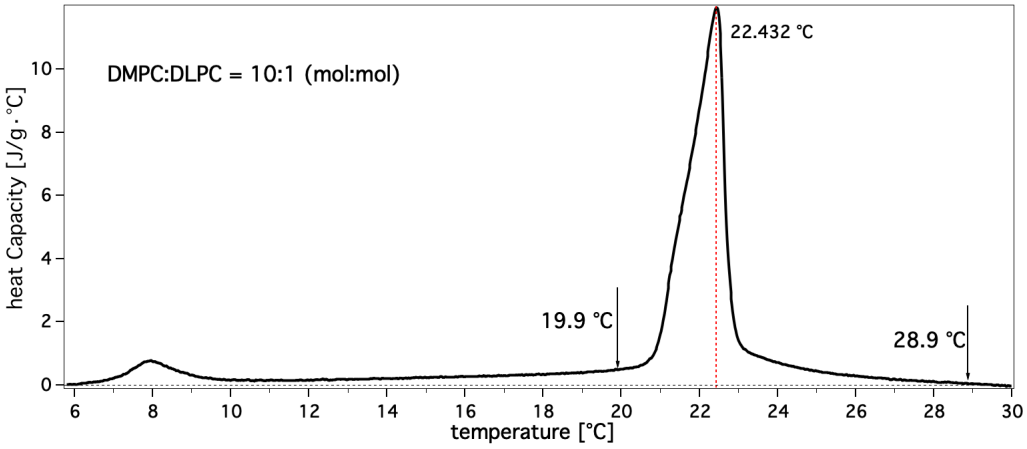

Figure 5.13: Heat capacity of 10 mM DMPC:DLPC=10:1(mol:mol) in electrolyte solution.The vertical red dash line indicate the main transition temperature of the sample is 22.432°C, the phase transition region is broad. 19.9°C is the temperature below phase transition, and 28.9 °C is the temperature above T_m.

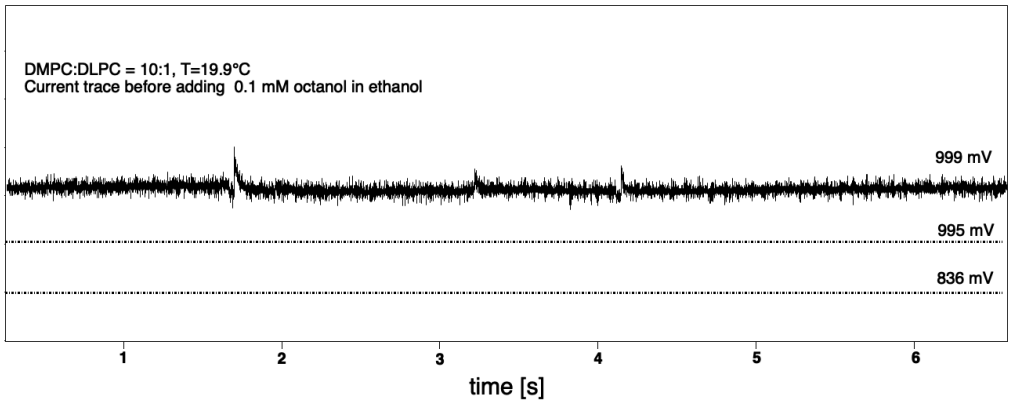

(a)

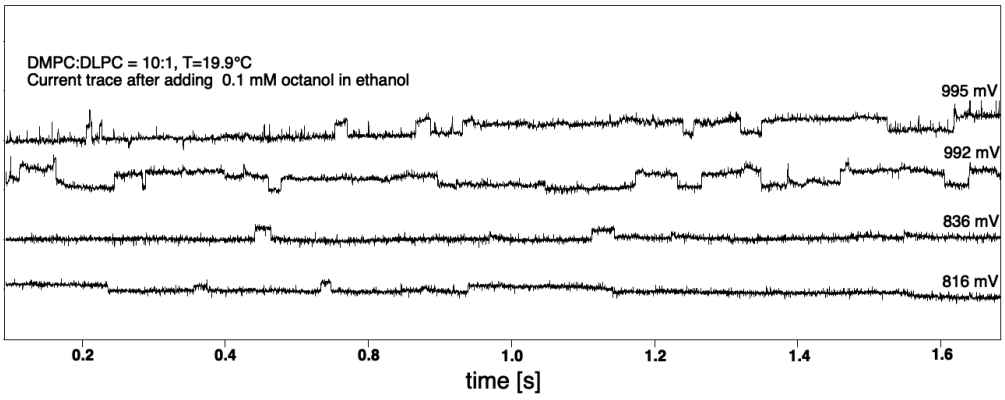

(b)

Figure 5.14: (a)Membrane current recorded by patch clamp technique at the temperture of 19.9°c,only the current trace under a voltage of 999mV is shown in this figure,no ion channel is found during the whole recording. (b)Lipid ion channel appear after adding a drop(8uL) of 0.1 mM octanol in ethanol.

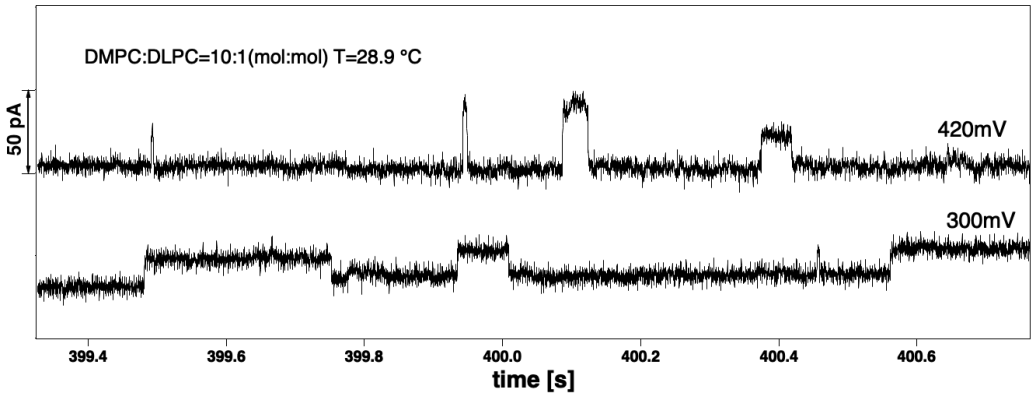

(a)

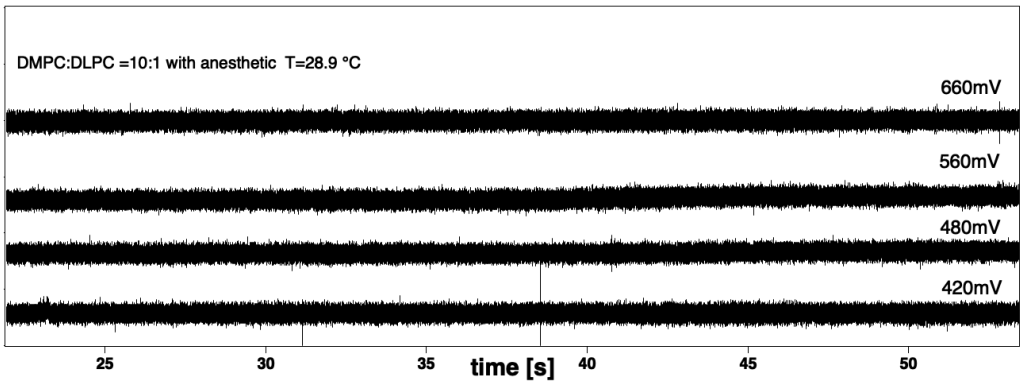

(b)

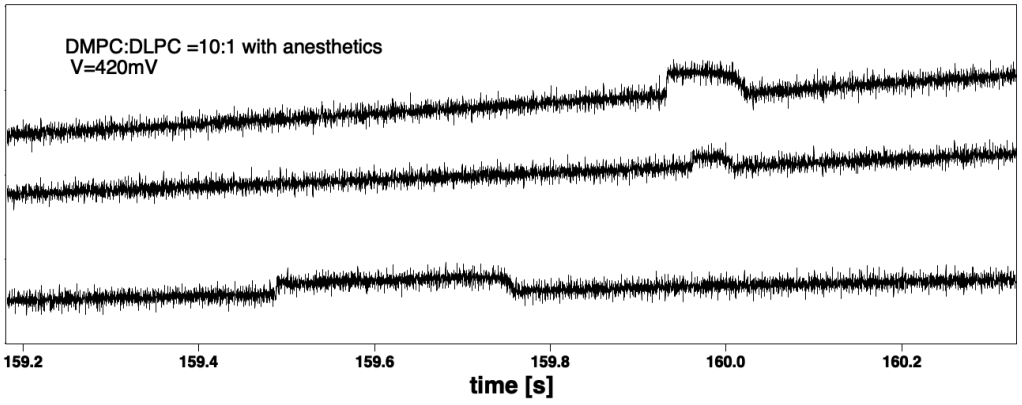

(c)

Figure 5.15: (a) Current traces recorded at the temperature of 28.9 °C(the temperature is higher than Tm). Two current traces with the lipid ion channel at voltage of 300mV and 420mV. (b) Current traces record at temperature of 28.9°C after adding a drop(8uL) of anesthetics solution at the voltage of 420mV. No channel is observed even at higher voltage 480mV,560mV,660mV. (c) Channels recorded from the membrane with anesthetic at a voltage of 420mV by cooling down the temperature.The temperature in changing during the recording, the channel events appeared again.

Chapter 6

Discussion and conclusion

6.1 Discussion

6.1.1 The Existence of Lipid Ion channel

Numerous scientific papers have documented the existence of lipid ion channels. In our own research, we have also observed channel events occurring in membranes without proteins, particularly during membrane phase transitions. The remarkable aspect of these channel events is their stochastic nature. The reported diameter of lipid ion channels is approximately 1 nm, which may vary slightly, and is comparable to the reported pore size of protein ion channels.

In reality, lipid ion channels are likely to exist in cell membranes because cell membrane phase transitions can occur slightly below their growth temperature in different cell types. Previous current recordings from lipid ion channels display similar characteristics to those of protein ion channels, suggesting the presence of lipid ion channels in natural cells that may have gone unnoticed. Furthermore, the observed membrane area in specific protein ion channel recordings is significantly larger than that of a protein itself. For instance, ion channel proteins like the potassium channel have a diameter of approximately 5 nm. This implies that even the smallest patch used in a patch-clamp experiment (with a diameter of around 1 μm) is 40,000 times larger than the cross-sectional area of the protein[28]. Therefore, it is inaccurate to attribute all channel events solely to protein ion channels.

Detecting lipid ion channels successfully is a challenging task that requires a keen sense to find channel events. But there is a high probability of discovering lipid ion channels when the membrane temperature approaches its melting point (T_m). In this thesis, the data obtained from patch clamp experiments may not accurately represent the average channel events. Although these channel events are from different membranes.

6.1.2 The pore size of the lipid ion channel

In Section 5.2.2, we concluded that the pore size may be influenced by changes in applied voltage. However, in Section 5.2.3, we reached a different conclusion, stating that the pore size is independent of the applied voltages. These seemingly contradictory conclusions can be reconciled by considering the pore model illustrated in Figure 2.4.

According to the pore model, a pore initially begins as a hydrophobic pore due to thermal fluctuation, and its size can increase with higher voltage. However, at a certain point, the pore undergoes a transition and becomes a hydrophilic pore through the reorientation of lipid molecules. This transition process is energetically favorable, meaning that it occurs with minimal energy expenditure.

Once the hydrophilic pore is formed, it can maintain a relatively larger size while requiring minimal energy to create and sustain it. The conclusion in Section 5.23 is based on these hydrophilic pores, which only need the minimum energy to form. As a result, the pore size in this state is almost unaffected by the applied voltage. However, it is important to note that higher voltages may increase the likelihood of new pore formation.

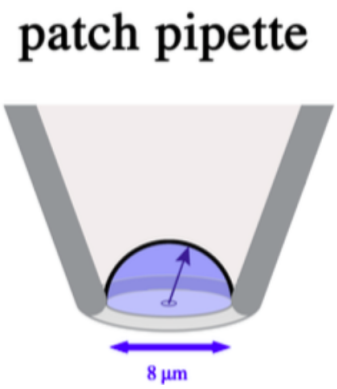

Figure 6.1: The curved lipid bilayer on the pipette tip(the pipette used in the experiment has a diameter around $8 - 12\mu m$). The arrow indicates the maxium radium of the curvature.

Therefore, both conclusions can be valid and consistent. The observation in Section 5.2.2 pertains to the initial stages of pore formation and enlargement under the influence of applied voltage, while the conclusion in Section 5.2.3 pertains to the stable hydrophilic pores that have already reached their optimal size and are minimally affected by further changes in applied voltage.

6.1.3 The Formation of Lipid Membrane on Pipette Tip

In patch clamp experiments, we measured the conductance of lipid membrane G_L before current recordings. Tables 5.3 and 5.4 show the conductance of different membranes formed on the pipette tip in the experiments. The conductance of membrane is in the order of $10^{-4}nA/mV$, if the conductance G_L is much smaller than $10^{-4}nA/mV$, it suggests the presence of a multilayer lipid membrane. Conversely, if G_L is much bigger, it indicates that the membrane is not intact.

Although we form the membranes on the same pipette, there can be variations in the values of G_L. This variation arises due to the inherent differences in the formation of lipid membranes, particularly with respect to the curvature of the membrane on the pipette tip. The schematic drawing in Figure 6.1 illustrates the bilayer curves due to the small diameter of the hole in the pipette tip. We can see the maximum curvature, is where the radius matches the radius of the hole. Another possibility is that the membrane may be anchored differently along the rim of the pipette.

Despite these variations in the formation of membranes on the pipette tip, it is surprising that the effect of a certain amount of octanol on different lipid membranes remains consistent (see Section 5.3). In the following section, we will primarily talked about how we select and analyze the data to examine the impact of anesthetics on lipid membranes.

6.1.4 Variety of Channel Events

The results of the effect of anesthetics on lipid membrane is unexpectedly consistent, but reasonable(Table 5.5). In the following, we will talked about several considerations when analyse the data.

Conductance change at a constant voltage in lipid membrane

During the patch clamp experiments, changes in lipid conduction were observed under a constant voltage in the same membrane. Figure 6.2 presents four segments of current traces obtained at a voltage of 100mV and a temperature of 22.4 °C. In Figure 6.2 (c), a two-step current jump is observed, indicating the presence of two pores in the membrane. Figures (a), (e), and (g) correspond to the current traces of one of these two pores, although it is difficult to determine which pore is open at any given time. However, the conductance of these two pores is comparable, suggesting that their sizes are similar. Figure 6.2 (d) demonstrates that when one pore opens, the current step is 61.99 pA, while the current step increases to 136.59 pA when both pores open simultaneously. It is worth noting that the current steps for individual pores show slight differences, which can be attributed to natural fluctuations and the inherent variability of the pores.

In summary, the observation of conductance changes at the same voltage and temperature can be

attributed to two main reasons. Firstly, slight fluctuations can cause variations in the conductance of the pores. Secondly, multiple pores may be present, and their openings can occur independently or simultaneously, as illustrated in Figure 5.6. It is important to note that the current trace used for analysis in Figure 5.10 (a) is the same as the one shown in Figure 6.2 (g). This choice was made because pores of this size were more frequently observed, and the current step of 59.99 pA is close to the first current step of 61.99 pA in the current trace (see Figure 6.2 (d)).

Current Traces at Lower Voltage

At lower applied voltages, such as 65 mV, 70 mV, and 75 mV (Figure 5.8, 5.12, and 5.9), only a single channel was observed, and the conductance of the individual pore did not exhibit significant changes. The conductance values of the channel events were found to be very similar when comparing multiple events within the same trace (data not shown). In some traces, a channel event was observed only once.

Interesting channel events

In Figure 6.3(a), the channel events observed in membrane 2 at a voltage of 65 mV are displayed. Figure 6.3(b) represents a subset of these channel events extracted from Figure 6.3(a). We have also observed similar channel events in some other current traces at relatively high voltages. Interestingly, it appears that there are channel events embedded within other channel events. We have made an attempt to determine the conductance of the embedded channel events and compare it to the channel events occurring in the same membrane at the same voltage.

Upon comparing the current steps in Figure 5.9(d) and Figure 6.3(c), we found that the conductance of the embedded channel events is almost equivalent to that of a single ion channel. However, the lifetime of the channel has undergone significant changes. The reasons behind this phenomenon are currently unknown. While This kind of channel events will not be considered during data analysis.

6.1.5 The Substantial Impact of Anesthetics on Lipid Bilayer

Due to the inherent variability in the conductivity of lipid ion channels, even when the cell membrane is under identical conditions. We observed surprising consistency in changes of lipid ion channel conductance after the addition of a certain amount of anesthetic agents. For 5 mol% octanol in membrane, the conductance of lipid ion channel will changed around 29%. And the conductance is expected to decrease by approximately 56% by adding 10 mol% octanol. This indicate the the possible addictive inhibition of octanol in lipid membrane permeability.

We can use our result to do some calculation. The critical anesthetics does is 2.6 mol% anesthetic in the membrane, this anesthetics does will produces the desired anesthesia effect in 50% of individuals or experimental animals[33]. This suggests that when the membrane contains a concentration of 2.6 mol% anesthetics, the inhibition of cell membrane permeability reaches approximately 15%. It is worth emphasizing that this inhibition effect is significant. Therefore, it is imperative for us to take into account the presence of lipid ion channels in cell membrane and further contemplate the substantial impact of anesthetics on the lipid bilayer.

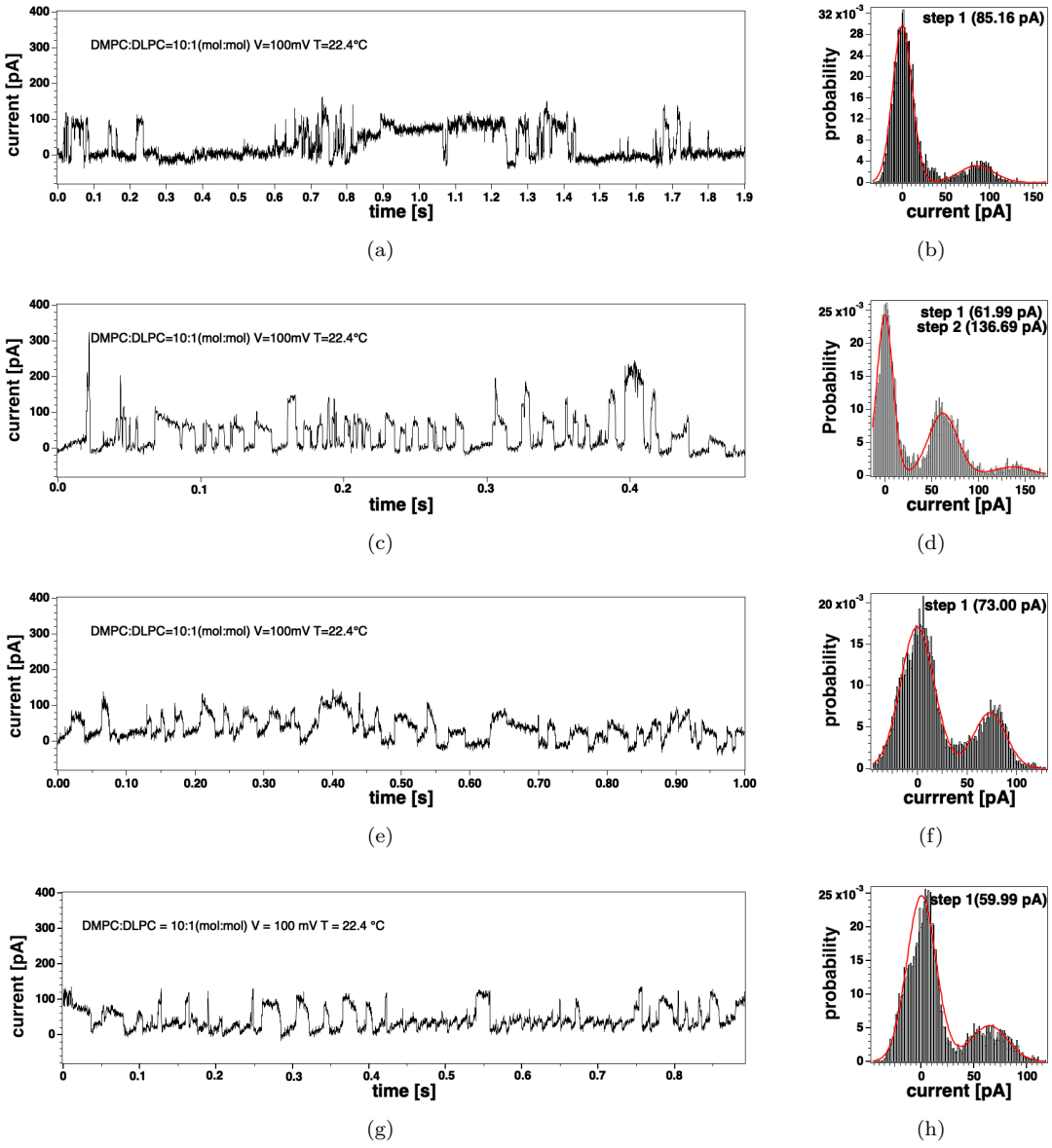

Figure 6.2: Different conductance of lipid ion channel observed at a voltage of 100mV, The temperature is 22.4°C.

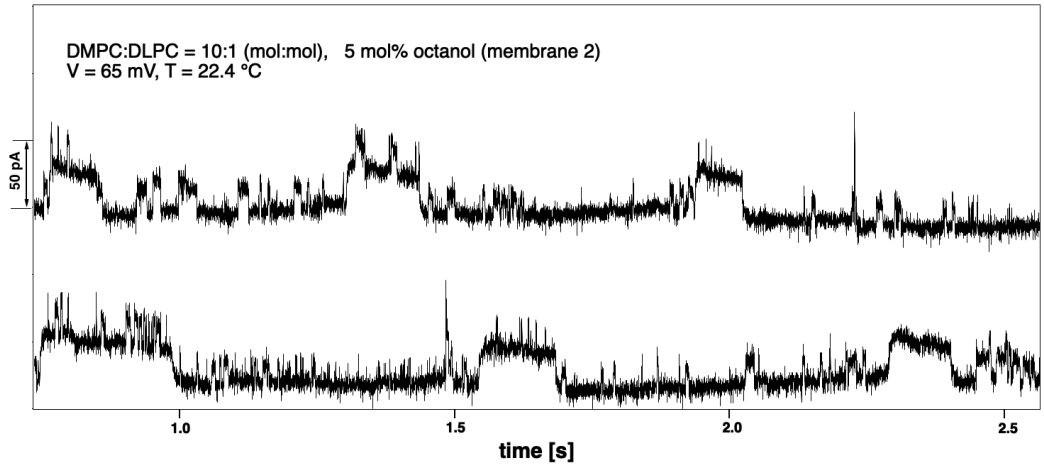

(a)

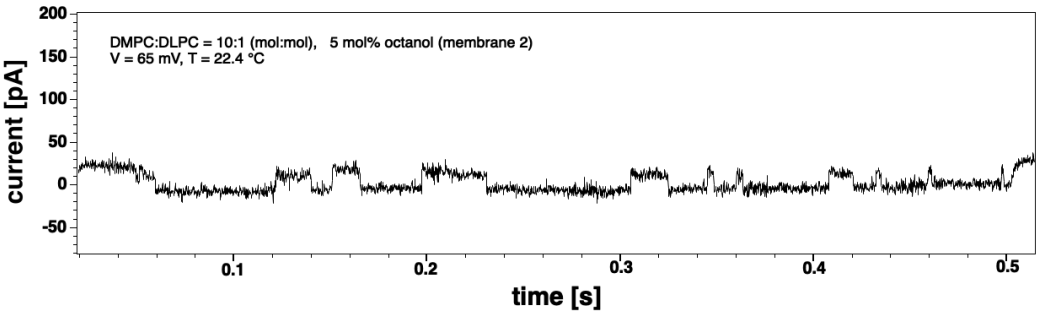

(b)

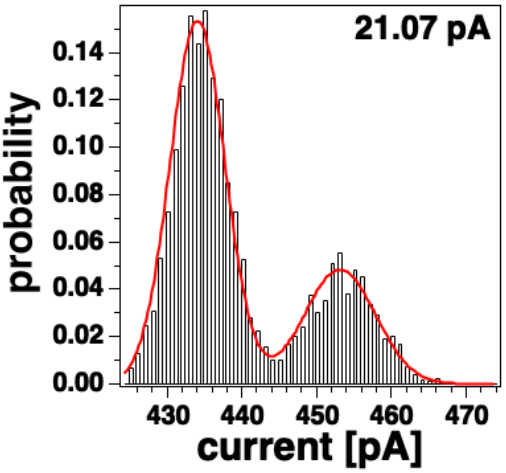

(c)

Figure 6.3: The channel events along with the phenomenon needed to be explained.

Bibliography

[1] V. F. Antonov, V. V. Petrov, A. A. Molnar, D. A. Predvoditelev, and A. S. Ivanov. The appearance of single-ion channels in unmodified lipid bilayer membranes at the phase transition temperature. *Nature*, 283(5747):585–586, 1980.

[2] V F Antonov, E V Shevchenko, E T Kozhomkulov, A A Mol'nar, and EYu Smirnova. Capacitive and ionic currents in blm from phosphatidic acid in ca2+-induced phase transition. *Biochem Biophys Res Commun*, 133(3):1098–1103, Dec 1985.

[3] Valerij F Antonov, Andrej A Anosov, Vladimir P Norik, and Elena Yu Smirnova. Soft perforation of planar bilayer lipid membranes of dipalmitoylphosphatidylcholine at the temperature of the phase transition from the liquid crystalline to the gel state. *European Biophysics Journal*, 34:155–162, 2005.

[4] VF Antonov, E Yu Smirnova, and EV Shevchenko. Electric field increases the phase transition temperature in the bilayer membrane of phosphatidic acid. *Chemistry and physics of lipids*, 52(3-4):251–257, 1990.

[5] Karis A.Zecchi. On polarization in biomembranes. *PhD Thesis,Neils Bohr Institute,Copenhagen University*, 2016.

[6] Andreas Blicher. Electrical aspects of lipid membranes. *PhD thesis. Neils Bohr Institute,Copenhagen University*, 2011.

[7] Andreas Blicher and Thomas Heimburg. Voltage-gated lipid ion channels. *PLoS One*, 8(6):e65707, 2013.

[8] Andreas Blicher, Katarzyna Wodzinska, Matthias Fidorra, Mathias Winterhalter, and Thomas Heimburg. The temperature dependence of lipid membrane permeability, its quantized nature, and the influence of anesthetics. *Biophysical journal*, 96(11):4581–4591, 2009.

[9] Rainer A Böckmann, Bert L De Groot, Sergej Kakorin, Eberhard Neumann, and Helmut Grubmüller. Kinetics, statistics, and energetics of lipid membrane electroporation studied by molecular dynamics simulations. *Biophysical journal*, 95(4):1837–1850, 2008.

[10] Rainer A Böckmann, Agnieszka Hac, Thomas Heimburg, and Helmut Grubmüller. Effect of sodium chloride on a lipid bilayer. *Biophysical journal*, 85(3):1647–1655, 2003.

[11] MARK S. BRETSCHER. Asymmetrical lipid bilayer structure for biological membranes. *Nature New Biology*, 236(61):11–12, 1972.

[12] Horridge GA Bullock TH. Structure and function in the nervous systems of invertebrates. *San Francisco : W. H. Freeman*, 1965.

[13] Andreas Carl and Kenton M. Sanders. Measurement of single channel open probability with voltage ramps. *Journal of Neuroscience Methods*, 33(2):157–163, 1990.

[14] Steven M Chrysafides, Stephen Bordes, and Sandeep Sharma. Physiology, resting potential. 2019.

[15] K S Cole and H J Curtis. Electric impedance of the squid giant axon during activity. *J Gen Physiol*, 22(5):649–670, May 1939.

[16] Edward F DeLong and A Aristides Yayanos. Adaptation of the membrane lipids of a deep-sea bacterium to changes in hydrostatic pressure. *Science*, 228(4703):1101–1103, 1985.

[17] Holger Ebel, Peter Grabitz, and Thomas Heimburg. Enthalpy and volume changes in lipid membranes. i. the proportionality of heat and volume changes in the lipid melting transition and its implication for the elastic constants. *The Journal of Physical Chemistry B*, 105(30):7353–7360, 2001.

[18] Alberts B. et.al. Molecular biology of the cell. 4th edition. 2003.

[19] Alan Finkelstein. Water movement through lipid bilayers, pores and plasma membranes. *Theory and Reality.*, 1987.

[20] Irene S Gabashvili, Bernd HA Sokolowski, Cynthia C Morton, and Anne BS Giersch. Ion channel gene expression in the inner ear. *Journal of the Association for Research in Otolaryngology*, 8:305–328, 2007.

[21] Jill Gallaher, Katarzyna Wodzińska, Thomas Heimburg, and Martin Bier. Ion-channel-like behavior in lipid bilayer membranes at the melting transition. *Physical Review E*, 81(6):061925, 2010.

[22] Ralf W Glaser, Sergei L Leikin, Leonid V Chernomordik, Vasili F Pastushenko, and Artjom I Sokirko. Reversible electrical breakdown of lipid bilayers: formation and evolution of pores. *Biochimica et Biophysica Acta (BBA)-Biomembranes*, 940(2):275–287, 1988.

[23] A. Gonzalez-Perez, L.D. Mosgaard, R. Budvytyte, E. Villagran-Vargas, A.D. Jackson, and T. Heimburg. Solitary electromechanical pulses in lobster neurons. *Biophysical Chemistry*, 216:51–59, 2016.

[24] Kaare Græsbøll, Henrike Sasse-Middelhoff, and Thomas Heimburg. The thermodynamics of general and local anesthesia. *Biophysical Journal*, 106(10):2143–2156, 2014.

[25] W Hanke, C Methfessel, U Wilmsen, and G Boheim. Ion channel reconstitution into lipid bilayer membranes on glass patch pipettes. *Bioelectrochemistry and Bioenergetics*, 12(3-4):329–339, 1984.

[26] Thomas Heimburg. Mechanical aspects of membrane thermodynamics. estimation of the mechanical properties of lipid membranes close to the chain melting transition from calorimetry. *Biochimica et Biophysica Acta (BBA) - Biomembranes*, 1415(1):147–162, 1998.

[27] Thomas Heimburg. A model for the lipid pretransition: Coupling of ripple formation with the chain-melting transition. *Biophysical Journal*, 78(3):1154–1165, 2000.

[28] Thomas Heimburg. Lipid ion channels. *Biophysical chemistry*, 150(1-3):2–22, 2010.

[29] Thomas Heimburg. *Phase Transitions in Biological Membranes*, pages 39–61. Springer Singapore, Singapore, 2019.

[30] Thomas Heimburg. Physics of biological nonequilibrium systems. 2020.

[31] Thomas Heimburg and Andrew D Jackson. On soliton propagation in biomembranes and nerves. *Proc Natl Acad Sci U S A*, 102:9790–9795, 2005.

[32] Thomas Heimburg and Andrew D Jackson. On the action potential as a propagating density pulse and the role of anesthetics. *Biophysical Reviews and Letters*, 2(01):57–78, 2007.

[33] Thomas Heimburg and Andrew D Jackson. The thermodynamics of general anesthesia. *Biophys J*, 92(9):3159–3165, May 2007.

[34] Thomas Rainer Heimburg. *Thermal Biophysics of Membranes*. Wiley-VCH, Germany, 2007.

[35] A L HODGKIN and A F HUXLEY. A quantitative description of membrane current and its application to conduction and excitation in nerve. *J Physiol*, 117(4):500–544, Aug 1952.

[36] Yuan Hu, Sudipta Kumar Sinha, and Sandeep Patel. Investigating hydrophilic pores in model lipid bilayers using molecular simulations: Correlating bilayer properties with pore-formation thermodynamics. *Langmuir*, 31(24):6615–6631, 2015.

[37] VP Ivanova, IM Makarov, TE Schäffer, and T Heimburg. Analyzing heat capacity profiles of peptide-containing membranes: cluster formation of gramicidin a. *Biophysical journal*, 84(4):2427–2439, 2003.

[38] K. Iwasa and I. Tasaki. Mechanical changes in squid giant axons associated with production of action potentials. *Biochemical and Biophysical Research Communications*, 95(3):1328–1331, 1980.

[39] Konrad Kaufmann and Israel Silman. The induction by protons of ion channels through lipid bilayer membranes. *Biophysical chemistry*, 18(2):89–99, 1983.

[40] Thomas Heimburg Lars D. Mosgaard, Karis A.Zecchi. Electrical properties of polar membranes. *Neils Bohr Institute,Copenhagen University*, 2014.

[41] Katrine R Laub, Katja Witschas, Andreas Blicher, Søren B Madsen, Andreas Lückhoff, and Thomas Heimburg. Comparing ion conductance recordings of synthetic lipid bilayers with cell membranes containing trp channels. *Biochimica et Biophysica Acta (BBA)-Biomembranes*, 1818(5):1123–1134, 2012.

[42] Katrine R. Laub, Katja Witschas, Andreas Blicher, Søren B. Madsen, Andreas Lückhoff, and Thomas Heimburg. Comparing ion conductance recordings of synthetic lipid bilayers with cell membranes containing trp channels. *Biochimica et Biophysica Acta (BBA) - Biomembranes*, 1818(5):1123–1134, 2012.

[43] Zoya V Leonenko and David T Cramb. Revisiting lipid general anesthetic interactions (i): Thinned domain formation in supported planar bilayers induced by halothane and ethanol. *Canadian journal of chemistry*, 82(7):1128–1138, 2004.

[44] Hari Leontiadou, Alan E Mark, and Siewert J Marrink. Molecular dynamics simulations of hydrophilic pores in lipid bilayers. *Biophysical journal*, 86(4):2156–2164, 2004.

[45] Fei Li, Pascal F Egea, Alex J Vecchio, Ignacio Asial, Meghna Gupta, Joana Paulino, Ruchika Bajaj, Miles Sasha Dickinson, Shelagh Ferguson-Miller, Brian C Monk, et al. Highlighting membrane protein structure and function: A celebration of the protein data bank. *Journal of Biological Chemistry*, 296, 2021.

[46] Drew Marquardt, Barbara Geier, and Georg Pabst. Asymmetric lipid membranes: towards more realistic model systems. *Membranes (Basel)*, 5(2):180–196, May 2015.

[47] Hans Meyer. Zur theorie der alkoholnarkose: Erste mittheilung. welche eigenschaft der anästhetica bedingt ihre narkotische wirkung? *Archiv für experimentelle Pathologie und Pharmakologie*, 42:109–118, 1899.

[48] JF Nagle and HL Scott Jr. Lateral compressibility of lipid mono-and bilayers. theory of membrane permeability. *Biochimica et Biophysica Acta (BBA)-Biomembranes*, 513(2):236–243, 1978.

[49] ERWIN NEHER and BERT SAKMANN. Single-channel currents recorded from membrane of denervated frog muscle fibres. *Nature*, 260(5554):799–802, 1976.

[50] Richard W Olsen and Werner Sieghart. Gaba a receptors: subtypes provide diversity of function and pharmacology. *Neuropharmacology*, 56(1):141–148, Jan 2009.

[51] D Papahadjopoulos, K Jacobson, S Nir, and I Isac. Phase transitions in phospholipid vesicles fluorescence polarization and permeability measurements concerning the effect of temperature and cholesterol. *Biochimica et Biophysica Acta (BBA)-Biomembranes*, 311(3):330–348, 1973.

[52] Reinhold Penner. A practical guide to patch clamping, chapter 1: Practical guide to patch clamping, pages 3–30. *Single-channel recording*, pages 3–30, 1995.

[53] Uwe Rudolph and Bernd Antkowiak. Molecular and neuronal substrates for general anaesthetics. *Nat Rev Neurosci*, 5(9):709–720, Sep 2004.

[54] Heiko M Seeger, Marie L Gudmundsson, and Thomas Heimburg. How anesthetics, neurotransmitters, and antibiotics influence the relaxation processes in lipid membranes. *J Phys Chem B*, 111(49):13858–13866, Dec 2007.

[55] S J Singer and G L Nicolson. The fluid mosaic model of the structure of cell membranes. *Science*, 175(4023):720–731, Feb 1972.

[56] Hermann Träuble and Hansjörg Eibl. Electrostatic effects on lipid phase transitions: membrane structure and ionic environment. *Proceedings of the National Academy of Sciences*, 71(1):214–219, 1974.

[57] BW Urban. Current assessment of targets and theories of anaesthesia. *British journal of anaesthesia*, 89(1):167–183, 2002.

[58] A.J Verkleij, R.F.A Zwaal, B Roelofsen, P Comfurius, D Kastelijn, and L.L.M van Deenen. The asymmetric distribution of phospholipids in the human red cell membrane. a combined study using phospholipases and freeze-etch electron microscopy. *Biochimica et Biophysica Acta (BBA) - Biomembranes*, 323(2):178–193, 1973.

[59] Tian Wang, Tea Mužić, Andrew D. Jackson, and Thomas Heimburg. The free energy of biomembrane and nerve excitation and the role of anesthetics. *Biochimica et Biophysica Acta (BBA) - Biomembranes*, 1860(10):2145–2153, 2018. Emergence of Complex Behavior in Biomembranes.

[60] Katarzyna Wodzinska. Pores in lipid membranes and the effect of anesthetics. *Master thesis. Neils Bohr Institute,Copenhagen University*, 2008.

[61] Katarzyna Wodzinska, Andreas Blicher, and Thomas Heimburg. The thermodynamics of lipid ion channel formation in the absence and presence of anesthetics. blm experiments and simulations. *Soft Matter*, 5(17):3319–3330, 2009.

[62] Dixon J Woodbury. Pure lipid vesicles can induce channel-like conductances in planar bilayers. *The Journal of membrane biology*, 109:145–150, 1989.

[63] Stephen Hong-wei Wu and Harden M McConnell. Lateral phase separations and perpendicular transport in membranes. *Biochemical and Biophysical Research Communications*, 55(2):484–491, 1973.

[64] B Wunderlich, C Leirer, A-L Idzko, UF Keyser, Achim Wixforth, VM Myles, T Heimburg, and Matthias F Schneider. Phase-state dependent current fluctuations in pure lipid membranes. *Biophysical journal*, 96(11):4592–4597, 2009.

[65] M Yafuso, S J Kennedy, and A R Freeman. Spontaneous conductance changes, multilevel conductance states and negative differential resistance in oxidized cholesterol black lipid membranes. *J Membr Biol*, 17(3):201–212, Jul 1974.

[66] Eric A Zizzi, Marco Cavaglià, Jack A Tuszynski, and Marco A Deriu. Alteration of lipid bilayer mechanics by volatile anesthetics: Insights from μs-long molecular dynamics simulations. *Iscience*, 25(3):103946, 2022.